

VOLUMETRIC YIELD MONITORING SYSTEM USING LASER SCANNER FOR CITRUS
MECHANICAL HARVESTER

By

UJWALA JADHAV

A THESIS PRESENTED TO THE GRADUATE SCHOOL
OF THE UNIVERSITY OF FLORIDA IN PARTIAL FULFILLMENT
OF THE REQUIREMENTS FOR THE DEGREE OF
MASTER OF SCIENCE

UNIVERSITY OF FLORIDA

2010

© 2010 Ujwala S Jadhav

To my family for their love and support

ACKNOWLEDGMENTS

I would like to give my sincere thanks to all those people who have offered me support, encouragement and help in completing my thesis successfully. I would like to thank my advisor Dr. Reza Ehsani, for his continuous guidance, valuable inputs and support throughout my master's studies. It was a wonderful experience and I am deeply indebted for giving me opportunity to work with him. My appreciation goes to Dr. Won Suk "Daniel" Lee for giving me guidance and direction during the course of my study and thesis completion. I am also grateful for the useful suggestions and discussion provided by my committee members Dr. John K. Schueller and Dr. Masoud Salyani. I am thankful for the funding provided by the Citrus Initiative of Florida to complete my research work. I would like to thank CREC members especially Mr. John Henderson from the packaging house, for providing me citrus fruits during my laboratory experiments. I am greatly indebted to my colleagues Dr. Mari Maja, Dr. Joa Camargo, Dr. Sindhuja Sankaran, Dmitry K, Bhargav Prasad, Ashish Mishra, Sherrie Buchanon, Sajith Udumala Savary and Raghav Panchapakesan for helping me during my experiments and giving me a fun filled lab environment.

My special thanks go to my husband Vijay, who was always there to help and support me. During my research work, discussion with him helped me understand the basic principles of engineering. It would be incomplete if I do not thank my mom and family members without whose continuous love, support, patience and encouragement any of this would not have been possible.

TABLE OF CONTENTS

	<u>page</u>
ACKNOWLEDGMENTS	4
LIST OF TABLES	7
LIST OF FIGURES	8
ABSTRACT	11
CHAPTER	
1 INTRODUCTION	13
Citrus Industry in Florida.....	15
Citrus Harvesting	17
Precision Agriculture and Yield Monitoring	18
Reasons for Yield Monitoring in a Mechanical Harvester	21
Objectives of This Study	21
Report Organization.....	22
2 HISTORY AND LITERATURE REVIEW	23
Citrus History.....	23
Citrus Yield Monitoring	24
Yield Monitoring Techniques.....	26
3 MATERIALS	39
Conveyor Systems	39
Continuous Canopy Shake and Catch (CCSC) Harvester	39
Trash removal Machine	40
Sensor and Communication	40
Infrared (IR) Laser Sensor.....	41
LIDAR	43
Labview Software.....	45
4 VOLUMETRIC YIELD MEASUREMENT	47
Yield Monitoring Using Linear Array of IR Distance Sensors	48
Volumetric Yield Calculation Algorithm	48
Overview of the Experiment	50
Materials and Methods	52
System Calibration	54
Laboratory Test	56
Results and Discussions	57
Conclusion.....	57

Yield Monitoring Using LIDAR (SICK Sensor).....	58
Volumetric Yield Calculation Algorithm.....	58
Error Sources	61
Method of Gridding Interpolation	66
Experiments on Horizontal Conveyor (Trash removal machine, f/h <0.5)	69
Overview of Experiment	69
Method and Materials.....	70
Experiment A.....	71
Experiment B.....	75
Results and Discussions	76
Experiments on Inclined Conveyor (CCSC, f/h \geq 0.5).....	81
Overview of Experiments.....	82
Material and Methods.....	82
Experiment A.....	83
Experiment B.....	86
Results and Discussions	87
5 YIELD MONITORING INTERFACE.....	94
Importance of Yield Monitoring Interface	95
Design and Development.....	95
Conclusion and Discussion.....	102
6 CONCLUSION AND FUTURE WORK.....	103
APPENDIX: LMS SICK DATA COLLECTION ALGORITHM	106
Algorithm for Horizontal Conveyor System in Trash Removal Machine.....	106
Algorithm for Horizontal Conveyor System in Citrus Mechanical Harvester Machine	115
LIST OF REFERENCES	125
BIOGRAPHICAL SKETCH	130

LIST OF TABLES

<u>Table</u>		<u>page</u>
3-1	Angular resolution and maximum scanning angle.....	45
4-1	Laboratory test results on True volume and Computed volume.....	56
4-2	Different parameters used the two experiments for volume calculation algorithm.....	71
4-3	Calibration data with speed 0.92 m/s with angle 180° and angular resolution 1°	72
4-4	Calibration data with speed 1.03 m/s with angle 180° and angular resolution 1°	73
4-5	Calibration data with speed 1.14 m/s with angle 180° and angular resolution 1°	74
4-6	Validation of the data after applying the calibration equations	75
4-7	Calibration data with speed 1.7 m/s.....	77
4-8	Calibration data with speed 1.34 m/s.....	78
4-9	Calibration data with speed 1.03 m/s.....	79
4-10	Validation data and error with speed 1.71 m/s	80
4-11	Validation data and error with speed 1.34 m/s	80
4-12	Validation data and error with speed 1.03 m/s	81
4-13	Different parameters used in volume calculation algorithm.....	82
4-14	Validation data and error with speed 1.1 m/s	84
4-15	Validation data and error with speed 1.1 m/s	85
4-16	Standard and the percentage error in the actual and predicted mass 1.1 m/s.....	86
4-17	Calibration data with speed 0.586 m/s.....	88
4-18	Calibration data with speed 0.785 m/s.....	89
4-19	Calibration data with speed 1.1 m/s.....	91
4-20	Validation data and error with speed 0.586 m/s	92
4-21	Validation data and error with speed 0.785 m/s	92
4-22	Validation data and error with speed 1.1 m/s	93

LIST OF FIGURES

<u>Figure</u>		<u>page</u>
1-1	U.S. citrus utilized production and value of production packing house-door equivalents. (Source: USDA Citrus Fruits 2009 Summary Report)	14
1-2	Components of grain yield monitoring system (Source: Basics of Yield Monitor Installation and Operation by Shearer et al., 1999)	15
1-3	Production of U.S Citrus by States (Ref. Florida Department of Citrus, Citrus facts 2008)	16
2-1	Different methods used for yield monitoring and yield estimation for specialty crops (Ref. Ehsani and Karimi, 2010)	26
2-2	Schematic of common yield monitoring systems for specialty crops (a), (b), (c), (d), (e) and (g) Load cell based yield monitoring systems, (f) Volumetric flow rate based yield monitoring system (Ref. Ehsani and Karimi, 2010)	27
3-1	(a) Continuous Canopy Shake and Catch (CCSC) and (b) Conveyor portion of the CCSC in laboratory.....	40
3-2	Trash removal machine.....	41
3-3	An IR laser sensor with connectors (Source: Sharp Electronic).....	42
3-4	Analog output voltage vs. distance to reflective object (Source: Sharp Electronic)	42
3-5	SICK LMS 200 Sensor	43
3-6	Fan shaped scan by an internal rotating mirror of SICK 200(Ref SICK Manuel)	44
3-7	Labview program interfaces and set parameters for SICK sensor.....	46
4-1	Schematic of IR sensors setup on the conveyor belt.....	49
4-2	3D view of volume calculation model.....	49
4-3	An array of sixteen sensors mounted on conveyor belt	51
4-4	Citrus mechanical harvester and the possible sensor location	53
4-5	Different Angles with Different Distance (Ref.: Acroname Robotics Inc. manual)	53
4-6	Sensor calibration test in the laboratory.....	54

4-7	Sensor output (v) vs. Length (cm)	55
4-8	R-square and RMS vs. Polynomial order	55
4-9	Schematic of SICK sensor setup on conveyor.....	59
4-10	Schematic of SICK sensor on conveyor	60
4-11	Flaps on trash removal machine conveyor system	62
4-12	(a) and (b) Spatial distribution of the raw data without removal of flaps and interpolating the data by gridding method	63
4-13	After removing the flaps in the data	63
4-14	Conveyor system with flaps to hold the fruits	65
4-15	Spatial distribution of the data showing flaps alone on the conveyor belt	65
4-16	(a) and (b) The distortion in the fruit shape due to the collection and transformation of data from polar co-ordinate system to Cartesian co-ordinate system.....	66
4-17	Fruits on conveyor belt	67
4-18	(a) and (b) The radial spikes observed in the shape of the fruit before applying gridding interpolation.....	67
4-19	After using gridding interpolation, uniformly spaced data points on the conveyor surface without radial spikes.....	68
4-20	After using gridding interpolation, uniformly spaced data points on the conveyor surface without radial spikes.....	68
4-21	The goat truck dumping the fruits on the top container of the trash removal machine	69
4-22	SICK LMS 200 location on trash removal machine	70
4-23	(a) Mass vs. Calculated volume calibration curve with speed 0.92 m/s and (b) Mass vs. Calculated volume with grid data interpolation technique, calibration curve with speed 0.92 m/s.....	73
4-24	(a) Mass vs. Calculated volume with speed 1.03 m/s and (b) Mass vs. Calculated volume with grid data interpolation technique with speed 1.03 m/s	73
4-25	(a) Mass vs. Calculated volume with speed 1.14 m/s and (b) Mass vs. Calculated volume with grid data interpolation technique, calibration curves with speed 1.03 m/s... <td>74</td>	74
4-26	% Error vs. Mass plot with different speeds	75

4-27	Actual mass vs. Calculated volume calibration curve with speed 1.71 m/s	78
4-28	Actual mass vs. Calculated volume calibration curve with speed 1.34 m/s	79
4-29	Actual mass vs. Calculated volume calibration curve with speed 1.03 m/s	80
4-30	% Error based on actual mass with respect to the speed of conveyor	81
4-31	LMS SICK 200 for laboratory test on the conveyor belt.....	83
4-32	Calibration plot of mass vs. Calculated volume of fruits calculated after correcting the data with gridding method and removing the flap error	85
4-33	Calibration curve with speed 0.586 m/s.....	90
4-34	Calibration curve with speed 0.785 m/s.....	90
4-35	Calibration curve with speed 1.1 m/s.....	92
4-36	Error spread with different speeds	93
5-1	Yield monitor components (left), Yield monitor 8" touch Screen Panel (right)	94
5-2	Snap shot of the data from GPS and load cell	96
5-3	Mechanical harvesting machines on top and bottom rows in the grove	97
5-5	Yield monitor interface with driver's input tab	98
5-6	Yield monitor interface with top row mechanical harvester information tab	99
5-7	Yield monitor interface with bottom row mechanical harvester information tab.....	99
5-8	Yield monitor interface with bottom row mechanical harvester information tab.....	100
5-9	Yield monitor interface top row mechanical harvester data communication port setting tab	101
5-10	Yield monitor interface bottom row mechanical harvester data communication port setting tab	101
5-11	(a), (b) Snap shot of raw data for the top and bottom row harvesters, (c) The processed data after combining raw data from top and bottom row harvesters.....	102

Abstract of Thesis Presented to the Graduate School
of the University of Florida in Partial Fulfillment of the
Requirements for the Degree of Master of Science

**VOLUMETRIC YIELD MONITORING SYSTEM USING LASER SCANNER FOR CITRUS
MECHANICAL HARVESTER**

By

Ujwala Jadhav

December 2010

Chair: Reza Ehsani

Major: Agricultural and Biological Engineering

Yield monitoring system is one of the important components in precision agriculture.

There is no commercial yield monitoring system available for citrus mechanical harvesters to date. Most of the large equipment manufacturer investments are focused on developing the efficiency of their machines but make little investments or none at all in the research and development of yield monitoring systems for these high value crops.

A yield monitoring system using an impact plate has been developed that uses the impact of the fruit to correlate to its mass. The system performs well in both laboratory and field tests but due to the impact created by the oranges falling on the plate, the durability of the system is poor. A non-contact method of collecting yield data will be very desirable to either augment the performance of the current system or eventually replace it.

A volume-based yield monitoring system was implemented as a means to estimate the mass of the fruit passing on the conveyor system on the mechanical harvester. A LIDAR (Light Detection and Ranging) technology was used to scan the cross sectional area passing on the conveyor system and send the distance related information to calculate the volume of fruits on the conveyor by integrating the data over time. The scanner used in the experimental work was a low-cost general-purpose SICK LMS-200 sensor. An algorithm was developed to analyze

the data and calculate the volume of fruit passing on the conveyor. The system was calibrated and the calibration curve information was used to convert the volume into a corresponding mass. The system performance was tested in laboratory setting on two conveyor systems; one with inclined conveyor used in mechanical harvesters (which has flap height of 8 cm) and other with horizontal conveyor system used in the trash removal machine (which has flap height \leq 3 cm). The tested conveyor speeds were from 0.586 m/s to 1.71 m/s. The conveyor system used on the mechanical harvester was tested for its maximum speed of 1.1 m/s and its performance was found encouraging with a coefficient of determination (R^2) of 0.98 and a RMSE was 1.69 kg while the conveyor system used on the trash removal machine performed very well with its maximum speed of 1.71 meters/sec, the coefficient of determination R^2 was 0.99 and the RMSE was 0.98 kg. The system performance was satisfactory for the complete range of the speeds used on both the conveyor systems. The results indicated the potential of using volumetric yield calculation method using LIDAR in yield monitoring of citrus in mechanical harvesters. Although this study was conducted for citrus fruits, the concept could be easily applied with little modifications to calculate the yield of other fruits and vegetables.

CHAPTER 1

INTRODUCTION

A yield monitoring system is one of the most important elements in precision farming (Pelletier and Upadhyaya, 1999). It gives quality information and direct feedback to the growers about the yield variability within the grove and is considered to be the first step in the process of site-specific crop management (Pelletier and Upadhyaya, 1999). Site-specific agriculture focuses on improving management to increase profitability and yield monitoring is essential for the creation of accurate yield maps (Persson et al., 2004). The growers can use this precise information, optimize farm profit, and minimize the effects on the environment.

Citrus fruit is among in Florida's most valuable agricultural products worth \$1.5 billion (packaginghouse-door equivalent) during 2008-09 season (USDA Citrus Fruits 2009 Summary Report). In 2008-09 season citrus production was 12 million tons as shown in Figure 1.1. Florida produced 71%; California produced 26%, and Texas and Arizona produced the remaining 3% of the total U.S. citrus production (National Agricultural Statistics Service, 2009). Figure 1-1 shows U.S. citrus utilized production and value of production packing house-door equivalents. Mechanical harvesting of citrus fruits in Florida is becoming more prominent due to the high demands and high costs associated with labor for harvesting. Tree canopy shakers are being used for automated citrus fruit harvesting. Mechanical harvesters such as canopy shake and catch type, have the conveyor belt which carries the harvested fruits to the containers that are attached to Oxbo machine. Once the container gets filled, it is carried to the processing plants for further operation. A yield monitor is used to give the farmer an accurate measure of the amount yields vary within the grove. A yield monitoring system can measure and store the yield related information and also give the on-the-go yield information to the operator. A typical yield monitor is a combination of several components as shown in Figure 1-2.

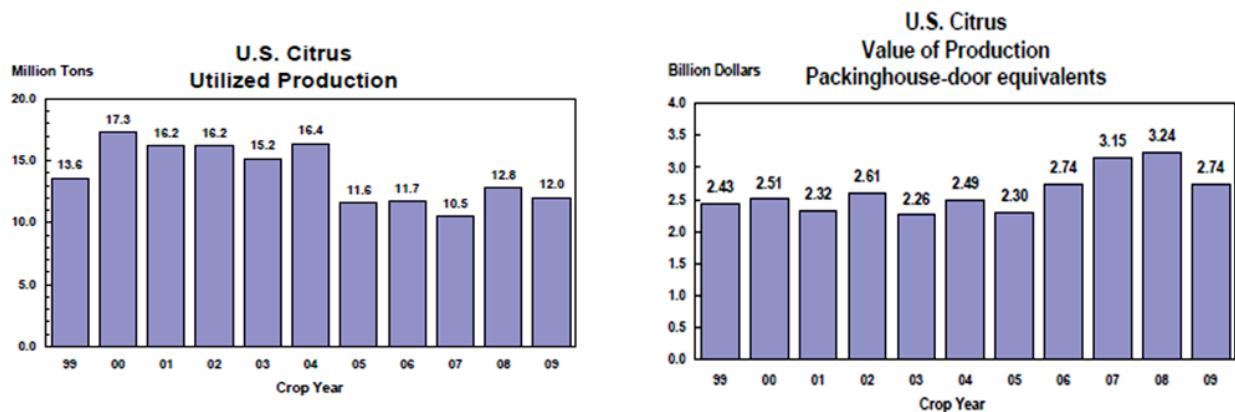


Figure 1-1. U.S. citrus utilized production and value of production packing house-door equivalents. (Source: USDA Citrus Fruits 2009 Summary Report)

It consists of several different sensors, a data storage device, a console installed in the operator's cab. These sensors measure the mass or volume flow of vegetables or grains (grain flow sensors), ground speed, separator speed and the grain moisture sensor. Depending upon the sensors specification, they might be connected to ADC and to the direct digital input. Using various parameters being calculated from the different sensors, the yield of the grain is determined. In order to understand the interaction of the yield monitor, combine cab operator and the combine dynamics, one should understand the function of various components.

A yield monitor consists of a main sensor to measure the actual mass or volumetric flow of the grain, fruits or vegetables. Yield monitors calculate the yield by dividing the crop volume or mass flow rate that is passing through the mechanical harvesting machine for the given time by the covered area (Ehsani and Karimi, 2010). The area covered by the mechanical harvester is calculated by using the speed related information collected from the ground speed sensors for a given time. The GPS receiver mounted on the mechanical harvester gives the position information which is integrated along with the yield information and then stored into the storage device for further processing.

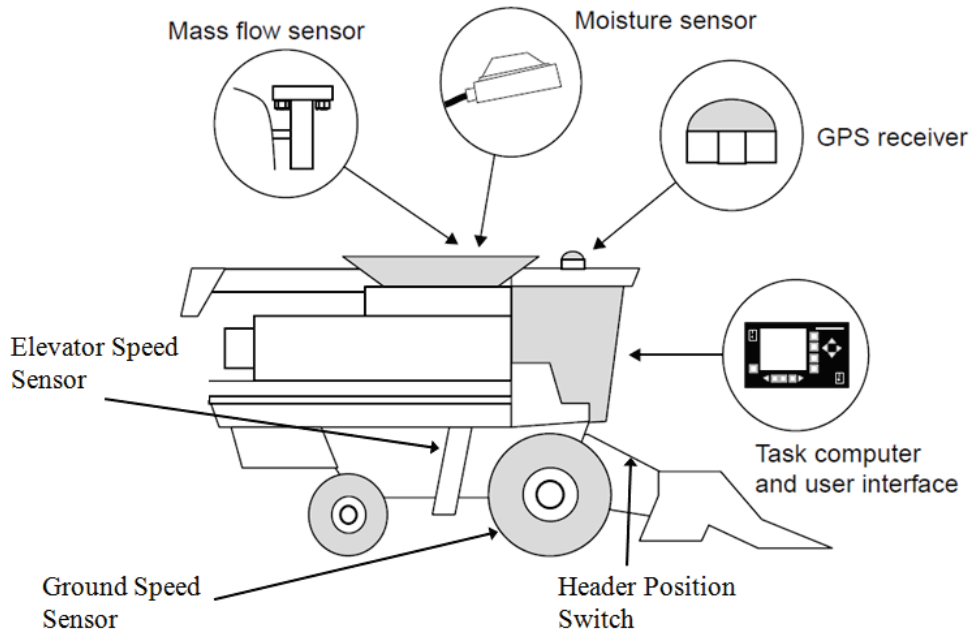


Figure 1-2. Components of grain yield monitoring system (Source: Basics of Yield Monitor Installation and Operation by Shearer et al., 1999)

In addition to the yield variability, growers can use this information wisely to manage the harvesting machine operation. The stored data can be used to extract the machinery management related information such as actual harvest time and total downtime. Also, the field efficiency, and the machine operator performance can be analyzed. This performance related information can be useful to the grove managers and it can help them improve the efficiency of the fruit harvesting operation. This will help to reduce the cost while making suitable management decisions (Ehsani and Karimi, 2010).

In this chapter, a brief discussion about the citrus industry in Florida, its history and the need for yield monitoring are provided. After some background information, the objectives of this study will be defined and the organization of the thesis will be provided.

Citrus Industry in Florida

In production of citrus, Florida has been the nation's largest producing state. During the last decade nearly three quarters of all U.S. citrus was grown in Florida (Figure 1-3) (Forecasting

Florida's Citrus Production, USDA's NASS, 2009). Florida growers produce several types of citrus including oranges, grapefruit, and specialty fruits including Temple oranges, tangerines and tangelos. The most commonly grown varieties of Florida oranges are Navel, Hamlin, Pineapple, Amber Sweet, and Valencia. The typical season for orange runs from October through June (Florida Department of Citrus, Citrus facts 2008).

Season	FL ^{1/}	CA	TX	AZ	U.S. total
<i>Thousand tons</i>					
1998-99	10,827	2,266	305	235	13,633
1999-00	13,305	3,457	308	206	17,276
2000-01	12,433	3,197	383	203	16,216
2001-02	12,824	2,907	310	153	16,194
2002-03	11,206	3,530	292	152	15,180
2003-04	13,045	2,855	298	162	16,360
2004-05	7,597	3,511	339	127	11,574
2005-06	7,832	3,460	277	185	11,745
2006-07	7,236	2,743	368	120	10,467
2007-08	9,119	3,470	318	90	12,997

^{1/} Does not include lemons. Limes and K-Early Citrus Fruit included through 2001-02.

Figure 1-3. Production of U.S Citrus by States (Ref. Florida Department of Citrus, Citrus facts 2008)

In market share, Florida is second to Brazil in global orange juice production and in the production of grapefruit Florida is the world's leading producer (Florida Department of Citrus, Citrus facts 2008). Florida produces more than 70% of the nation's supply of citrus, with majority export markets to Canada, Japan, France and the U.K. More than 80% of U.S.A's orange juice is made from Florida-grown oranges and nearly 87% of Florida citrus is processed into orange and grapefruit juices (Florida Department of Citrus, Citrus facts 2008).

In Florida, citrus groves cover nearly 569,000 acres of land and there are more than 74 million citrus trees. Most of the citrus groves are cultivated in the southern part of the Florida where there is low probability of a freeze. Florida citrus fruit is harvested when it is ripe. Once picked, the fruit does not continue to ripe. The picked or harvested fruits are placed into canvas

bags, transferred to the tubs and then put into specialized vehicles called ‘goat trucks’. Citrus produced for the fresh consumption is brought to the packaging houses where it is washed, graded and packed. Citrus produced for juice extraction is transported to the processing plants (Florida Department of Citrus, Citrus facts 2008).

The citrus industry generates close to \$1 billion in tax revenues which helps in supporting schools, highways, and healthcare services (Florida Department of Citrus: Citrus Facts, 2008). The citrus industry gives employment to nearly 75,000 Floridians (Florida Department of Citrus: Citrus Facts, 2008).

Citrus Harvesting

Citrus harvesting is a labor intensive process and depending upon the size of the grove, the demand for workers to harvest the citrus fruits increases. Mechanical harvesting and many other improvements in harvesting of citrus fruits in Florida began in the mid-1950s. In the 1950s, the harvesting operations were mechanized reducing the labor required by at least two-thirds (Whitney, 1995). The acreage along with the yield of Florida citrus was steadily increasing and finding the labor to harvest was getting difficult and expensive. The Florida Department of Citrus, United States Department of Agriculture, and the University of Florida started research development on a citrus mechanical harvesting system to aid in the removal of fruits from the trees thereby reducing the number of hand harvesters needed.

In early 1960s, the focus was on the development of mass harvesters. Some of the initial efforts to mechanize the picking of fruits were towards the development of machines that could duplicate manual harvesting. The goal was to develop a system that could be used for both process and fresh market oranges. Research was done on trunk shakers, limb shakers, air shakers, and canopy shakers. Such a system could be very useful to the Florida citrus industry by reducing the picking/harvesting costs. In 1970s, air shakers and the canopy shakers were

designed and implemented. These systems apply force to the canopy and limb portion of the tree. Hedden and Coppock (1971) used canopy or foliage and limb shakers to do series of tests and came to the conclusion that the foliage shakers had better selectivity. Despite of this, during the late season harvest, a considerable amount of young fruit was removed and also the fruits were bruised during the following year. Whitney (1968), Whitney and Patterson (1972) developed the air shaker which did not come in contact, but this system was only efficient when used along with the abscission chemical, but in that case it caused defoliation and peel damage too.

In 1990s, Peterson (1998) designed and developed a prototype similar to the current canopy shaker. The removal efficiency of these harvesters ranged from 80 to 90% which could be improved by finding the optimal operating parameters and changing the configuration of the system. Now using these machines, the fruit can be picked off the tree, more research was needed to collect or catch these fruits. The mechanical pickers were classified into two categories. In the first category, fruits were dropped onto the ground and then deposited by machines or manual workers into bins and to goat trucks and later transferred to hauling trailers. In the other category, the mechanical harvesters had catch frame which caught the harvested fruits and deposited directly into goat trucks. These harvest machines with catch frames were designed and developed with the mechanical pickers (Coppock (1967); Coppock and Hedden (1968); Churchill et al., (1976); Coppock (1976); Sumner and Churchill (1977)). The main disadvantage of these methods is the damages caused to the fruit due to bruising when falling from the tree. Sometimes these bruises are too severe for fruits that are intended for processing.

Precision Agriculture and Yield Monitoring

In precision farming each of the crop production inputs, e.g., fertilizer, limestone, herbicide, insecticide, seed, etc. are managed on a site-specific basis which helps in reducing waste and increase profits while maintaining the quality of environment (Kuhar, 1997). In

precision farming small units of land are treated instead of treating the whole field. A grower analyzes, applies fertilizers, pesticides, maps, and treats these small units of a field considering infield spatial variability. Using precision farming techniques a grower can monitor the crop yield more precisely; a grower can control the application of fertilizers, pesticides, etc. In order to apply precision farming techniques, a farmer needs to be able to measure and record yield at different locations in the field as the crop is being harvested or processed. This site-specific yield data then used to generate a yield map showing yield variations for each unit of a field.

In applying precision farming techniques for grain production, yield monitoring systems have been used. In grain harvesters or a combine, yield monitors are installed and used to gather the real time yield data as the grain is weighed or measured on the harvester. When the yield information is related to the geographic information system (GIS) of that particular location, this gives advantage to the farmers in being able to know the productivity of each unit of the field, through which units with low yield can be targeted, insect infestations can be outlined, different soil types can be identified and plotted, diseases can be identified, and fertilizer quantities can be adjusted.

Precision agriculture is a management technology that responds to the spatial and temporal variability found on agricultural landscapes. Using precision agriculture technique, one can determine the yield variability in the field, determine cause of low yield, come up with solutions based on economic justification, implement new techniques, and repeat the procedure in cyclic approach. These techniques could be used to improve economic and environmental sustainability in crop production. Major technologies and techniques used for precision farming such as Global Positioning System (GPS), yield monitoring and mapping, soil testing, remote sensing (RS), GIS and mapping, variable rate technology (VRT), and information technology have enabled the farmer to visualize the entire field in a way, that could help manage the agricultural operations

efficiently and improve overall productivity. Using these technologies, the farmer can effectively manage the crop throughout its life cycle, starting from preparing soil, sowing seeds, applying fertilizers/pesticides, and finally measuring yield during harvesting based on each individual plant, which helps reduce the waste of resources due to in-field variability.

Yield monitoring and mapping plays a major role and is the first step to implement site-specific crop management on a field. A yield monitoring and mapping system measures and records the amount of crop harvested at any point in the field along with the position of the harvesting system. The position and yield data could be used to generate yield map using mapping software. Yield maps are useful to identify variability within a field. A yield variability may be due to seasonal change in weather pattern or rainfall over several years or improper distribution of irrigation/drainage facilities for field and excessive/deficit application of farm inputs.

Various yield monitoring and mapping systems have been researched and commercialized for various crops over the two decades. Whitney et al. (1998) and Schueller et al. (1999) developed the first yield monitor system for citrus industry. Schueller and Bae (1987), and Searcy et al. (1989) extensively studied and opted yield mapping system during grain harvesting. Examples of yield mapping and monitoring for other crops include cotton (Wilkerson et al., 2001; Roades et al., 2000), sugarcane (Benjamin 2002), potatoes (Campbell et al., 1994), citrus (Annamalai, 2004; Ehsani et al., 2009; Maja and Ehsani, 2009a), tomatoes (Pelletier and Upadhyaya 1999), silage (Lee et al., 2002), and tuber (Persson et al., 2004). Being able to evaluate the entire farm graphically, with respect to the yield and other associated field characteristics would tremendously help farmers to more meticulously know the variability in the field and thus help them to make important decisions in an efficient manner.

Reasons for yield monitoring in a mechanical harvester

Currently, there is no yield monitoring system available for ‘Citrus Mechanical Harvesters’ up to date. Canopy shake and catch harvesters and tree canopy shakers are the automated citrus fruit harvesting machines used by citrus growers in recent years. These machines lack the reliable method of yield monitoring. Canopy shake and catch harvesters have the conveyor mechanism that carries the citrus fruits and transports to a level where the fruits roll along a ramp into the container. A system can be implemented on the citrus carrying conveyors, which can measure the amount of citrus fruit volume passing along the conveyor and can convert this volume into mass to get the citrus mass carried per unit time in the collection bin.

Yield monitoring systems for mechanical harvesting machines create real time data for maximum efficiency (Ehsani, 2007). Yield monitoring is the process of measuring fruit yield for a given location in the citrus grove. The yield variability for a particular section or part of the grove is unknown to the growers, yield monitoring can provide and document the yield variability at a smaller scale and can lead to a way to manage the needs of each individual tree rather than treating the entire block of trees uniformly.

Yield monitoring system would not only provide information of the mass loaded into the container but also provide fruit yield of the area and approximate individual tree yield.

Objectives of This Study

The main objectives of this research was to

1. Study and evaluate different sensors for volumetric yield calculation
2. Design a volumetric yield measurement system using the mass flow sensor using LIDAR (Light Detection And Ranging) technology for citrus mechanical harvester and Trash removal machine
3. Develop an algorithm for the laser based sensors that can estimate the volume of the fruits on the conveyor belt
4. Develop a yield measurement model to relate the volume to the mass of the fruits

Report Organization

Chapter 2 is about the history of yield monitoring of citrus, different techniques used for yield monitoring of specialty crops and the literature review related to this study. Chapter 3 explains about the materials used during the laboratory experiments involved in this study. Chapter 4 describes the volumetric yield measurement technique and the experiments performed. The performance of different sensors was analyzed in the laboratory conditions. The analysis and validation are explained in this chapter. Chapter 5 discusses the yield monitoring interface development for the impact plate type yield monitor. Chapter 6 provides main conclusions from the study and indicates possible future research direction.

CHAPTER 2

HISTORY AND LITERATURE REVIEW

Citrus History

Citrus fruit can be of different types such as orange, tangerine, lemon, lime, and grapefruit. The evergreen citrus species grow and produce fruit under varied climate conditions, ranging in the latitude over 40° North to 40° South from equatorial hot-humid climates through warm-subtropical and even cooler maritime climates (Spiegel-Roy and Goldschmidt, 1996). The exact origin of citrus fruit is not clearly known but the various species of citrus are native to the subtropical and tropical regions of South-East Asia including South China, north-eastern India and Burma, and have spread from there to other regions of the world, by least 4000 BC (Spiegel-Roy and Goldschmidt, 1996). The genus spread was very slow from one part of the world to the other. The first member of the group - Citron, mentioned about 310 BC by Theophrastus, was cultivated and known for several hundred years to European civilization. The sour and sweet oranges and lemon introduced after Citron several centuries apart. Sweet oranges had been grown in China for many centuries and then it became known to Europeans. Many older references to oranges may be found in ancient Chinese manuscripts and documents (Spiegel-Roy and Goldschmidt, 1996).

By the middle of sixteenth century, citrus was succeeded to establish in the West Indies and Brazil. There is no any exact date when the citrus was brought to California, the first citrus seeds were introduced to California when the mission of the Franciscans was established in San Diego in 1769. Citrus was first introduced to Florida sometime between 1513 and 1565 by the Spanish voyagers. Spanish explorers, most likely Ponce de Leon, planted the first orange trees around St. Augustine, Florida (Florida Department of Citrus, 2008). A first grapefruit seed was planted in Florida around 1809 (Hume, 1926). Florida's unique sandy soil and subtropical

climate proved to be ideal for growing the seeds that the early settlers planted and since then has flourished.

Citrus Yield Monitoring

Yield monitoring systems are available in market for grains but very few yield monitoring systems are available for specialty crops. Specialty crops are high valued commodities that need special care and are more sensitive to the growth conditions. Lack of yield monitoring systems limits the site-specific crop management and considered as one of the bottlenecks in applying precision agriculture techniques for specialty crops (Upadhyaya et al. 1999). Citrus yield monitoring system was not developed for several decades. Miller and Whitney (1999), and Schueller et al. (1999) developed the first yield monitoring and mapping system for citrus and evaluated the system for site specific crop management for citrus in Florida. Citrus yield was measured by installing three electronic sensor systems on a specialized vehicle called a goat, which is used to transfer the fruits from grove to the roadside containers. A GPS unit (GOAT, Geo-Focus, Gainesville, FL) was attached to the sensor systems to record the location of bins as it was picked by the goat truck. This GPS unit was used to coordinate all the operations of the goat truck. A crop harvest tracking application (GeoFocus, LLC, Gainesville, FL) was installed on the unit to record the pallet bin or tub pickup location. This application was also programmed and modified later to incorporate two channel A/D data acquisition capability for A/D voltage measurements. This unit was used by the goat truck operator and the data logging process was triggered by a button push. This initiates the recording of GPS location and the A/D voltage acquisition corresponding to the bin or tub. A LCD display on the unit indicated the acquisition process status and number of events recorded. The data then transferred to the computer through RS-232 port connection for further post processing. The LCD display was mounted on the goat truck such a way that it was accessible by the truck operator. It was found that this system

sometimes produced incorrect maps due to the fact that the driver failed or forgot to record the location of the tub. Salehi et al. (2000) developed a system to overcome the problem in the previous system. An automatic triggering system was developed to record the location of the bin or tub. The pressure switch was used to detect the load on the dump cylinder and on the boom lift cylinder. The position switch detected whether the tipping head was located over the truck bulk bin and then the system identifies that the truck was in the process of picking the bin or tub for collecting the fruit and data gathering circuit was activated for a given time using the timer and relay circuit for collecting the DGPS data. However, the automatic triggering system also encountered problem in recording the tub locations, which could be the problems related with the delay timer, pressure switch settings and hardware connections. Annamalai (2004) and Ehsani et al. (2009) developed yield estimation techniques by counting individual fruits or vegetables on the citrus trees.

Maja and Ehsani (2009b) developed a load cell based yield monitor for citrus mechanical harvesters. Two load cells were attached to a carbon fiber plate and mounted at the end of the conveyor system of a shaker machine. The carbon fiber plate was used to measure the force created by the rolling oranges on the conveyor. The system performed very well in field conditions with coefficient of determination of 0.97 with an average error of 7.8%. Along with the harvested fruits the conveyor carries the foreign objects also called as trash, such as citrus tree limbs, leaves, stems, and trunks. Because of the impact produced by the fruits and the trash, it cannot withstand for longer duration of time in the field and the system failed. The large diversity in the type and harvesting methods of specialty crops have provided little incentive for commercial companies to invest in developing yield monitoring systems for specialty crops.

Yield Monitoring Techniques

Yield monitoring is the process of measuring crop yield per unit area and integrating this yield along with the GPS coordinate information. In earlier time, the yield-monitoring attempts have been done in manual harvesting by counting and locating the containers at particular locations in the field (Schueller et al., 1999; Whitney et al., 2001).

There are a number of ways to measure the yield of crops. Most of the methods developed over the years have involved weighing the crop after it has been threshed, separated and cleaned. This method is oldest method and it is still being used. The second method is batch-type yield monitor, which weighs grains in the grain tank of combine's operator on a monitor. This method is considered forerunner of modern, site specific yield monitoring. The third and last method is instantaneous crop yield monitoring which measures and records yield on-the-go. The most commonly used methods in developing yield monitoring systems for specialty crops are mass/volume flow rate sensors, direct weighing, and cumulative weighing. These methods are used for yield estimation and yield monitoring of specialty crops. These methods can be categorized as shown in Figure 2-1 and 2-2.

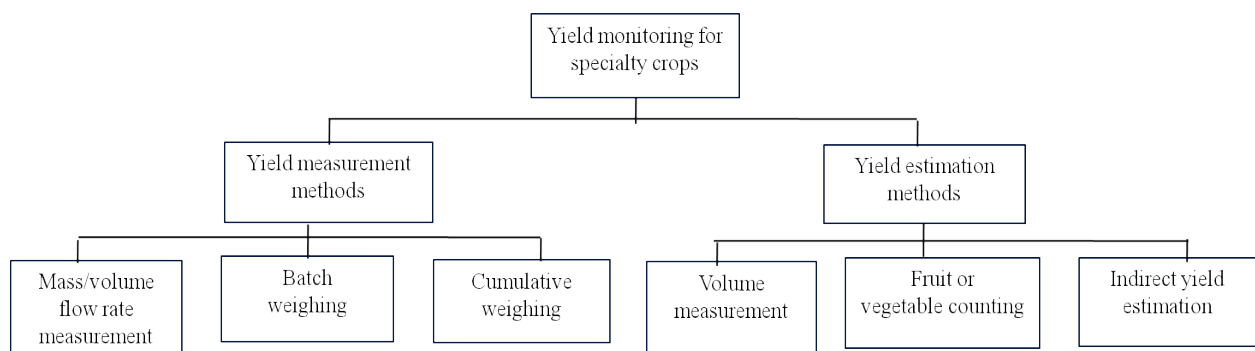


Figure 2-1. Different methods used for yield monitoring and yield estimation for specialty crops
(Ref. Ehsani and Karimi, 2010)

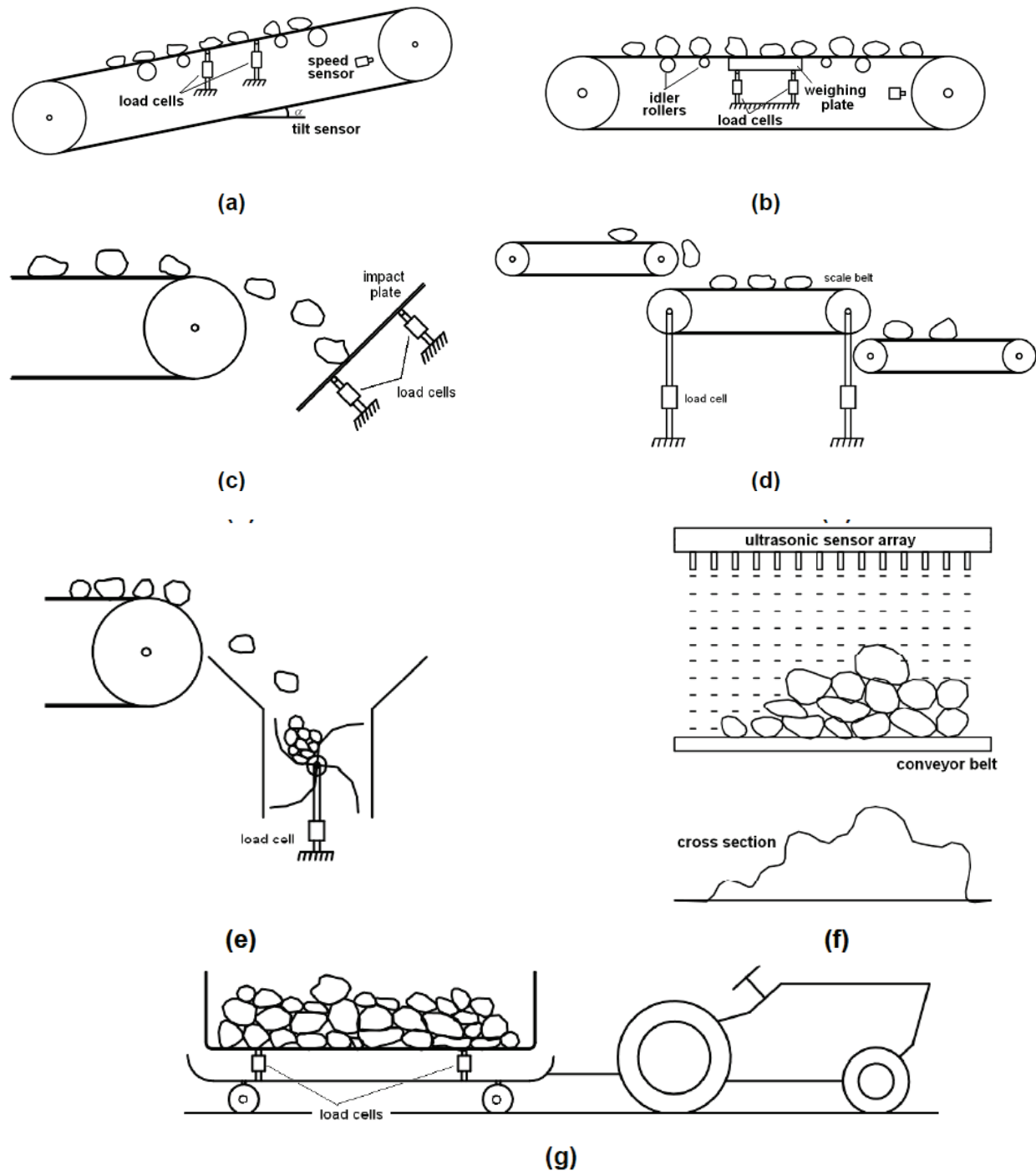


Figure 2-2. Schematic of common yield monitoring systems for specialty crops (a), (b), (c), (d), (e) and (g) Load cell based yield monitoring systems, (f) Volumetric flow rate based yield monitoring system (Ref. Ehsani and Karimi, 2010)

Yield monitoring of grains and other crops vary in different methods of measuring grain or crop flow. There are some popular yield monitoring systems which use different flow sensors in

the path of clean grain/fruit flow. The grain flow sensor is typically mounted at the top of the clean grain elevator or conveyor belt in harvesters. Grain or fruit flow can be sensed by placing the impact plate in the path of grain or fruits and then the force applied by impact of grains or fruits are measured. In mechanical harvesters developed for specialty crops, the mass or volume measurement of harvested crop is done at the end of the conveyor belt before the fruit get transferred into containers (Figure 2-2a and 2-2b). Yield monitors for grain crops based on mass flow have been developed for the measurement of specialty crops. Either an optical sensor or a load cell has been used for such measurements. The impact plate is mounted on the load cell which measures the force impacted and converts this load into an electrical signal. The strain gauge bonded with the load cell converts the load into an electrical signal. A very slight deformation of the load cell causes the measureable change in the resistance offered by the strain gauge to electrical current flow. Ehlert (2000) tested a rubber coated bounce plate with a force measuring instrument for potato harvesters by placing it in different positions in the discharge trajectory of a conveyor belt running at 3 different speeds. The vibrations in actual potato harvesters were simulated by moving the measurement device at five different frequencies and four amplitudes. The result showed a linear relationship between the mass flow and the force. For many parameter combinations, the coefficient of determination was more than 0.99 and in some cases; standard error was less than 0.083 kg/s which indicates that the bounce plate provides a basis for measurement in potato harvesters for yield mapping. Lee et al. (2002) developed a silage yield mapping system using DGPS, load cells, moisture sensor and bluetooth for wireless data transmission. A shear beam type load cells were installed on the four corners of the bottom of the trailer silage box. To compare the load cell weight and the actual weight, the axle of a silage trailer without the box was measured on a platform scale. In order to compare the

weight measured by a platform scale and load cell, the weight of a trailer axle was subtracted from a total trailer weight. The error was calculated between the two measurements and was found to be in the range of 0.37~1.96%, which was very small. Benjamin (2002) developed a technique for yield monitoring of sugarcane. They evaluated the system performance based on the variety of sugarcane, maturity levels and flow rates. The yield sensor predicted the sugarcane yield with a slope of 0.90 and coefficient of determination (R^2) of 0.96. The average error was 11.05%. Results showed that for the simple weight scale system, sugarcane maturity level and flow rate (induced by two different travel speeds of the combine) did not significantly change the yield monitor readings but the effect of sugarcane variety was significant. The percentage error ranged from 0 to 33% and 14 out of 118 tests showed an error of higher than 20%. Molin and Menegatti (2004) developed a similar system for sugarcane harvesters. Average error in field evaluations was from -3.5% to 8.3%. Several different methods used to estimate weight from a weigh scale, these methods ranged from inclusion and exclusion of slat speed, tilt sensor data, and different processing algorithms. The standard deviation ranged from 4 to 10% on absolute value error numbers. Bora et al. (2006) developed a mass-flow citrus yield monitor under laboratory conditions. They found mass-flow yield monitor is most accurate when the mass flow rates that are used in the calibration phase are in the same range in the actual measurements.

In impact type mass flow sensor based system, harvested crop grains hit the impact plate and the output measurement corresponding to the impact and velocity used to calculate the mass of the crop flow. The coefficient of restitution of the crop should be accurate for the accuracy of impact plate yield monitors. The coefficient of restitution is a constant, representing the ratio of its velocity before and after an impact. If the coefficient of restitution of a crop significantly depends on its maturity, moisture content then the impact-type yield monitors will not result in

accurate measurements (Pelletier and Upadhyaya, 1999). Grift et al. (2006) developed three methods for yield monitoring system for citrus fruits. They found the first method which was based on large sensor array was inaccurate in measuring the lengths of clumps and spacing due to defocus problems. The second method based on the interruption of a low placed single laser beam showed promising results for higher mass flow densities. A third method which used gutters that forced fruits in single file was deemed most reliable and robust for application of tree canopy shakers. Magalhães and Cerri (2007) designed and implemented a sugarcane yield monitor consisting mass flow sensor which was mounted on a weigh plate. The weighing plate was set up on the upper part of the harvester side conveyor, just before the sugarcane billets are dropped in an in-field trailer. Additional sensors were used to measure the conveyor inclination angle and speed. Performance reports indicated that the maximum error of yield measurement did not exceed 6.4% and the mean error detected without any compensation was 4.3%. Qarallah et al. (2008) designed an impact-based yield sensor consisting of two load cells, an acrylic plate and a polyurethane cushion for measuring the individual weights of onion bulbs. The precision of the sensor was maintained with a 30 mm cushion resulting in a relative error of less than 2.0% during validation. The accuracy of measurement was independent of the orientation of the onion bulb on the conveyor belt or their orientation as they hit the impact plate.

In batch weighing method, the fruits get divided into batches which are weighed before they get dropped into hauling truck or containers (Figure 2-2e). Heidman et al. (2003) introduced similar kind of yield monitor for pistachio. This system was field tested on the commercial pistachio harvester and found the 0.97 as the coefficient of determination between the true and the measured yield. Abidine et al. (2003) and Cerri et al. (2004) described the development and improvement of yield monitor for tomato. In this, a weigh bucket was mounted on the boom

elevator of the tomato harvester. An impact plate was mounted on the four load cells continuously weighed the tomatoes in the bucket. Field test analysis showed that the coefficient of correlation ($R^2 > 0.99$) between yield monitor load cell output and the true weight of the harvested tomato was highly correlated.

Several techniques were implemented on cumulative weighing and yield monitoring system for specialty crops. In cumulative weighing, harvested crop is collected in a container on the harvesting machine (Figure 2-2g) and the system measures the total weight of the harvested crop over time. Behme et al. (1997) developed a system with a drawbar load cell and two weigh axle load cells to estimate the bale weight in a round baler. The output from the three load cells were summed to measure the weight of the bale. Field experiments showed an error between 2.5% and 5.2%. Wild and Auernhammer (1999) developed a weighing system for local yield monitoring of forage crops in round balers. The mounted weighting system was based on load cell in the drawbar coupling and strain gauges in the axle similar to the work of (Behme et al., 1997). The static tests and weighing during vehicle stops could be carried out with errors of less than 1%. Weight measurement on-the-go needs further investigation to eliminate the sources of errors.

Vellidis et al. (2001) developed and tested a peanut yield monitoring system over a 3 year period. This system was evaluated by 11 users and they were able to use the resulting yield maps to evaluate management practices. This yield monitor uses load cells for instantaneous load measurement and was accurate between 2-3% on a trailer basis and 1% on basket-load basis. The error due to sloping terrain was found to be negligible. The noise due to vibrations of the harvester and uneven field surface were measured and dealt with using appropriate filtering. Rains et al. (2002) developed similar yield monitoring system for pecans. Yield was measured by

weighing the pecan wagon as it is loaded by the harvester in the field. They conducted field experiments and developed a simple linear equation to estimate the net pecan yield from the gross weight of the pecan and the foreign material. The total pecan yield measurements were closely correlated with the gross weight of pecans for the individual pecan trees ($R^2 = 0.84$). One of the challenges was separating the foreign material picked up by the harvester from the collected pecans.

In volumetric flow rate measurement system, volume or volumetric flow rate is measured and then converted into the corresponding weight or mass of flowing fruits (Figure 2-2f). Different optical laser scanners are being used to measure the volume of fruits carried on the conveyors and then convert the measured volume into mass of the grain or fruits. These systems need calibration first and then use the calibration curve to get the weight or mass of the fruits on the conveyor. Along with the optical techniques such as laser scanners, computer vision systems are also widely used for the volume or volumetric flow rate measurement. Persson et al. (2004) tested an optical sensor for the tuber yield monitoring. The laboratory and field test showed that the errors in size determination by the sensor were in the order of 1% to 2% on average. The mean of optical sensor from the load cell in the field experiments showed the deviation of 3.2%. The laboratory tests were performed on the spherical objects and the sensor was very accurate in measuring the size and the number of objects. The field tests were performed on the potato harvester which showed that the number of pixels in the tuber image and the tuber weight has a coefficient of correlation 0.91. The possible errors were due to the differences in the tuber orientation with respect to the camera and moisture content. Gogineni et al. (2002) developed vision based sweet potato yield and grade monitor. The estimation of weight was based on multiple-linear regression and neural networks, while grade classification was based on linear

discriminant analysis and neural networks. In order to identify the sweet potatoes from soil clods, the images captured by the camera were transformed from RGB to YUV color space, where pixels were characterized by their brightness and color characteristics. Once the algorithm detected the sweet potatoes in the image; the other parameters such as area, polar moment of inertia, rectangular width and height, and major and minor axes were determined and using linear regression and neural networks, the weight was calculated. The multiple linear regression method was more accurate ($R^2 \geq 0.95$) than the neural networks. The system was tested under real field conditions. The coefficient of determination between the number of sweet potatoes detected by the image analysis algorithm and manual count had a $R^2 \geq 0.91$ for the neural network method and $R^2 \geq 0.80$ for the discriminant analysis method. They suggested that the reduced accuracy could be due to muddy field conditions and poor lighting in the boundaries of the field of view of camera. Bora et al. (2006) developed similar type of vision based system for citrus yield estimation. The system consisted of three CCD progressive scan digital color camera and an algorithm was developed for counting the number of fruits and measuring the size from the images. The system was tested in laboratory conditions and the test analysis showed that the system performed well in identifying the fruits that appeared as full in the image. However, when the fruit image was not complete, the recognition error rates were very high. The overall fruit detection accuracy was 85.5%. Hofstee and Molema (2003) have estimated the volume of individual potato tubers using machine vision on the conveyor of a harvester. Cundiff and Sharobeem (2003) developed a procedure to measure the mass flow and volumetric yield monitoring system for round balers. The system consisted of displacement sensors to measure the windrow cross section. This measurement were combined with the velocity and the volumetric flow rate was calculated, which was then multiplied by a mass factor to give the mass

flow rate. Field experiments showed that the yield estimations were within 4% of the true value. Rains et al. (2005) tested the cotton yield sensor on a peanut combine. A pair of optical sensor was installed in the deliver chute between air fan and basket. The optical sensors were strategically adjusted such a way that the sensors were not covered by the dust and were not hit by to the peanut flow. The peanut yield monitoring system performance was evaluated in three harvesting seasons in real field conditions. The absolute mean error for three different field harvested was 3-9%. They concluded that to maximize the performance of the yield monitor, the yield monitor needs to be recalibrated every time the field conditions or harvester adjustments change. Thomasson and Sui (2004) also developed, fabricated and tested an optical yield monitor for peanut. Field evaluation on commercial peanut harvesters showed that this yield monitor was capable of estimating peanut yield with very high accuracy. The coefficient of determination between the two optical sensor outputs and true peanut weight was 89- 96%. There were two major challenges that need to be addressed, peanut moisture content and nonlinear behavior of the sensor output for high mass flow rates. Konstantinovic et al. (2007) developed non-invasive ultra-wideband (UWB) ground penetrating radar system to detect sugar beets in soil. The system was successful in detecting the sugar beets with visual detectability from 90% to 96%. They were able to relate the reflected energy to the mass of individual sugar beets with a correlation over 80%. Laboratory tests showed that the detectability of beets buried in the soil depended on the size, the depth of the beets in the soil, the soil moisture content, and roughness of the soil surface. Beets which were small and deeper in the soil were more difficult to detect, and high moisture contents and rougher soil surfaces were less favorable. Price et al. (2007) developed a yield monitor for sugarcane harvesters where three optical sensors were mounted in the flooring of the harvester conveyor. This system was tested in laboratory conditions and the result showed

the linear relationship with coefficient of correlation between estimated yield and true yield of 0.93. The system was found to be rugged in the field conditions and did not need frequent maintenance. Chinchuluun et al. (2007) developed a machine vision based system for citrus yield mapping and quality inspection. The image processing algorithm was implemented to count the number of citrus fruits passing on the harvester conveyor belt. The system was tested in laboratory and actual field conditions with coefficient of correlation 0.96 and 0.89, respectively. They concluded that the system needs improvement in image acquisition (speed and quality of images).

In yield estimation methods, yield of the crop is estimated before or after the fruits get harvested. These are the systems which use the vision based approach or other technologies to count the number of fruits or to measure the volume of the fruits and estimate the yield of the crops but such systems require the density or the mass of individual fruit as constant. These systems use non-contact, non-intrusive measurement approach which could be a major advantage for certain crops.

In volume estimation method, the system estimates the volume or the volumetric flow of the crop. The machine vision system was developed by Annamalai (2004) for yield estimation and mapping of the yield data in the real time in citrus grove. These systems estimate yield by counting the individual fruits on the tree or in the mechanical harvester. In this system, a color CCD camera was used to capture the citrus tree images and using an image processing algorithm, the number of fruits on the citrus trees were identified and counted. Using the test data, the yield prediction model was developed and the results were then compared with the hand harvested fruits. When the yield estimated using the prediction model and hand harvest were compared, a R^2 of 0.46 was achieved. The reason for such poor relationship could be that a single camera was

used to capture the image of the whole canopy and it was difficult to cover the citrus canopy sides of the tree. In addition, the fruits which were hidden inside the canopy by leaves cannot be identified and are not visible in the image. Therefore, the algorithm was not able to count these fruits. Zaman et al. (2008) estimated the wild blueberry fruit yield using a digital camera. This digital color camera was used to take top-view images of wild blueberry crop. An algorithm was developed to process these images and count the number of blue pixels in each image. The system was calibrated in field and the true blueberry yield was determined during hand harvesting. A linear regression analysis was performed to relate the percentage of blue pixels in each image to the blueberry yield data. The analysis showed a very high coefficient of determination of 0.98. The correlation between the two variables was used to predict the blueberry yield in another field. The model predictions were close to the true yield with $R^2 = 0.99$. They concluded the potential of estimation of blue berry yield using digital photography within wild blueberry fields.

Ehsani et al. (2009) developed two fruit counting techniques for citrus mechanical harvesting machines. In the first method, the arrival process of fruits was random whereas the second method relied on counting single fruits using five channels. The fruits were counted using laser-based photo-interruption sensors installed at the channel exits. The system performed very well in laboratory conditions, counting individual fruits with an accuracy of 99.8%. The other method where the fruit arrivals at the sensor were assumed to be a Poisson process failed because laboratory experiments showed that this assumption was invalid.

In the method or indirect yield estimation, the yield is estimated using related parameter(s) such as tree canopy size. Whitney et al. (2001) developed a DGPS based yield monitoring system for Florida Citrus along with the three fruit weighing systems for hand harvested citrus

fruits. The results showed that the “lift cylinder”, scale unit utilizing the pressure transducer has the lowest errors ranging from 0.08 to 2.13% than that of the “load cells”, mounted on the truck frame and the “loader boom”. The load cell output was recorded every 0.1 s and the yield was computed. The real time prototype DGPS receiver eliminated the post processing of GPS data and gave the position information accurate enough to locate the citrus bin loads and to plot their location in the map. Tumbo et al. (2002) designed a microprocessor-based citrus yield monitoring system which automatically counts the number of tubs dumped in the goat truck. This system was implemented successfully with 100% accuracy. The microcontroller system was interfaced with the DGPS to record the position of each tub when dumped into the goat truck with an accuracy of 98% of the time. Field evaluations showed that this system was accurate 89% of the time. Zaman et al. (2006) developed a system for estimating yield of citrus trees using the ultrasonically-sensed tree canopy size. An ultrasonic sensor was used to measure the volume of tree canopy. The tree location was mapped with the weight of fruit tubs as they were picked by goat truck. The canopy volume and yield data showed a strong correlation ($R^2 = 0.80$). The regression model was used to estimate the yield based on the canopy volume for a new set of trees. The estimated and true values of fruit yield showed a correlation with $R^2 = 0.42$. It was hypothesized that poor flowering or fruit set, fruit drop, and disease might be some of the factors that reduce the yield, but they not necessarily affect the canopy volume, which could have contributed to the low validation accuracy. Ye et al. (2008) used aerial hyperspectral imagery to estimate the yield of individual citrus trees. From the images, the canopy features of individual trees were identified using pixel based spectral reflectance values at various wavelengths. The features were used to develop the yield prediction models. Authors used the two-band vegetation index (TBVI) and multiple linear regression analysis to relate the spectral characteristics of the

pixels of a tree canopy in the image to the yield of the tree. Analysis showed that the yield was highly correlated with the hyperspectral image from the period of fastest vegetation growth. They concluded that due to the alternate bearing of citrus trees, the size of tree canopy alone cannot be used to estimate the yield and canopy size should be used along with TBVI to predict the yield at individual tree levels. Hall and Louis (2009) reported the relationship between the grapevine canopy size and vegetation density and grape yield. They found statistically significant relationships between the canopy density and grape yield in the same year. Also, they conclude that the canopy density at flowering stage in one year was correlated with the yield in the next year. This study suggested that canopy area and density information from the previous years can be useful in predicting next year grape yield.

CHAPTER 3 MATERIALS

The basic components for all the experiments were the same, differing only in their setup and how they were used. Experiments were carried on different type of conveyor systems. Two kinds of sensors were tested to evaluate their performance in measuring the volume of citrus fruits on the conveyor. After evaluating their performance, one type of sensor was selected for further experiments. Different conveyor systems, sensor (s) and communications are explained in detail in this chapter.

Conveyor Systems

Continuous Canopy Shake and Catch (CCSC) Harvester

Continuous shake and catch systems currently used in Florida citrus are manufactured by Korvan Industries, Inc. of Lynden, Washington, and OXBO International Corp. of Clear Lake, Wisconsin (Ref. <http://edis.ifas.ufl.edu/hs239>). The mechanical harvester (Figure 3-1) consists of whirls stacked horizontally and has an array of approximately 6-foot long, 1.5 to 2 inch diameter tines mounted to the whirls which are connected to a central drum. These tines go about 5 feet inside the tree canopy and shake it horizontally to remove the fruit. The machines have the fruit catching frame on the ground below the canopy, which catches and separates the fruit from leaves and stems, reducing the amount of trash delivered to the processing plant. These fruits are then carried and forwarded through the conveyor system to the containers or directly to a goat-type truck.

The location where the conveyor system installed on the CCSC is shown in the Figure 3-1(a). This conveyor system as shown in the Figure 3-1(b) was used in laboratory for the experiments. The conveyor system was driven by a small hydraulic motor that operates the conveyor belt. The conveyor system has the area above the surface where the laser sensors can

be installed. Different types of sensor(s) were installed on the conveyor system to measure the volume of fruits on the conveyor system. The volumetric yield measurement system was installed above the fruit carrying conveyor at 30-50 cm distance as shown in 3-1(b) system.

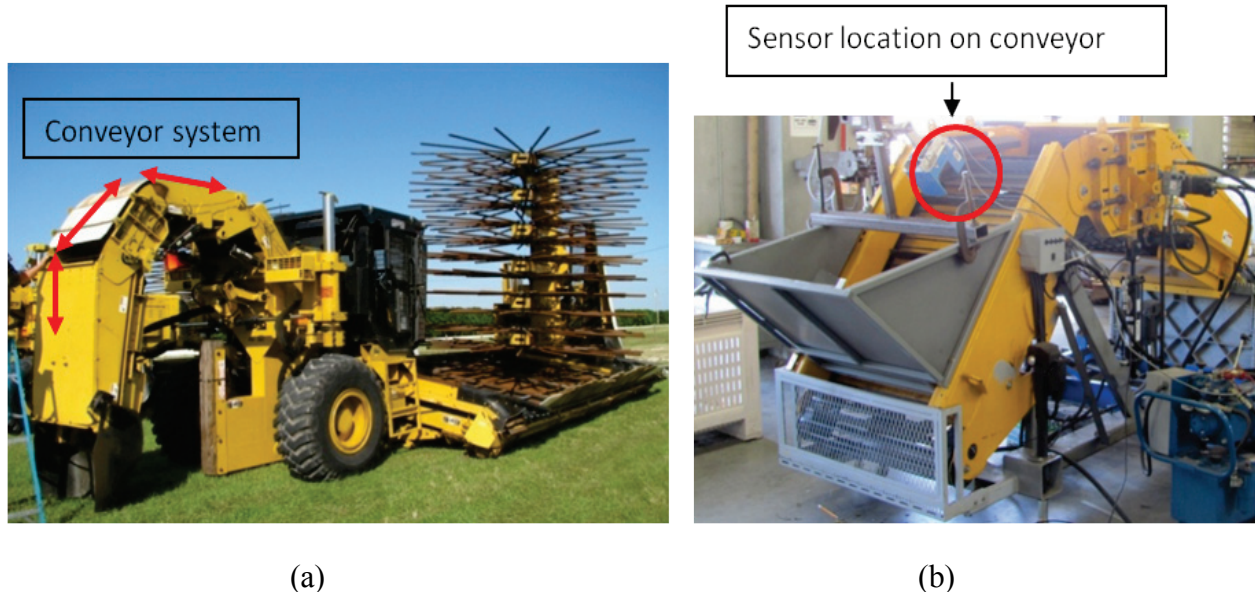


Figure 3-1. (a) Continuous Canopy Shake and Catch (CCSC) and (b) Conveyor portion of the CCSC in laboratory

Trash removal Machine

A trash removal machine as shown in the Figure 3-2 was developed by Dr. Ehsani and his team at the Precision Agriculture Laboratory, Citrus Research and Education Center, Lake Alfred, Florida. The trash removal machine was built specifically for the application of trash removal from the harvested citrus fruits and also used for mounting the yield monitoring system. The volume measurement system was installed, calibrated and also tested on the trash removal machine.

Sensor and Communication

Two types of sensors were tested to see the performance of the system with different speeds of the conveyor. The first type of sensor was an optical laser sensor, Sharp GP2Y0A02, and the other type was LIDAR based LMS SICK 200 laser scanner. Both these sensors were

used and tested in the laboratory conditions. An algorithm was developed to analyze the data collected from these sensor and then determine the fruit volume on the conveyor system. Several laboratory tests were performed and the data were analyzed to evaluate the performance of each sensor. The sensor properties and parameters are discussed as follows.

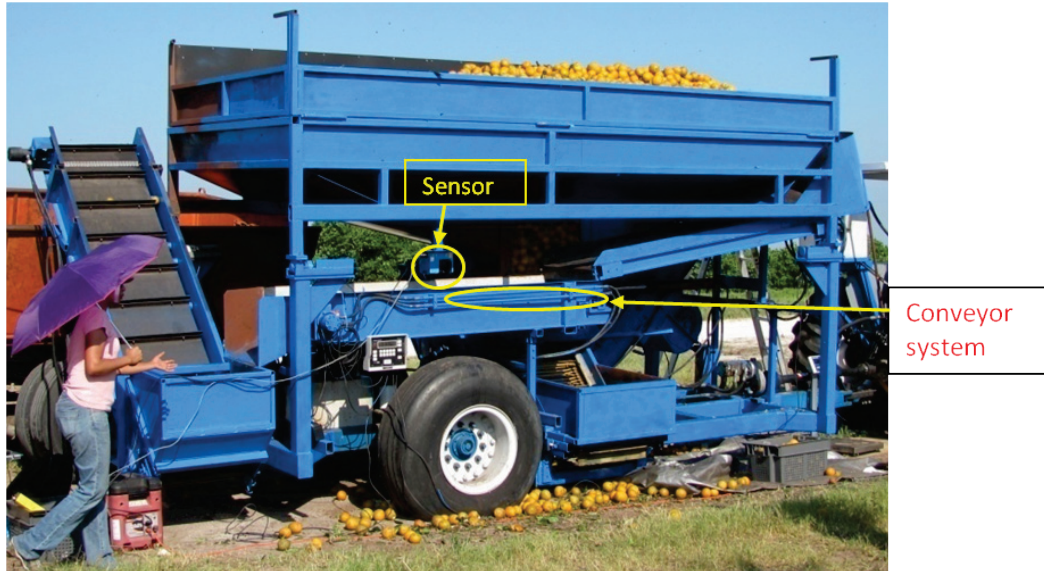


Figure 3-2. Trash removal machine

Infrared (IR) Laser Sensor

In the laboratory test an array of 16 IR laser (Figure 3-3) sensors, was installed on the aluminum plate. The Sharp GP2Y0A02 developed by Sharp Electronic Components has detection range of 20 cm to 150 cm. All these sensors were connected to the PIC controller and then the output from the PIC controller was connected to the laptop. The analog to digital conversion (ADC) was done using a microprocessor chip with 10-bit, 16 channel analog-to-digital converter. The operating supply voltage required for this sensor is 4.5 to 5.5 V.



Figure 3-3. An IR laser sensor with connectors (Source: Sharp Electronic)

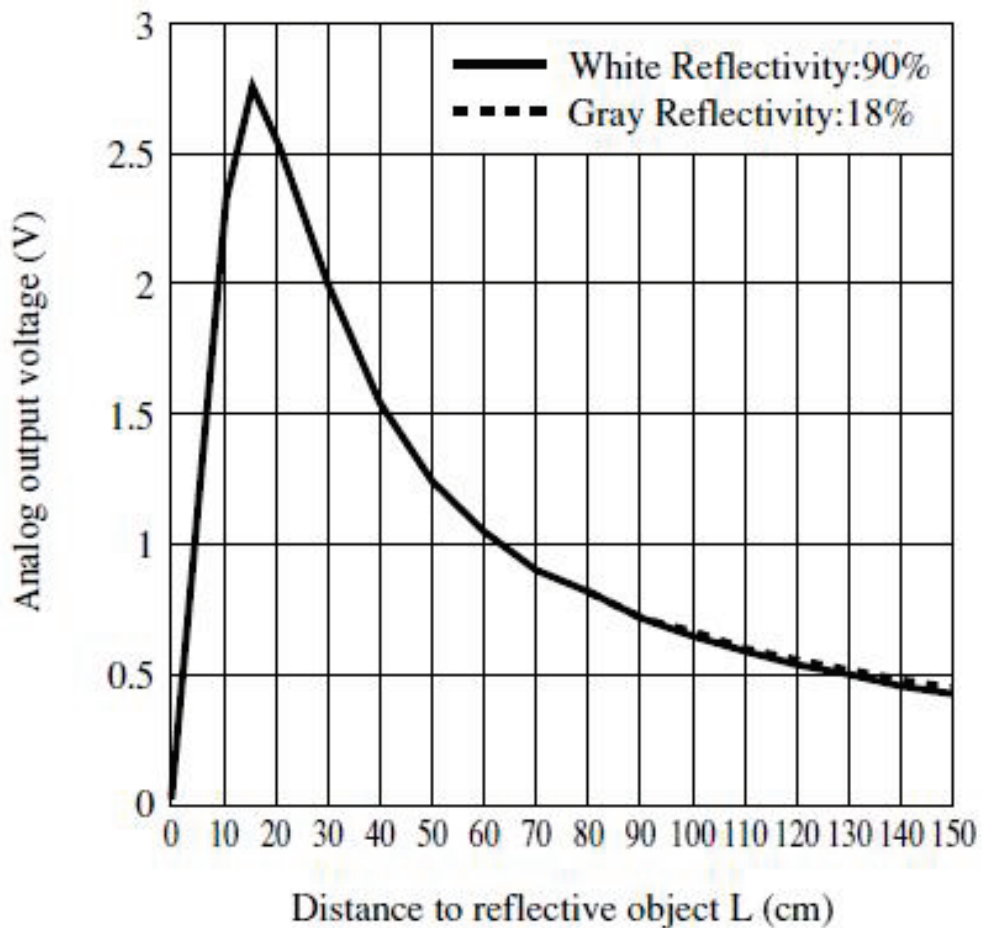


Figure 3-4. Analog output voltage vs. distance to reflective object (Source: Sharp Electronic)

The above Figure 3-4 shows a typical output from these IR sensor detectors. As it shows in the graph, the output of these detectors within the stated range (10 cm - 80 cm) is not linear but

rather it is logarithmic. As per the specification given in the sensor manual, the calibration curve varies slightly from detector to detector and the sensors need to be calibrated before use.

LIDAR

The SICK LMS 200 laser scanner as shown in Figure 3-5 uses the LIDAR (Light Detection and Ranging) technology and was used for volumetric yield measurement of citrus fruits.



Figure 3-5. SICK LMS 200 Sensor

The scanner used in this experimental work was a general-purpose LMS-200 model (SICK, Düsseldorf, Germany). The sensor will be called LIDAR hereafter. The LIDAR sensor scans the space in polar co-ordinate system and in two-dimension and sends the distance-related data in real time for further evaluation via a serial interface. The LIDAR sensor can aim its laser beam in a wide range as its head rotates horizontally and a mirror flips vertically. The laser beam

is used to measure the distance to the first object on its path. The LIDAR system operates on the principle of measuring the time of flight of laser light pulses. A pulsed laser beam is emitted and reflected if it sees an object and the receiver's scanner receives the reflection from the object.

The time between transmission and reception of the impulse is directly proportional to the distance between the scanner and the object (time of flight). The pulsed laser beam is deflected by an internal rotating mirror so that a fan-shaped scan as shown in Figure 3-6 is made of the surrounding area (laser radar). The shape of the target object is determined from the sequence of impulses received (LMS 200 Manual).

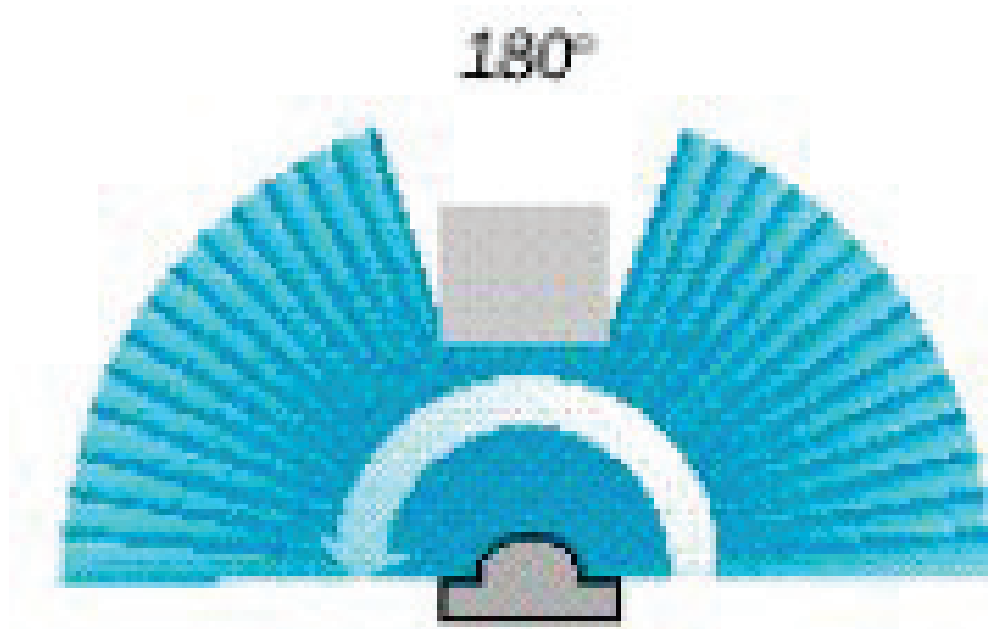


Figure 3-6. Fan shaped scan by an internal rotating mirror of SICK 200(Ref SICK Manuel)

Fundamentally, the distance per individual impulse is evaluated. This means that a distance is provided every 0.25° , 0.5° or 1° , depending on the angular resolution of the scanner (Table 3-1). Angular resolution is set using a software telegram. The LMS 200 model has accuracy of $\pm 150\text{mm}$ and 50mm standard deviation in a range up to 8m . In this study, an angular resolution of 0.5° or 1° and a scanning angle of 180° were used.

Table 3-1. Angular resolution and maximum scanning angle

Angular resolution (°)	0.25	0.25	0.5	0.5	1	1
Max. scanning angle (°) (Symmetrical from the center)	100	180	100	180	100	180
Max. no. of measured values	401	721	201	361	101	181
Frequency Achieved (Hz)	13-18	13-18	26-36	26-36	68-75	68-75

The LMS-200 has a standard RS-422 serial port for data acquisition. Labview 8.6 (National Instruments Corporation, Austin, TX, USA) and MATLAB®7.8 software (The Mathworks Inc., Natick, MA, USA) were used for data acquisition and data processing, respectively.

A program in Labview software available online were used to interface the SICK sensor through RS-422 port and store the data on the disk in the form of .dat file. An algorithm was implemented in Matlab software to post-process the data and for calculating the volume of the fruits carried onto the conveyor during the experiment. A 24 V DC input power supply was given to the sensor.

Labview Software

The Labview program as shown in Figure 3-7, developed for the SICK sensor data collection was used to set the parameters and to set the output file to store the data. The program interface has settings for the port to read the data from, LMS resolution, baud rate, maximum distance and the file path to store the data from the SICK sensor. The frequency of the SICK sensor depends on the LMS resolution. The data collection frequency increases as the resolution over the angle increases as shown in Table 3-1 such as for 0.25° , 0.5° , 1° degree interval over

angle 180°, 100°, the frequency will be 18, 36, and 75 Hz respectively. An average size of an orange fruit is about 8 cm; therefore, to calculate the volume of a fruit, minimum of 3 data points are required along the conveyor. With the setting 180°/1° (180° scanning angle and 1° resolution), the sensor gives 75 Hz frequency and to get the at least 3 data points on the fruit the conveyor speed can be increased up to 1.9 meters per second.

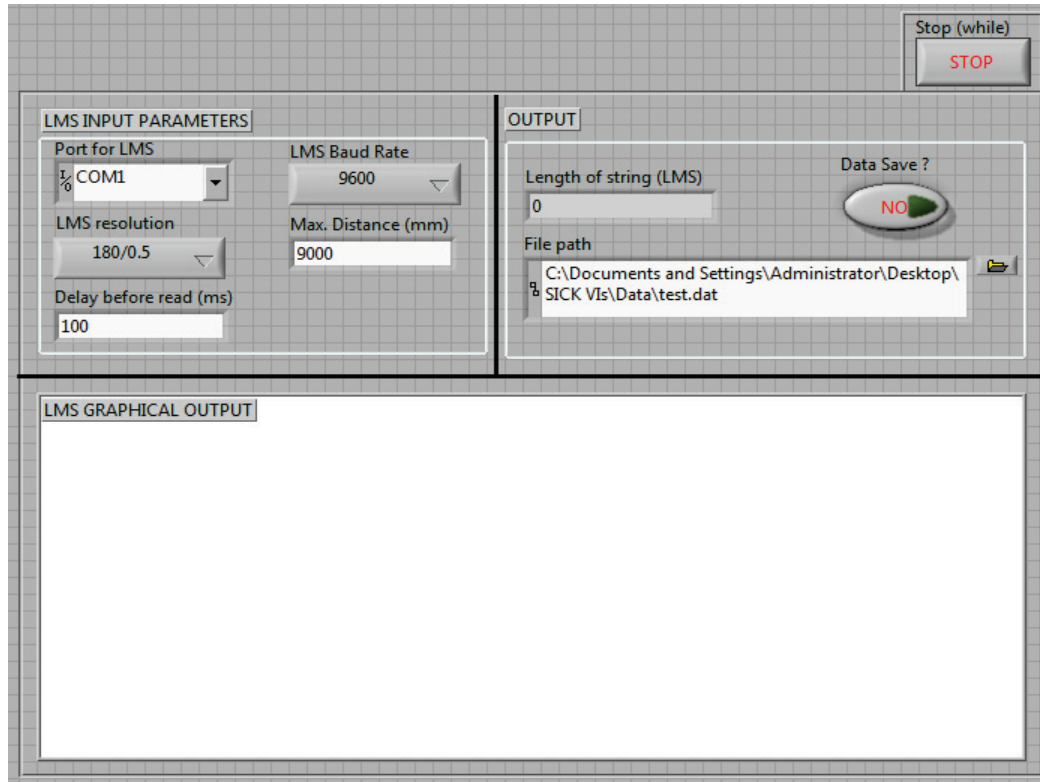


Figure 3-7. Labview program interfaces and set parameters for SICK sensor

CHAPTER 4

VOLUMETRIC YIELD MEASUREMENT

Continuous canopy shake and catch type harvesters used to harvest the citrus tree and removes the fruit, which are conveyed by the conveyor system to the fruit collecting containers or goat trucks. A load cell based yield monitoring system for citrus mechanical harvester was developed by (Maja and Ehsani 2009) that uses the impact of the fruits on the plate and correlate the yield to its mass. The system performed well in both laboratory and field tests but due to the impact created by the citrus fruit falling on the plate, the durability of the system is low. In the field the mechanical harvesters work continuously to harvest the fruits, and because of the continuous impact of these fruit, and the trash in the harvested fruit, the system failed. A non-contact method of measuring the yield of citrus fruits was very much desirable to either augment the performance of the current system or eventually replace it.

This chapter describes testing and analysis of different sensors on the conveyor system and to evaluate their performance with respect to the volumetric yield measurement of the fruits on the conveyor, in the laboratory. This chapter provides the background about the hardware system, the experimental setup used on different conveyor systems, and development of the volume measurement algorithm and its performance with respect to the amount of fruits on the conveyor. The conveyor systems on which the volumetric yield measurement system was tested had difference in their orientation and height of flaps present on them. The first section describes the performance of the IR sensors with respect to the yield calculation. This section begins with an algorithm used for volumetric yield calculation of fruits using the IR sensors then gives an overview of an experiment, calibration of the sensors and summarizes the performance of the system with results and conclusion. In the second section, the chapter discusses about the experiments performed using the LIDAR technology using the SICK LMS 200 sensor. This

section begins with an algorithm developed for volumetric yield calculation using LIDAR. The performance of this system was tested on two conveyor systems; one on the mechanical harvester conveyor system and other on the trash removal machine.

Yield Monitoring Using Linear Array of IR Distance Sensors

The objective of this experiment was to assess the performance of the infrared IR sensors on the conveyor system in the laboratory conditions. This section details the yield calculation algorithm implementation, overview of experimental setup, materials used during the experiment and the yield measurement results and discussion.

Volumetric Yield Calculation Algorithm

The volumetric yield calculation algorithm uses discrete point data captured using linear array of optical sensors mounted on the top of the conveyor. The number of sensors and the spacing between them ensures some minimum number of data points per fruit. By using the discrete data points, amount of citrus fruit volume passing on the conveyor system can be calculated. Since array of sensors would give only two dimensional cross sectional data (along conveyor width), information in third direction (along conveyor length) is achieved by acquiring data from sensors at some sampling frequency.

The linear array of optical IR sensors was mounted on the aluminum plate as shown in Figure 4-1. The co-ordinate system is chosen such that the X-axis is along the conveyor with positive X direction being against the movement of the conveyor. Y-axis is across the conveyor width and the Z-axis is perpendicular to the conveyor surface with positive Z pointing upwards (Figure 4-2). Each sensor was installed at a distance of 4.5 cm apart from each other. Distance from the left side and the right side conveyor wall to the respective nearest sensor was 3.5 cm. The distance between two consecutive sensors represents ‘dy’ value as shown in Figure 4-2. The distance from the sensor to the conveyor surface was 40 cm. In operation, each of the infrared

distance sensor measures distance from itself to the fruit surface or conveyor, whichever is closer or appears first. This distance was subtracted from the total distance (40 cm) between the sensor and the conveyor surface to achieve ‘z’ values as shown in the Figure 4-2. By correlating conveyor travel speed with the sensor scanning frequency we can achieve data along the conveyor length and the distance between two consecutive data points that is referred to as ‘dx’.

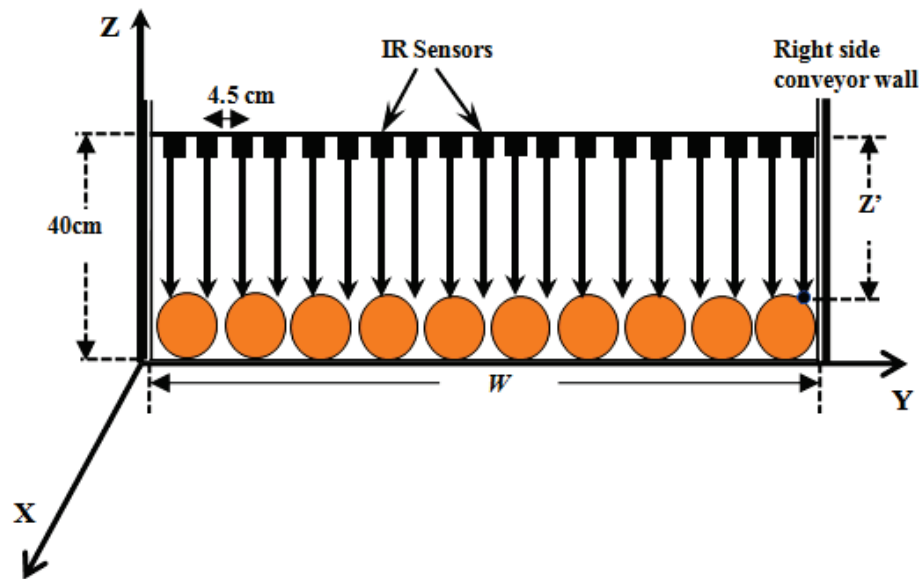


Figure 4-1. Schematic of IR sensors setup on the conveyor belt

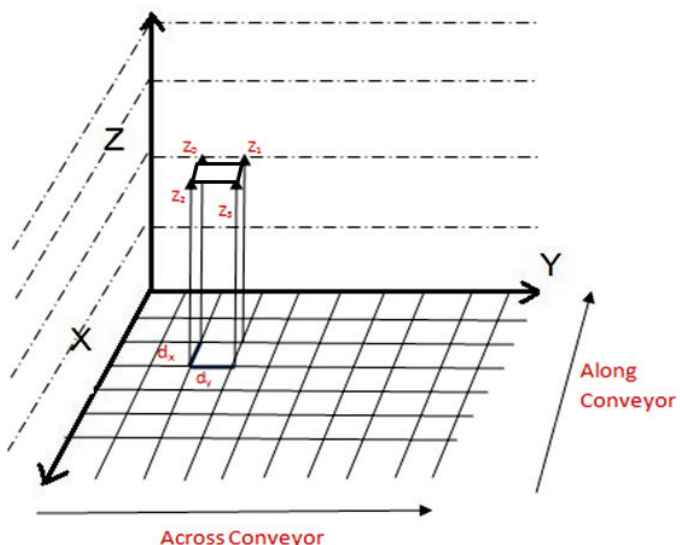


Figure 4-2. 3D view of volume calculation model

As discussed in Chapter 3, the Sharp GP2Y0A02 IR sensor gives analog voltage output corresponding to the measured distance, so all the 16 sensors were calibrated before the actual experiment. The calibration equations thus achieved were used to convert the analog voltage data into distance in cm.

The unit cell volume is calculated as the volume of a parallelepiped having base of ($dy \times dx$) with a height of Z_{avg} as shown in Figure 4-2. The measured height values (z values) were averaged (Equation 4-4) and used to calculate the unit cell volume (Equation 4-2). Summation of all such unit cell volumes along the conveyor width and the conveyor length gives the total volume of all the fruits/objects on the conveyor.

$$\text{TotalVolume} = \text{SumAll}(\text{UnitCellVolume}) \quad (4-1)$$

$$\text{UnitCell Volume} = dx * dy * Z_{avg} \quad (4-2)$$

$$dx = dt * \text{ConveyorSpeed} \quad (4-3)$$

$$Z_{avg} = \frac{Z_0 + Z_1 + Z_2 + Z_3}{4} \quad (4-4)$$

where,

$$dt = 1/f, \quad f = \text{Sensor scanning frequency in Hz},$$

Z_0, Z_1, Z_2, Z_3 as shown in Figure 4-2 are the distance values from sensor to the object on the conveyor

Overview of the Experiment

A series of laboratory tests were conducted with different speeds and setup. A small conveyor system as shown in Figure 3-1 (b) similar to the actual fruit conveyor belt of an Oxbo self-propelled, canopy shake and catch harvester, model 3220 was used to simulate the citrus flow during the harvesting. An array of sixteen sensors were installed on an aluminum plate each

sensor apart at the distance 4.5 cm on the conveyor belt. The aluminum plate mounted away from the surface of conveyor was as shown in Figure 4-3.



Figure 4-3. An array of sixteen sensors mounted on conveyor belt

The output terminal of all the sensors was connected to the ADC and then the data were transferred using the RS-232 output port to .dat file. The output voltage data from each sensor were combined together and a continuous string was sent and stored in a file on the laptop. The conveyor system in the laboratory has different flow controls from 1 to 10 and with different speeds increasing from 1 to 10. The system was tested with four speeds of 0.35, 0.53, 0.72, 0.86 m/s. The conveyor speed was measured and adjusted using the CDT-2000HD digital tachometer (ELECTROMATIC Equipment Co., Inc). The digital tachometer was set to measure the revolutions per minute (RPM). The conveyor rotating shaft diameter and the revolutions per minute were used to calculate the speed of the conveyor system. The tachometer was inserted

into the conveyor shaft for four speeds and the RPM was recorded. When the system was ready, the conveyor system was operated, and the computer program was used to start data collection and store the data continuously in a file on the laptop. For each run, different volume of fruit was put on the conveyor and their respective volume was recorded into an Excel file. Once the fruits passed the sensor plate on the conveyor, the computer program was stopped and the file was stored. This procedure was repeated for different set of fruits. An algorithm was developed in Matlab software to post-process the data stored into a file and calculate the volume on the conveyor. This experiment was performed to see the error between the actual volume of fruits passed on the conveyor and the volume calculated by the algorithm. The conveyor system was run by a hydraulic motor (Eaton Corporation, Eden Prairie, MN, USA). A hydraulic unit was used to power the system (Foster Manufacturing Corp., Racine, WI, USA) and allowed a wide range of flow and pressure rates. By changing the set point on the flow rate control valve, it was possible to change the speed of the conveyor system from zero up to 10 (maximum setting of the flow control).

Materials and Methods

The Sharp GP2Y0A02 (Figure 3-3), an optical IR laser was selected for volume calculation of the fruits because of its operating range and the accuracy in detecting an object. As shown in the Figure 4-4, the possible location of the sensors is the area where the fruits carrying conveyor is located in a citrus mechanical harvester. The distance available on top of the conveyor belt is not more than 50 cm and there is no scope to increase this distance, so the sensors whose detection range matches the available range were chosen. The operating range of this sensor was from 20 cm to 150 cm which resulted in a voltage of 0.5 to 2.5.

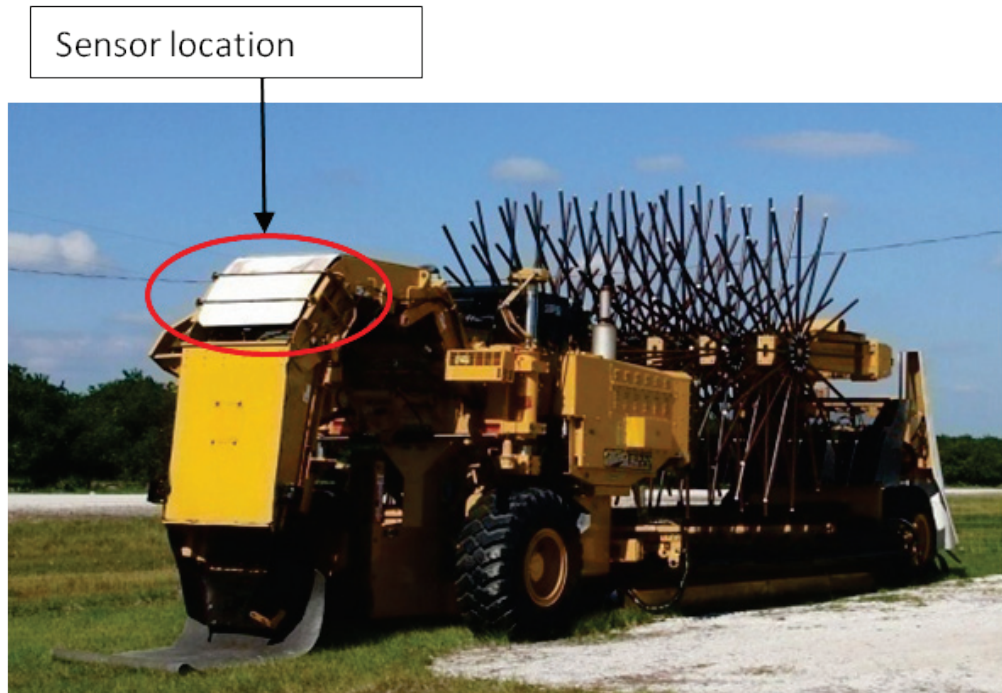


Figure 4-4. Citrus mechanical harvester and the possible sensor location

The Sharp GP2Y0A02 IR sensor uses triangulation method and a small linear CCD (charge coupled device) array to compute the distance from the object in the field of view. A pulse of infra-red light is emitted by the emitter and when this light hits an object, the light reflects off an object and it returns to the detector and creates a triangle between the point of reflection, emitter and the detector as shown in Figure 4-5. In absence of an object in the range, the light is not reflected back and the sensor does not detect any object.

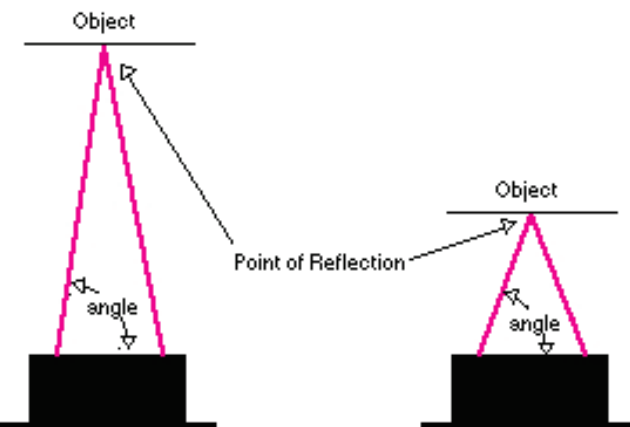


Figure 4-5. Different Angles with Different Distance (Ref.: Acroname Robotics Inc. manual)

As the distance to the object varies, the angle in the triangle changes. The receiver portion of the sensor transmits the reflected light onto various portions of the linear CCD array based on the angle. The CCD array determines what angle the reflected light came back at and therefore, it can calculate the distance to the object and gives the voltage related to the distance. This sensor takes a continuous distance reading and returns a corresponding analog.

System Calibration

Sensor calibration was required because of the non-linear relationship between the sensor output and the depth measurement. All the sensors were calibrated using static tests before the laboratory test. An array of sixteen laser sensors was installed on an aluminum plate as shown in the Figure 4-6. The output voltage for each of the sensor was recorded by keeping a flat plane surface of a wooden plank starting from the distance 15 cm to 65 cm at the increment of 1 cm each. For each of the distance, the analog voltage data were recorded into a file for 30 s. For each distance, the analog voltage data were averaged and stored.

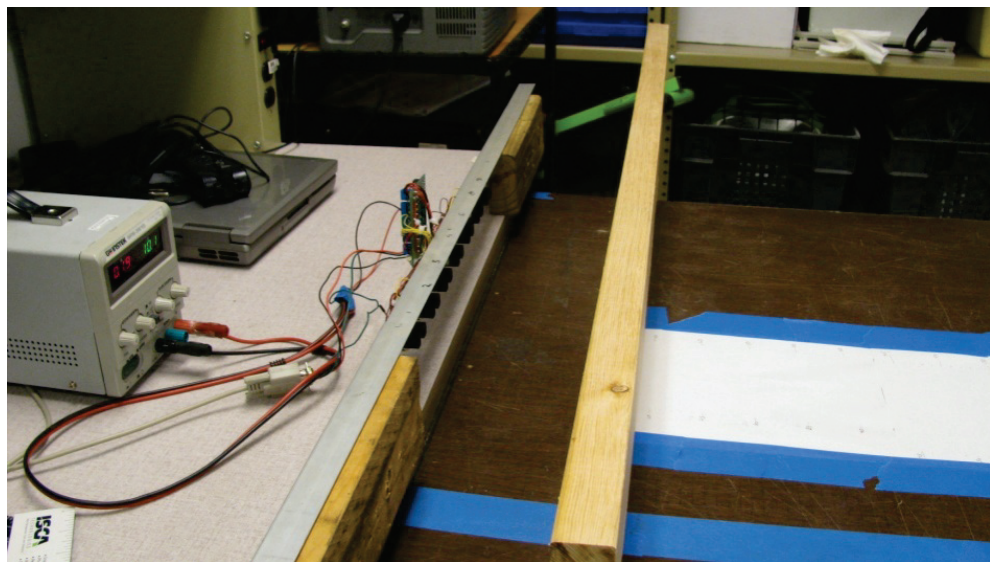


Figure 4-6. Sensor calibration test in the laboratory

When the recorded voltage and the corresponding distance data were plot as shown in Figure 4-7, the calibration curve was non-linear as expected behavior of the sensor. When the R-

square and RMS versus Polynomial order was plot as shown in Figure 4-8, a 3rd degree polynomial fit observed to be the best fit for the data. For each of the sensor a 3rd degree polynomial calibration equation was generated and was used in the volume calculation algorithm.

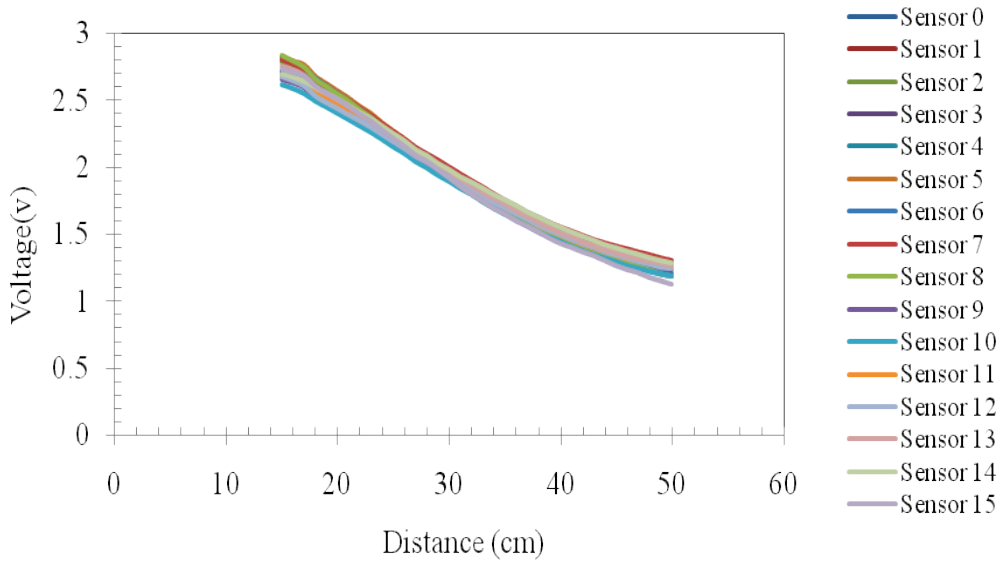


Figure 4-7. Sensor output (v) vs. Length (cm)

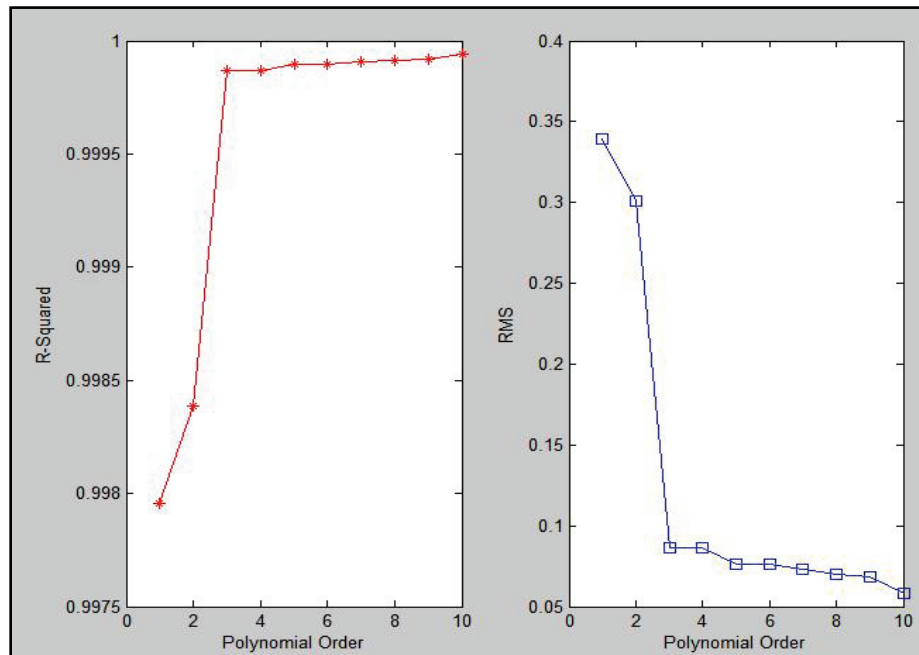


Figure 4-8. R-square and RMS vs. Polynomial order

Laboratory Test

In the laboratory test, a number of citrus fruits were grouped into a set so that each set was of different volume than the other set. Volume of each set was calculated by measuring the diameter of each fruit and summing up the volumes of each fruit into a set. The conveyor system was operated with speeds of 0.35, 0.53, 0.72, 0.86 m/s and for each speed the fruit set was put on the conveyor and the data were collected. Each test was repeated 4-8 times to check the repeatability of the volume for each set. Then the data were processed using the volume calculation algorithm and the fruit volume on the conveyor was calculated for each run. Table 4-1 shows the true volume and the computed volume of the fruits. The mean computed volume is generated by averaging the computed volume of repeated runs.

Table 4-1. Laboratory test results on true volume and computed volume

True Volume $\times 10^3(\text{cm}^3)$	Compute Volume $\times 10^3(\text{cm}^3)$	%Error
3.22	3.71	15.17
3.22	4.35	35.26
3.22	3.47	7.72
3.22	5.94	84.67
5.78	6.33	9.42
5.78	5.75	-0.45
5.78	7.55	30.59
5.78	5.81	0.60
5.78	5.61	-3.01
2.26	2.07	-8.52
2.26	2.27	0.32
2.21	1.91	13.76
2.21	1.40	36.88
4.48	3.83	14.53
4.48	3.60	19.68
4.48	3.99	10.85
4.48	5.75	28.57
270.00	6.22	97.73
270.00	55.00	79.95
270.00	4.96	98.19

Results and Discussions

The laboratory tests show that for speeds 0.35, 0.53, 0.72, 0.85 m/s the percentage error is not consistent. To confirm the results, the system was recalibrated and percentage error between the true volume and the actual volume was found to be less as 1 percentage to high as more than 100%. The reason for such variation in the volume error can be the data collection frequency and the synchronization between the sensors. All the sensors are not synchronized with each other so the data collection from each sensor varies and because of this the error in the calculated volume varies. The result shows that as the speed increases the error has increased and authors reached to the conclusion that these sensors would not work for conveyor speed more than 1.1 m/s. For the conveyor with speed more than 1 m/s, the data collection frequency should be more than 75Hz, so the number of points on a single fruit would be at least 3. The frequency of the sensor is 21 Hz which will reduce the number of data points on a fruit ($110/21 = 5.2$ cm, data at 5.2 cm). These sensors when kept close to each other, interfere and records wrong voltage and the distance between two sensors cannot be reduced which might be the cause of inconsistent error. Also, these sensors do not work in outdoor and different lighting conditions.

Conclusion

The IR sensors used for volume calculation were not suitable for yield monitoring in the mechanical harvesters as they interfere with each other which introduce an error in the distance measured by these sensors. The conventional mechanical harvesters run with the speed higher than 1 m/s, so there was a need of sensors which has frequency more than 75Hz. There was a need to do some research on other sensors which can be used for volume calculation purposes and has data collection frequency more than 75Hz.

Yield Monitoring using LIDAR (SICK Sensor)

LMS SICK 200 sensor was tested on different conveyor belts in the laboratory. The objective of this section is twofold; first to explain the volumetric yield calculation algorithm implemented to post process the sensor data, different types of error sources in calculating the volume and the method of gridding interpolation to reduce the error in volume calculation. The second part details the experiments conducted to calibrate and validate the volume calculation algorithm.

Volumetric Yield Calculation Algorithm

The volumetric yield calculation algorithm uses discrete point data captured using SICK LMS 200 sensor mounted on the top of the conveyor. As discussed in Chapter 3, the sensor scans the space in polar co-ordinate system, in two-dimension and captures the distance related information. After converting the data in Cartesian co-ordinate system, it represents the cross sectional information (along the conveyor width), information along the conveyor length was achieved by acquiring data from sensor at some sampling frequency. Figure 4-9 shows the conveyor system and the chosen three dimensional co-ordinate systems. The X-axis is along the conveyor with positive X direction being against the movement of the conveyor. Y-axis is across the conveyor width and the Z-axis is perpendicular to the conveyor surface with positive Z pointing upwards as shown in the Figure 4-9. The angular resolution setting used for the sensor determines the number of discrete data points along Y- axis and the spacing between them is selected to ensure some minimum number of data points per fruit. By using the discrete data points along X, Y and Z axis, amount of citrus fruit volume passing on the conveyor system can be calculated.

To calculate y' & z' distances, the LMS SICK polar co-ordinate data were converted into the Cartesian co-ordinate system. As shown in Figure 4-9, the sensor scanning direction is from

right to left side of the conveyor wall in 180° angle with the angular resolution of 0.5° or 1° . As discussed in the chapter 3, these parameters were set using the Labview program. The perpendicular distance z' , between the point shown in the Figure 4-9 on the fruit and the point 'P', is equal to $r1 \cdot \sin \Theta'$, where $r1$ is the distance from sensor to the point on the fruit which is given by the sensor and Θ' is the scanning angle or included angle between the starting position (horizontal in our case) and the current scanning location. Also, the distance between the sensor location and the point P (y') is equal to $r1 \cdot \cos \Theta'$.

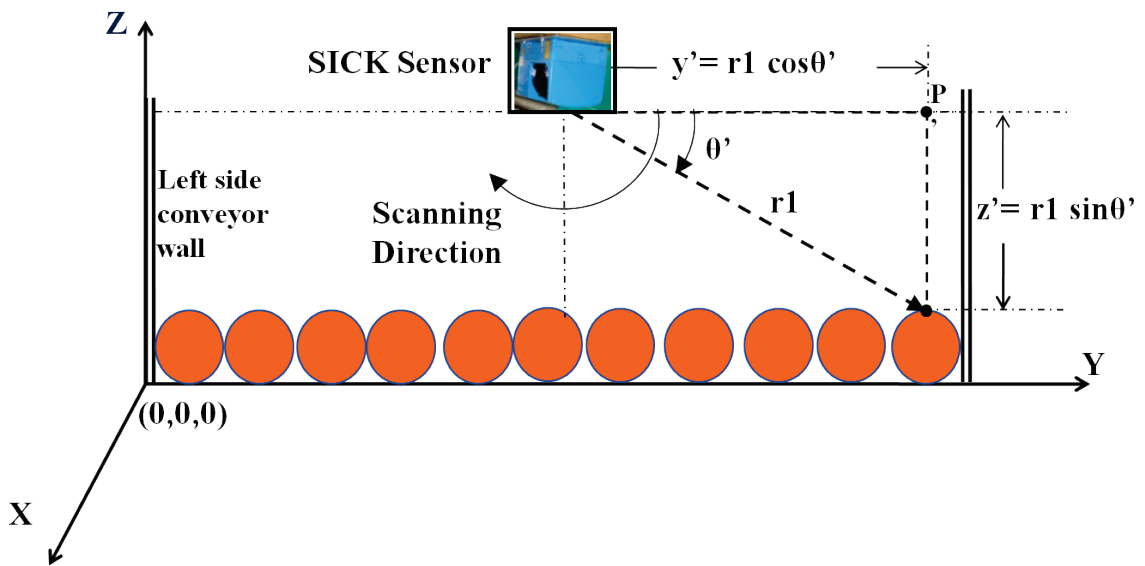


Figure 4-9. Schematic of SICK sensor setup on conveyor

The sensor gives 181 data points along the sensor scanning direction with the scanning angle set to 180° and angular resolution set to 1° . Similarly, we get 361 data points with setting of 180° and 0.5° angular resolution. For each of the data point, the values of z' and y' were calculated. Data outside the conveyor width was not useful and not considered for calculating the volume. If we just consider information equal to conveyor width then due to the nature of the scanning, partial data for the fruits close to the side walls will be obtained. Hence, appropriate side wall height was included in the data analysis. The average size of a fruit was considered to

be 8 cm and hence side wall data equal to 8 cm height was included in the analysis. If we consider the sensor and conveyor setup, we can calculate the useful included angle ‘ α ’ over which data should be analyzed. The distance between the conveyor and the SICK sensor was set to 25 cm so that there would be a minimum distance for the fruits to pass on the conveyor system, hence the height ‘ h ’ was calculated (refer Figure 4-10) to be equal to $25 - 8 = 17$ cm. The angle ‘ α ’ was calculated using the conveyor width ‘ W ’ and height ‘ h ’ to be equal to $2 \cdot \tan^{-1} \left(\frac{W}{2h} \right)$. Volume of the fruits or objects was calculated in the included angle ‘ α ’.

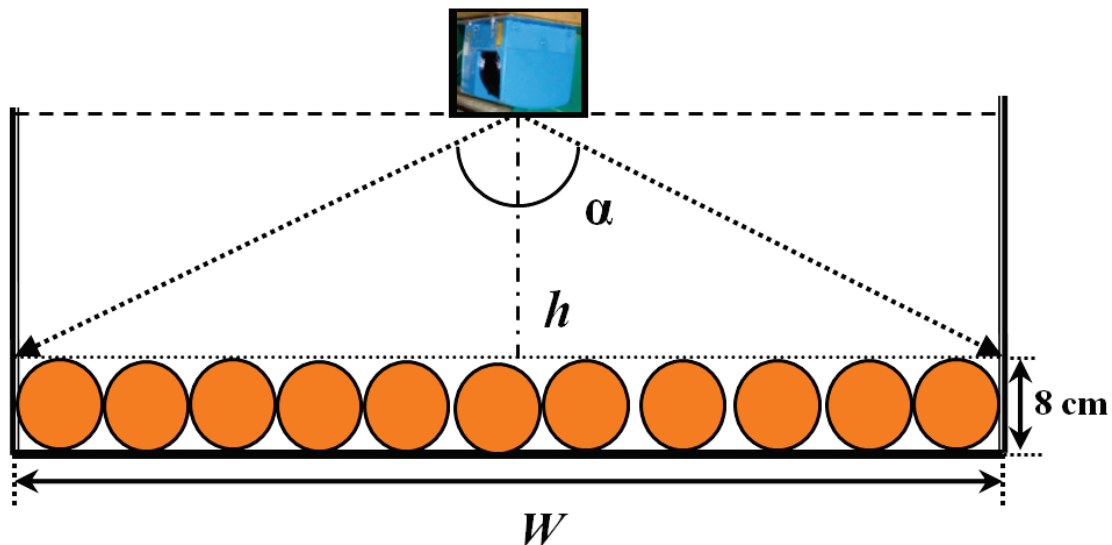


Figure 4-10. Schematic of SICK sensor on conveyor

The distance between two consecutive data points along Y-axis represents ‘ dy ’ as shown in Figure 4-1 was calculated using the distance between two consecutive y' values. The distance z' , was subtracted from the total distance (25 cm) between the sensor and the conveyor surface to achieve ‘ z ’ values as shown in the Figure 4-2. By correlating conveyor travel speed with the sensor scanning frequency, we can achieve data along the conveyor length and the distance between two consecutive data points is referred to as ‘ dx ’. The unit cell volume and the total volume were calculated as explained in section 4.1.

The calculated volume was the volume generated for the different objects on the conveyor. This volume does not contain the volume of fruits alone but some other objects such as the conveyor flaps, conveyor side walls, foreign objects / trash. These error sources and the method to reduce the error associated with them are discussed in the next section.

Error Sources

When the fruits get harvested, along with fruits other foreign objects get carried on the conveyor and then to the fruit carrying containers or goat trucks. Foreign objects include citrus tree leaves, stems and limbs. The volume calculation algorithm can't separate out these objects and the volume calculation adds up the error in the actual volume of the fruits. Also, the conveyor contains flaps and conveyor side wall which add to the error in the volume.

Flaps on Conveyor. The LMS SICK sensor was mounted and tested on two machines. The first one was the trash removal machine and the other was Continuous Shake and Catch type mechanical harvester (CCMH). These two machines have a conveyor system which differs in their orientation and the height of flaps present on them. The trash removal machine has a horizontal conveyor with flap height of approximately 3 cm while the CCMH machine has inclined conveyor system with flap height of approximately 8 cm. Depending upon the height of the flap to fruit height ratio, different methods were used to reduce the error produced by these flaps.

Flap height to fruit height ratio < 0.5. In this method, the experiment was performed on the trash removal machine which has horizontal conveyor system and has flaps with height 3 cm as shown in Figure 4-11. These flaps add an error in the fruit volume calculated by the volume calculation algorithm. If the flap height to fruit height ratio is less than 0.5, which means the flap size is less than half the size of the fruit and the flaps can be easily removed from the data without removing the fruit related data. If the calculated z value is less than 3 cm (which is less

than half of the fruit height) then the corresponding z value is set equal to zero. Since the sensor scans only top surface of the fruits, such an operation is not expected to remove the useful data points lying on the fruit surface. By using this technique, most of the volume error produced by the flaps and the foreign objects which has less than 3 cm size was removed and the error was minimized. The error in volume produced by the foreign objects such as stems, leaves, limbs which lay on the conveyor and have height less than 3 cm can also be removed using this technique.

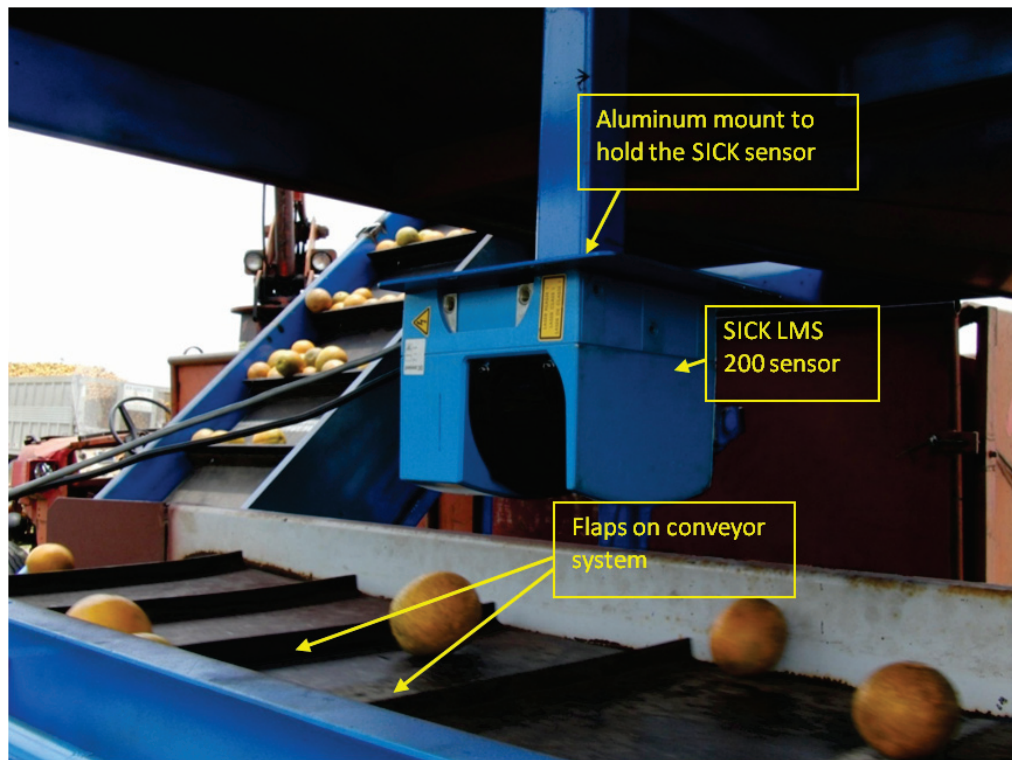


Figure 4-11. Flaps on trash removal machine conveyor system

The flap correction technique was applied and implemented in the algorithm. When the data were plotted as shown in Figure 4-12, the conveyor flaps and the citrus fruits were visible on the conveyor system.

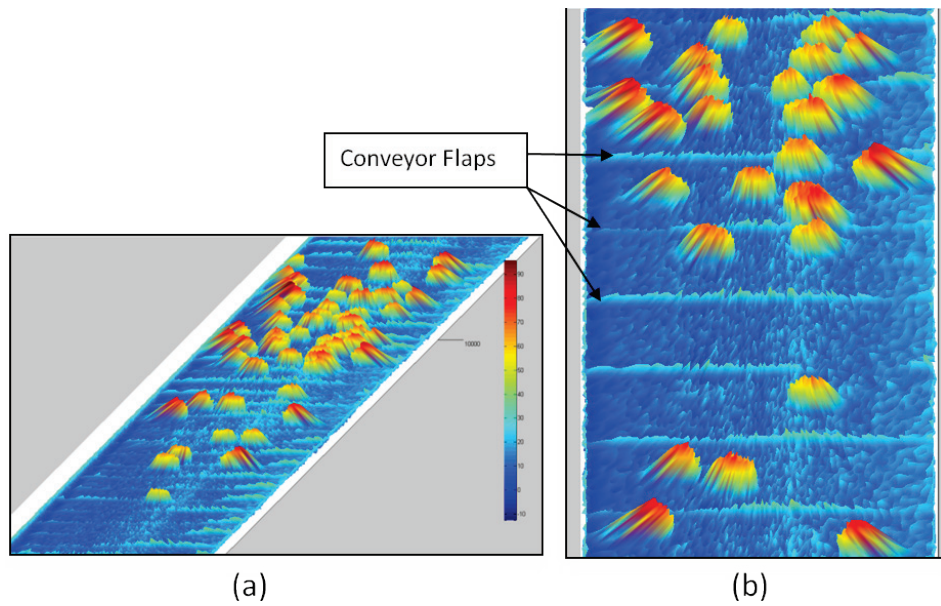


Figure 4-12. (a) and (b) Spatial distribution of the raw data without removal of flaps and interpolating the data by gridding method

After removing the flap error, the spatial distribution of the data as shown in Figure 4-13, shows just the fruits on the conveyor system, though the fruits appear to be distorted in the shape. Gridding interpolation technique was used to remove the distortion in the fruit shape and correct the spatial distribution of the data. This technique is explained in detail in the later part of this chapter.

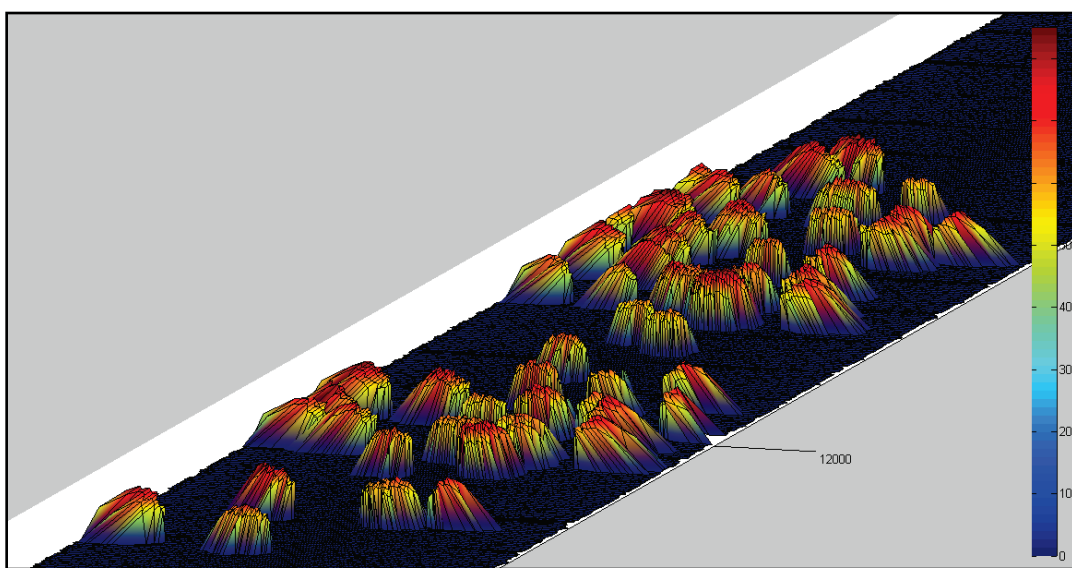


Figure 4-13. After removing the flaps in the data

Flap height to fruit height ratio ≥ 0.5 . As discussed in Chapter 3, Continuous canopy shake CCMH shakes the citrus canopy causing fruit to fall from the tree and onto a catch frame. These fruits then carried by fruit carrying conveyor system of mechanical harvester and dropped to the containers or the goat truck. The conveyor is oriented in such a way that it makes 50° angles with respect to the horizontal. These conveyors have the vertical flaps (height = 7 to 8 cm) as shown in Figure 4-14 which hold the fruits on the conveyor and forward those to the end of the conveyor belt into the container. The flap height to fruit height ratio is ≥ 0.5 with the height of the flaps being equal to the average size of the fruits. Hence the earlier flap correction technique is not applicable as it will remove useful fruit data. A different technique was used to remove the error produced by these flaps and the conveyor side wall. When the algorithm calculates the volume, the data contain the information about the fruits as well as the flaps as shown in Figure 4-15 which needs to be removed when the actual volume is calculated. Therefore, to remove the error added by flaps and side wall of the conveyor, before collecting the data for actual fruits, data were collected by operating the conveyor empty for 30 s for each test speeds. This data were processed and the amount of volume generated by the empty conveyor was referred as an ‘error volume’. The distance between two flaps was measured on the conveyor and from the test time and the speed; length of the conveyor covered in analysis was calculated. Using this information, the total number of flaps present on the conveyor was determined.

The error volume contribution per flap was calculated and then removed from the actual test data. However, the error volume produced by foreign objects (trash, leaves, and branches) cannot be removed using this technique.

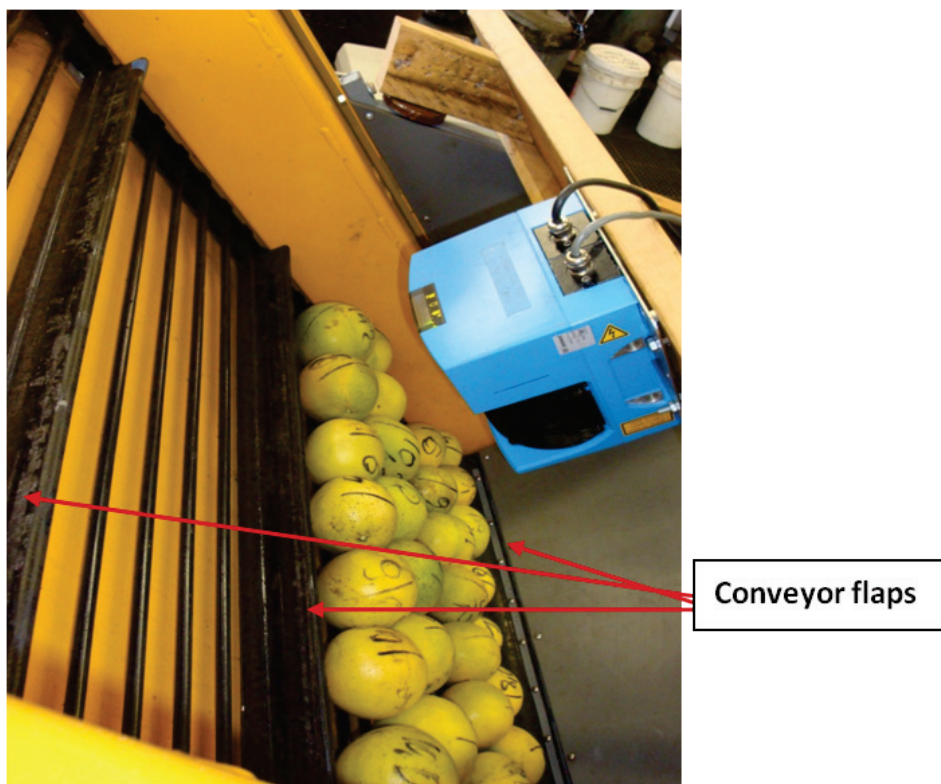


Figure 4-14. Conveyor system with flaps to hold the fruits

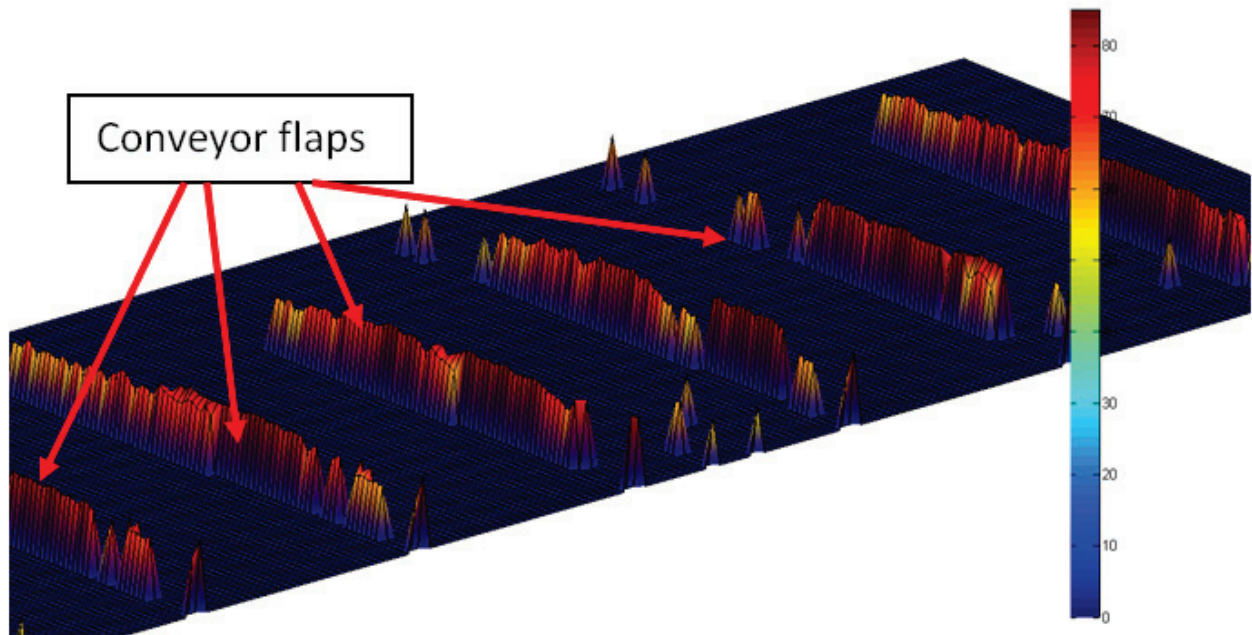


Figure 4-15. Spatial distribution of the data showing flaps alone on the conveyor belt

The sensor data in polar co-ordinate system when converted into Cartesian system; shows distortion in the shape of the fruits as shown in Figure 4-16. When we consider the cross sectional data (Y-Z plane data) attained from the sensor, due to the polar sweeping nature of the scanning, once we encounter the end of the fruit, the co-ordinates of the next point on the conveyor surface lay considerable amount away from the previous data point on the fruit. These results in the spikes being observed directed towards the sensor mounting location. This distortion in fruit shape can add a huge error in volume calculation, so this data needs to be corrected. A method of gridding interpolation was used to correct this data and the error in volume was minimized.

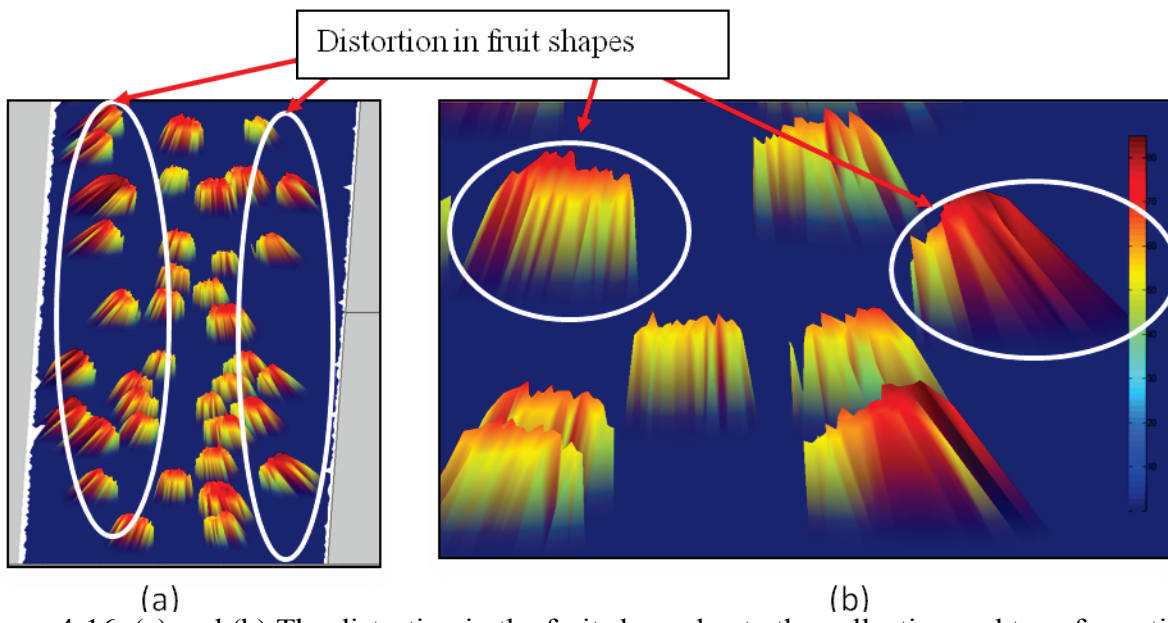


Figure 4-16. (a) and (b) The distortion in the fruit shape due to the collection and transformation of data from polar co-ordinate system to Cartesian co-ordinate system

Method of Gridding Interpolation

The radial spikes observed in the raw data leads to erroneous volume being calculated using the volume calculation method employed in this research. To take care of this, uniformly spaced ‘Y’ vector is created having the same dimension as the original raw data and data gridding interpolation was performed using the Matlab native function ‘griddata’.

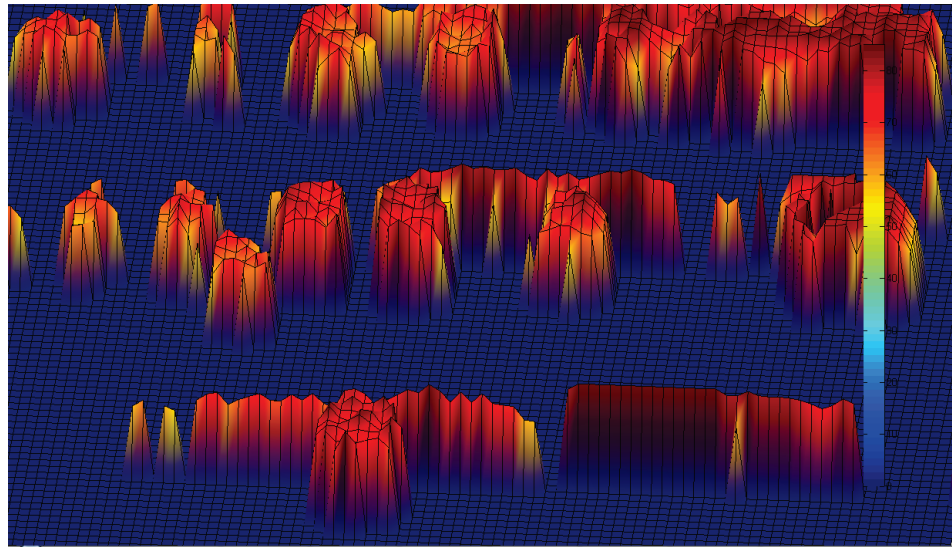


Figure 4-17. Fruits on conveyor belt

In the process ‘griddata’ fits a cubic surface to the original raw data and then interpolates this surface at the points specified by the uniformly spaced X and Y arrays to produce Z at these newly formed data points. The cubic surface is created such that it always passes through the original raw data points.

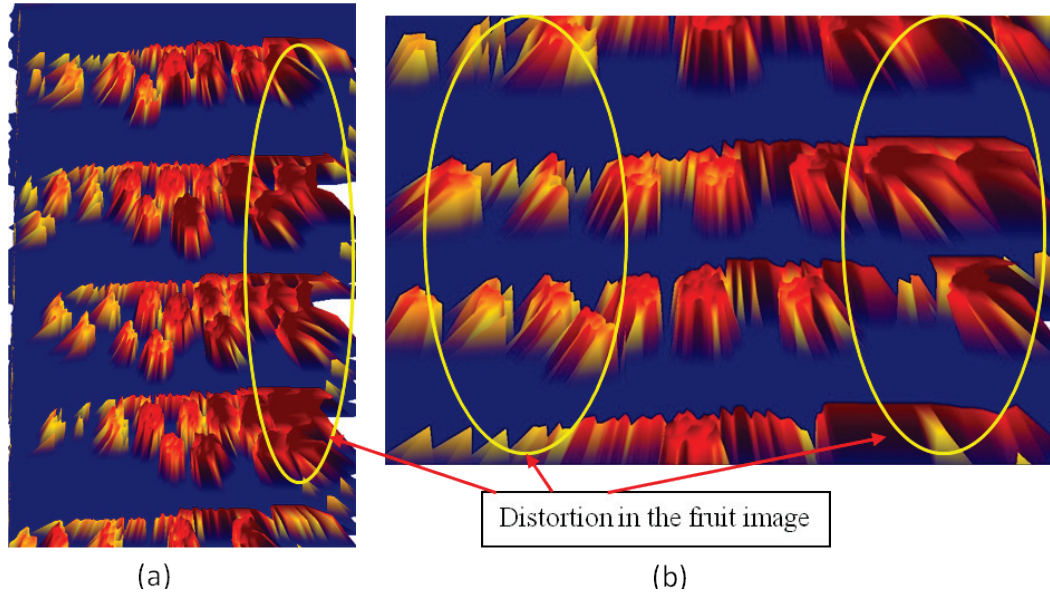


Figure 4-18. (a) and (b) The radial spikes observed in the shape of the fruit before applying gridding interpolation

By using gridding interpolation we get uniformly spaced data points on the conveyor surface and no radial spikes were observed (refer Figures 4-17, 4-18, 4-19 and 4-20). The volume calculated based on the gridding data points was observed to be more accurate than the volume calculated based on the original raw data.

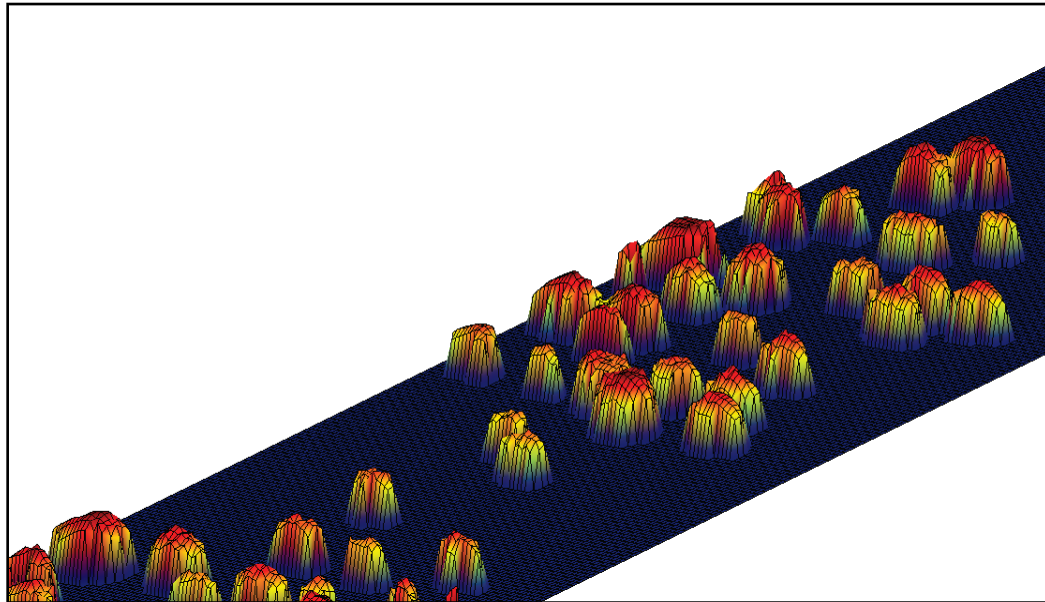


Figure 4-19. After using gridding interpolation, uniformly spaced data points on the conveyor surface without radial spikes

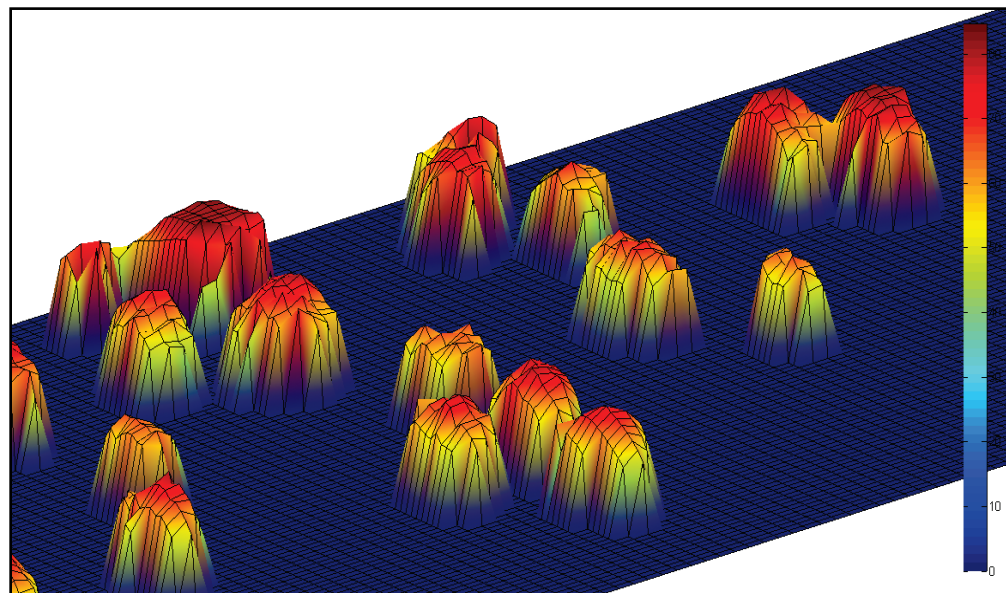


Figure 4-20. After using gridding interpolation, uniformly spaced data points on the conveyor surface without radial spikes

Experiments on Horizontal Conveyor (Trash removal machine, f/h <0.5)

Overview of Experiment

The catch and shake type of mechanical harvester (CCMS) can't be stopped frequently during the field operation. These systems are very expensive; so the growers use them efficiently with maximum utilization for harvesting the citrus fruits in the grove. To avoid interruption and downtime of these mechanical harvesters a system was built called Trash removal machine shown in the Figure 3-2 and discussed in Chapter 3. The performance of the trash removal machine was tested in the real field conditions during the summer of 2010 at Fort Basinger, FL. The top portion of this system as shown in Figure 4-21 was where the fruits from the goat truck were dropped for trash removal and volume measurement purpose using SICK sensor.



Figure 4-21. The goat truck dumping the fruits on the top container of the trash removal machine

The SICK sensor was mounted as shown in Figure 4-22 on the top of the conveyor where the fruits were carried after removal of the stems, leaves and other trash from the trash removal machine.

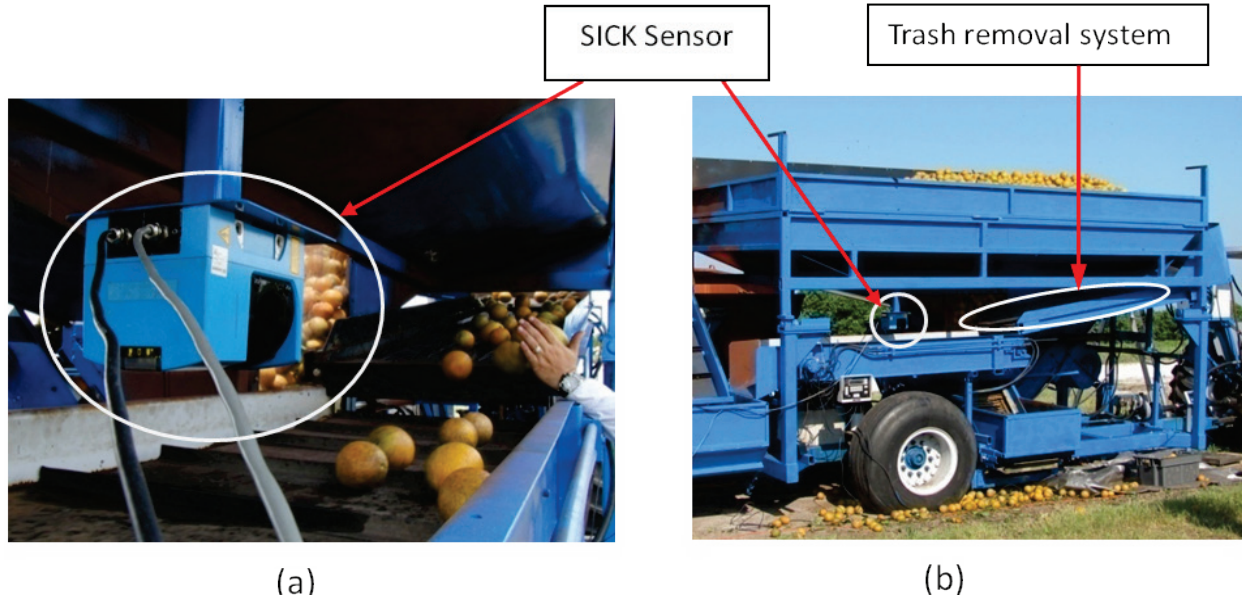


Figure 4-22. SICK LMS 200 location on trash removal machine

Two experiments were performed on the trash removal machine. In the first experiment citrus fruit loads from 4 to 41 kg were used to calibrate the system and then two loads of 11 and 22 kg were used to evaluate the performance of the system using the developed calibration equation. The volumetric yield calculation system performed very well with the percentage error less than 8%. In the second experiment, loads from 4 to 41 kg were used to calibrate the system and then system was validated with five different loads. In both the experiments SICK sensor was set to 180° angle with 1° angular resolutions. The parameters used for the volume calculation algorithm are shown in Table 4-2. These parameters were measured and recorded before the experiment was performed.

Method and Materials

The SICK sensor was mounted on an aluminum plate perpendicular to the conveyor surface as shown in Figure 4-22. The aluminum plate was welded on top and at the center of the conveyor such that the sensor will be at the center of the conveyor belt. The distance from the sensor to the conveyor surface was about 25 cm. The sensor has supplied a power of 24 V and

the output with RS-422 port was connected to a sea level port to the computer. The sea level port converts the RS-422 input to USB port. Different parameters such as the distance from the SICK LMS to the conveyor surface, width of the conveyor, the flap length, average distance between two consecutive flaps, distance from sensor midpoint to left and right side conveyor wall, frequency of the sensor and different speeds were recorded before the experiment as shown in Table 4-2. For this experiment around 90 kg of oranges were collected from the orange field present at the Citrus Research and Education Center, Lake Alfred, FL. These fruits were divided into seven bins with mass from 4 to 41 kg and 11 and 22 kg.

When the volumetric yield calculation system was ready, the conveyor was started using the hydraulic power and adjusted to a particular speed. Data were collected by pouring the fruits from each bin manually on the conveyor system.

Table 4-2. Different parameters used the two experiments for volume calculation algorithm

	Experiment A	Experiment B
Date of experiment	16-Jul-10	22-Jul-10
Sensor Frequency (Hz)	75	75
Conveyor Speeds (m/s)	0.92, 1.03, 1.14	1.7, 1.3, 1.0
Angle / resolution	180°/1°	180°/1°
Conveyor width (cm)	63	63
Distance from sensor to right side conveyor wall	32	32
Distance from sensor to conveyor surface (cm)	25	25
Distance between two flaps (cm)	27	27

Experiment A

Calibration. The system was calibrated by putting the citrus fruits from each bin of different mass. The trash removal machine conveyor was operated for three different speeds of 0.92, 1.03, 1.14 m/s and for each speed a mass from 4 to 41 kg at the increment of 4.5 kg was put onto the conveyor system. For each mass the data were collected three times to check the repeatability

and the volume variation for that particular mass. After performing the tests for calibrating the system, validation data were collected with mass 11 and 22 kg. For each run the data were stored to respective .dat file on the computer and then this data were post processed using the Matlab program developed on the basis of the volume calculation algorithm explained in the earlier part of this section.

Tables 4-3, 4-4 and 4-5 shows the calibration data for speeds 0.92, 1.03 and 1.14 m/s. As discussed, the experiment was repeated three times for each mass, the volume for each mass were calculated and the average volume was used to plot the data.

Table 4-3. Calibration data with speed 0.92 m/s with angle 180° and angular resolution 1°

Mass (kg)	Calculated Volume x 10 ³ (cm ³)	With Grid data Calculated Volume x 10 ³ (cm ³)
4.54	4.85	4.68
9.08	13.55	11.03
13.62	17.46	15.43
18.16	23.22	21.15
21.51	29.04	25.40

When the actual mass versus the calculated volume using grid data as shown in Figure 4-23 (b), 4-24 (b) and 4-25 (b), for respective speeds were plot, linear trend was observed between the mass and calculated volume with $R^2 = 0.99$. Also, if the actual mass versus the volume calculated without using the grid interpolation technique as shown in Figure 4-23 (a), 4-24 (a) and 4-25 (a), were plot it showed a linear trend with $R^2 = 0.98$.

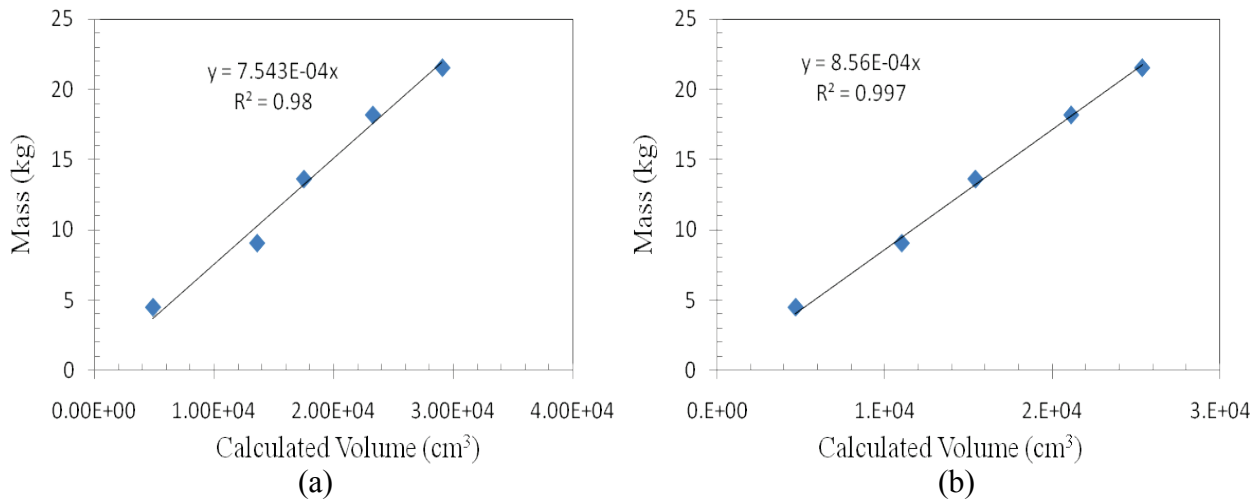


Figure 4-23. (a) Mass vs. Calculated volume calibration curve with speed 0.92 m/s and (b) Mass vs. Calculated volume with grid data interpolation technique, calibration curve with speed 0.92 m/s

Table 4-4. Calibration data with speed 1.03 m/s with angle 180° and angular resolution 1°

Mass (kg)	Calculated Volume x 10 ³ (cm ³)	With Grid data Calculated Volume x 10 ³ (cm ³)
4.54	5.18	4.87
9.08	12.77	10.61
13.62	17.83	15.68
18.16	23.06	20.42
21.51	27.96	25.64

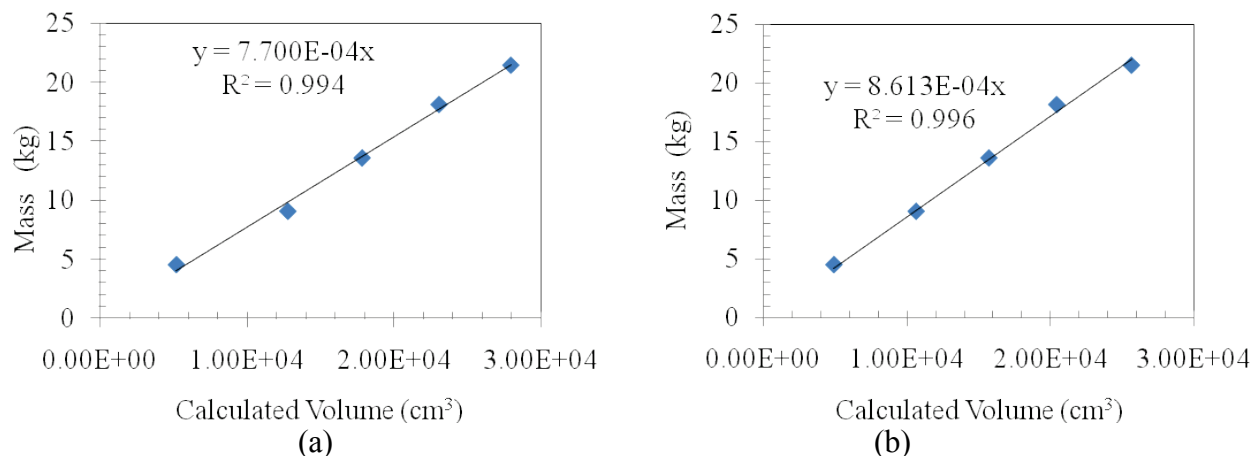


Figure 4-24. (a) Mass vs. Calculated volume with speed 1.03 m/s and (b) Mass vs. Calculated volume with grid data interpolation technique with speed 1.03 m/s

Table 4-5. Calibration data with speed 1.14 m/s with angle 180° and angular resolution 1°

Mass (kg)	Calculated Volume x 10 ³ (cm ³)	With Grid data Calculated Volume x 10 ³ (cm ³)
4.54	5.55	5.02
9.08	12.06	10.65
13.62	17.82	14.94
18.16	26.44	23.94
21.51	30.06	25.87

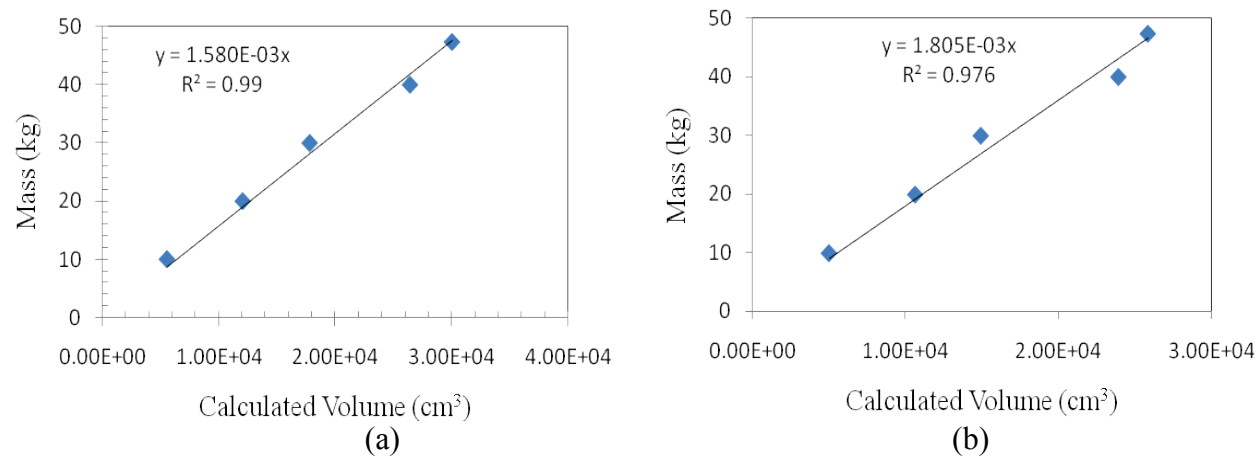


Figure 4-25. (a) Mass vs. Calculated volume with speed 1.14 m/s and (b) Mass vs. Calculated volume with grid data interpolation technique, calibration curves with speed 1.03 m/s

Validation. Two validation tests were performed with mass 11 and 22 kg for each of the 3 speeds. When the calibration equations were used to predict the mass of fruits on the conveyor, the % error shows very promising results with percentage error less than 8%. Table 4-6 shows the calculated volume and percentage error between the actual and calculated mass in kg.

Results and Discussion. When the % Error versus the mass of the fruits on the conveyor was plotted as shown in Figure 4-26 with respect to the speed, it shows that as the mass increased, the error decreased. The calibration data and the validation data were not sufficient to prove the results so more tests are needed to confirm the error with respect to speed and mass of the citrus

fruits on the conveyor system. Also, experiments with high speed need to be repeated to verify the performance of the system with speeds higher than 1.14m/s.

Table 4-6. Validation of the data after applying the calibration equations

Speed (m/s)	Mass (kg)	Calculated Volume $\times 10^3$ (cm 3)	With Grid Data Calculated Volume $\times 10^3$ (cm 3)	With Grid data Calculated Mass (kg)	With grid %Error
0.92	11.35	14.67	12.95	11.09	-2.32
0.92	22.70	27.56	24.26	20.78	-8.47
1.03	22.70	27.69	24.74	21.31	-6.13
1.14	11.35	16.29	13.46	11.03	-2.84
1.14	22.70	28.86	25.87	21.20	-6.60

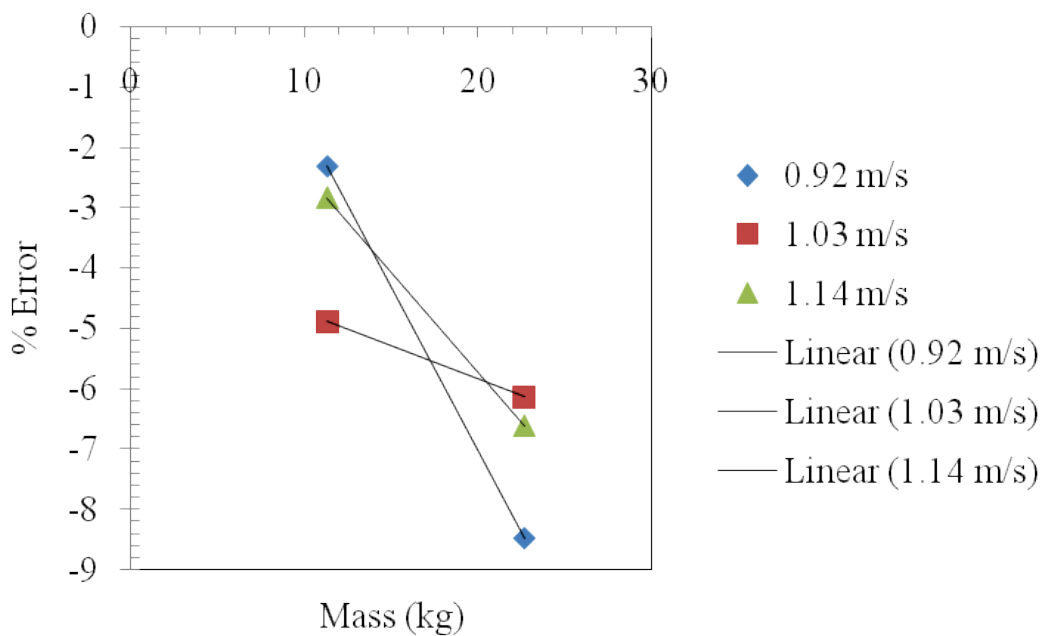


Figure 4-26. % Error vs. Mass plot with different speeds

Experiment B

Calibration. In this experiment the volumetric yield calculation system was recalibrated with mass from 4 to 41 kg at the increment of 4.5 kg. The experiment was repeated three times for

each mass and for 1.7, 1.3, 1.0 m/s conveyor speeds and the system performance was analyzed. The conveyor speed of 1.7, 1.3, 1.0 m/s were chosen to evaluate the system performance when the speed of the conveyor belt increases and reaches its higher speed of 1.7 m/s. Once the calibration data were collected, system was validated using with different mass citrus fruit bins on conveyor. After collecting the calibration data, it was analyzed using the volume calculation algorithm and the amount of fruit volume on the conveyor was determined. As shown in Tables 4-7, 4-8, 4-9 for each mass and speed the volume is calculated with and without applying the gridding interpolation.

When the volume calculated using gridding interpolation technique and the mass were plot for different speeds as shown in Figures 4-27, 4-28, 4-29, it showed the linear trend and coefficient of determination R^2 equal to 0.99. The calibration equations for each speed were used for validating the data.

Validation. The calibration equations derived by plotting the actual mass and the calculated volume for each speed were used to validate the next set of data. Table 4-10, 4-11, 4-12 shows the actual mass and the calculated volume using those calibration equations.

Results and Discussions

The validation data shows that as the speed was increased the root mean squared error was reduced. As shown in Table 4-10, 4-11, 4-12 for speed 1.71 m/s the RMSE error was 0.98 kg. This RMSE error was increased as the speed was decreased. For speeds 1.34 m/s, 1.03 m/s the RMSE error was 0.81 kg and 3.21 kg respectively.

When the percentage error versus the mass of the fruits on the conveyor was plot as shown in Figure 4-30 with respect to the speed, it shows that as the mass increases error decreases, so for the mechanical harvesters with continuous stream of fruits the error might go down. Also, the

plot shows that for speeds higher than 1.71 m/s, the system performed well with an error less than 8 % for mass greater than 20 kg and less than 5% for the speed 1.34 m/s.

Table 4-7. Calibration data with speed 1.7 m/s

Mass (kg)	Calculated Volume x10 ³ (cm ³)	With Grid data Calculated Volume x10 ³ (cm ³)
4.54	5.52	5.18
9.08	12.25	10.93
13.62	19.78	16.74
18.16	25.62	21.94
22.70	33.93	29.35
27.24	37.96	32.45
31.78	45.12	37.61
36.32	51.68	44.53
40.86	58.53	49.77
4.54	6.95	6.07
9.08	13.70	11.55
13.62	20.28	17.59
18.16	27.29	22.85
22.70	33.23	29.37
27.24	39.32	33.83
31.78	45.45	37.18
36.32	52.26	44.38
40.86	57.95	48.84
4.54	7.39	6.22
9.08	13.58	11.65
13.62	20.85	18.36
18.16	28.04	23.93
22.70	33.75	28.93
27.24	38.78	32.74
31.78	42.33	35.85
36.32	55.05	48.96
40.86	60.09	51.60

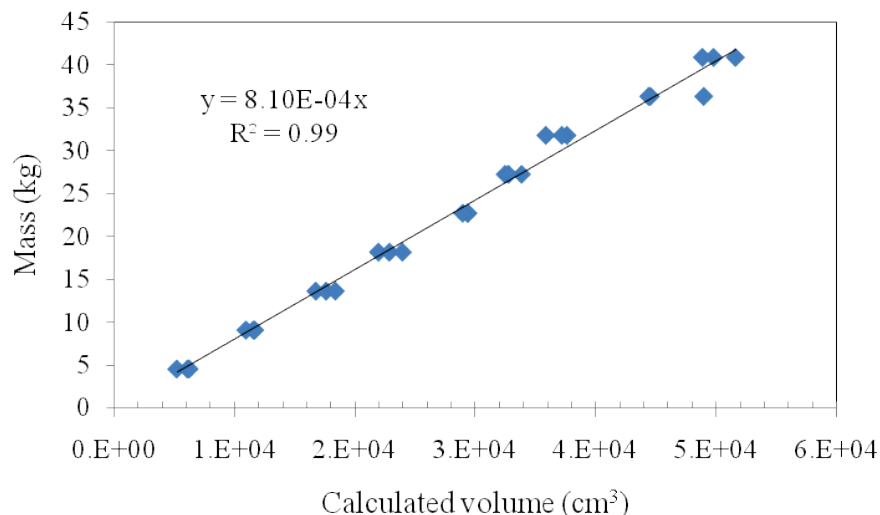


Figure 4-27. Actual mass vs. Calculated volume calibration curve with speed 1.71 m/s

Table 4-8. Calibration data with speed 1.34 m/s

Mass (kg)	Calculated Volume x10 ³ (cm ³)	With Grid data Calculated Volume x10 ³ (cm ³)
4.54	6.05	5.17
9.08	13.72	12.67
13.62	19.17	16.66
18.16	24.19	20.51
22.70	31.53	27.09
27.24	34.96	31.54
31.78	43.91	37.54
36.32	48.27	42.11
40.86	53.04	44.88
4.54	6.05	5.17
9.08	11.86	10.95
13.62	20.05	17.52
18.16	26.38	23.22
22.70	29.79	25.71
27.24	38.75	34.17
31.78	43.12	36.38
36.32	48.30	41.51
40.86	52.05	45.88
4.54	6.77	6.33
9.08	12.53	11.13
13.62	20.12	18.02
18.16	26.17	22.68
22.70	32.30	28.00
27.24	39.32	34.26
31.78	39.33	33.30
36.32	46.65	39.68
40.86	45.93	39.65

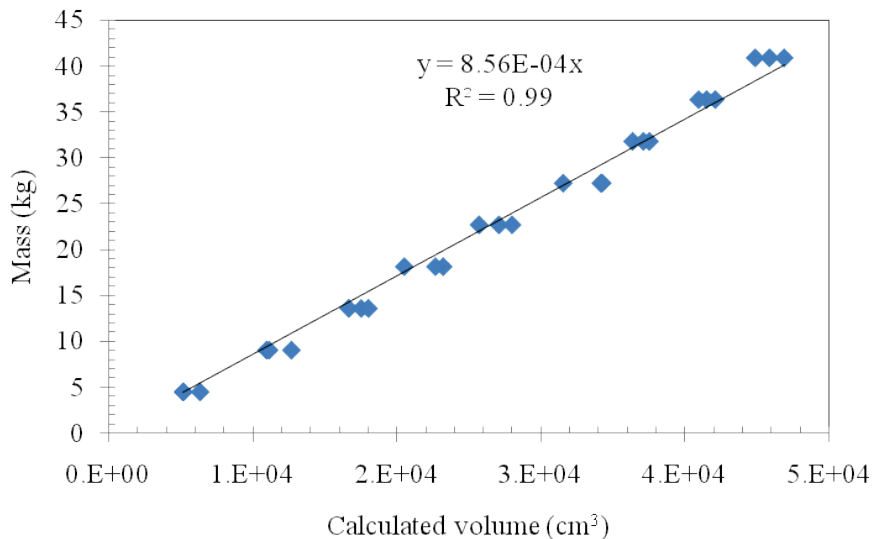


Figure 4-28. Actual mass vs. Calculated volume calibration curve with speed 1.34 m/s

Table 4-9. Calibration data with speed 1.03 m/s

Mass (kg)	Calculated Volume $\times 10^3 (\text{cm}^3)$	With Grid data Calculated Volume $\times 10^3 (\text{cm}^3)$
4.54	5.18	4.87
9.08	12.77	10.61
13.62	17.83	15.68
18.16	23.06	20.42
21.51	27.96	25.64
27.24	30.21	24.37
31.78	36.78	31.73
36.32	47.14	40.05
40.86	48.54	40.86
27.24	30.72	26.74
31.78	38.66	33.85
36.32	39.09	33.68
40.86	45.69	39.24
27.24	30.48	25.88
31.78	39.33	33.30
36.32	46.65	39.68
40.86	45.93	39.65

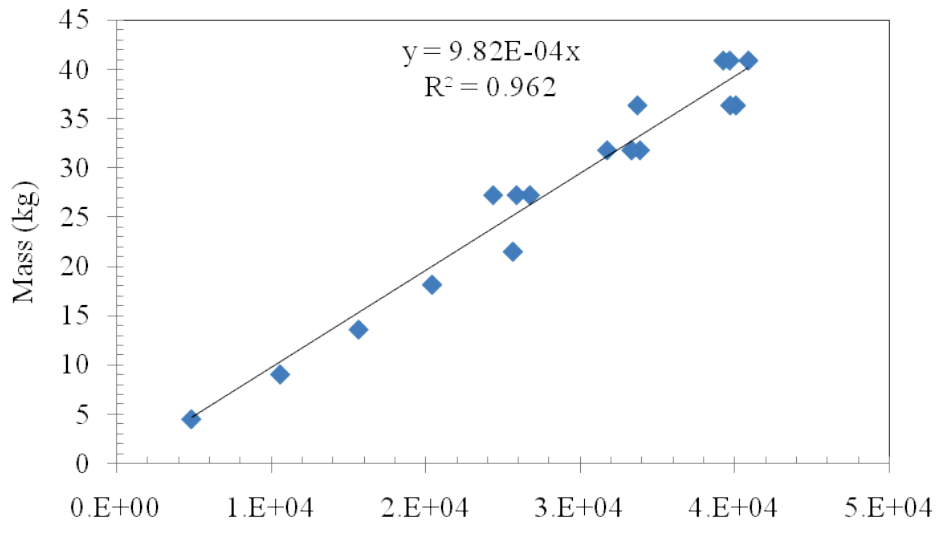


Figure 4-29. Actual mass vs. Calculated volume calibration curve with speed 1.03 m/s

Table 4-10. Validation data and error with speed 1.71 m/s

Actual Mass (kg) (Y)	With Grid data Calculated Volume $\times 10^3$ (cm^3)	Calculated Mass $\times 10^3$ (cm^3) (Y')	%Error	$(Y-Y')^2$
9.19	14.57	12.09	6.83	0.39
23.24	33.45	28.40	-0.70	0.03
16.12	26.27	21.60	8.92	2.07
35.66	54.11	45.62	3.95	1.99
29.94	45.05	37.63	2.13	0.41
				RMSE (kg) 0.98

Table 4-11. Validation data and error with speed 1.34 m/s

Actual Mass (kg) (Y)	With Grid data Calculated Volume $\times 10^3$ (cm^3)	Calculated Mass $\times 10^3$ (cm^3) (Y')	%Error	$(Y-Y')^2$
9.19	13.51	11.20	4.55	0.18
23.24	31.69	27.46	1.36	0.10
16.12	21.47	18.82	0.21	0.00
35.66	48.07	40.69	-2.09	0.56
29.94	37.64	33.06	-5.25	2.47
				RMSE (kg) 0.81

Table 4-12. Validation data and error with speed 1.03 m/s

Actual Mass (kg) (Y)	With Grid data Calculated Volume x10 ³ (cm ³)	Calculated Mass x10 ³ (cm ³) (Y')	%Error	(Y-Y') ²
9.19	12.88	10.51	12.07	1.23
23.24	29.22	25.81	8.88	4.26
16.12	21.78	19.38	17.94	8.36
35.66	48.65	41.91	15.24	29.55
9.94	38.30	33.49	9.70	8.43
RMSE (kg)				3.21

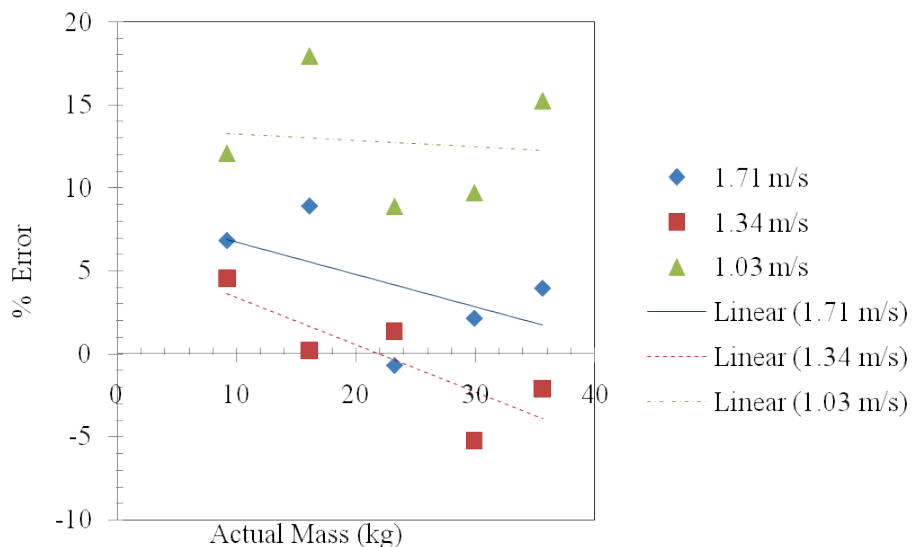


Figure 4-30. % Error based on actual mass with respect to the speed of conveyor

Experiments on Inclined Conveyor (CCSC, f/h ≥ 0.5)

As discussed in the section 4.2, different types of error sources introduce an error in volume calculation of fruits on conveyor. This section describes few methods that were used to minimize the errors. The conveyor system present on CCSC machines are inclined and the flap to fruit size ratio was ≥ 0.5 . The performance of volume measurement system was tested on the conveyor system used in the CCSC. This section will discuss the experiments performed, material and method used, the calibration and validation tests and the results in detail.

Overview of Experiments

Two experiments were performed in the laboratory on a small conveyor system as shown in Figure 4-31. The conveyor system was used to simulate the flow of citrus fruits during the harvesting using CCMH. The volume measurement system was mounted on the conveyor system as shown in Figure 4-31. Different parameters used in both the experiments as shown in Table 4-13 were recorded before the experiment.

Table 4-13. Different parameters used in volume calculation algorithm

	Experiment 1	Experiment2
Date of experiment	12-Jan-10	27-Jul-10
Sensor Frequency	24 Hz	75 Hz
Conveyor Speeds (m/s)	1.1	0.587, 0.785, 1.1
Angle / resolution	180°/0.5°	180°/1°
Conveyor width (cm)	76	76
Distance from sensor to right side conveyor wall (cm)	36.9	36.5
Distance from sensor to conveyor surface (cm)	28.7	35.6
Distance between two flaps (cm)	40	40

The system was calibrated and then the calibration data were used to validate the next set of data. System performance was analyzed by the amount of error in calculated mass of fruits with respect to the actual mass of fruits on the conveyor system.

Material and Methods

The SICK sensor was mounted as shown in Figure 4-31 on the top of the fruit carrying conveyor present and then fruits were dropped on to the conveyor system.

During the first experiment the SICK sensor was set on 180° scanning angle and 0.5° angular resolutions while the second experiment was performed with 180° scanning angle and 0.5° angular resolutions set using the Labview program.

The conveyor system has different flow controls from 1 to 10. The speed of the conveyor was measured using Digital tachometer. The tachometer was inserted into the conveyor shaft by setting the flow control on 10 and the RPM was recorded. The diameter of the conveyor shaft was 20 cm and was used to calculate the shaft revolutions per min and then calculate the speed of the conveyor system.



Figure 4-31. LMS SICK 200 for laboratory test on the conveyor belt

Experiment A

Calibration. In this experiment, the system was calibrated for speed 1.1 m/s with heavy loads from 11 kg to 85 kg. For each mass, three tests were carried out, the average volume was

calculated for each set of mass, and this averaged volume was used to calibrate the system. Table 4-14 shows the calculated volume for the fruits on the conveyor for each run while Table 4-15 shows the averaged mass and the volume for each set of mass.

The calibration plot of actual mass and the calculated volume as shown in Figure 4-32 has linear trend between the actual mass and the calculated volume with good coefficient of correlation of 0.99.

Table 4-14. Validation data and error with speed 1.1 m/s

Actual Mass (kg)	Calculated Volume $\times 10^3$ (cm 3)
11.80	31.00
11.78	34.99
11.76	40.01
23.31	77.37
23.24	62.39
23.24	75.97
34.82	102.72
34.57	94.11
34.57	107.18
48.19	107.18
48.03	135.81
48.12	145.09
62.18	102.03
62.08	126.00
61.97	139.63

Table 4-15. Validation data and error with speed 1.1 m/s

Actual Mass (kg)	Calculated Volume $\times 10^3$ (cm 3)
11.78	35.33
23.27	71.91
34.65	101.34
48.08	140.45
84.58	215.50

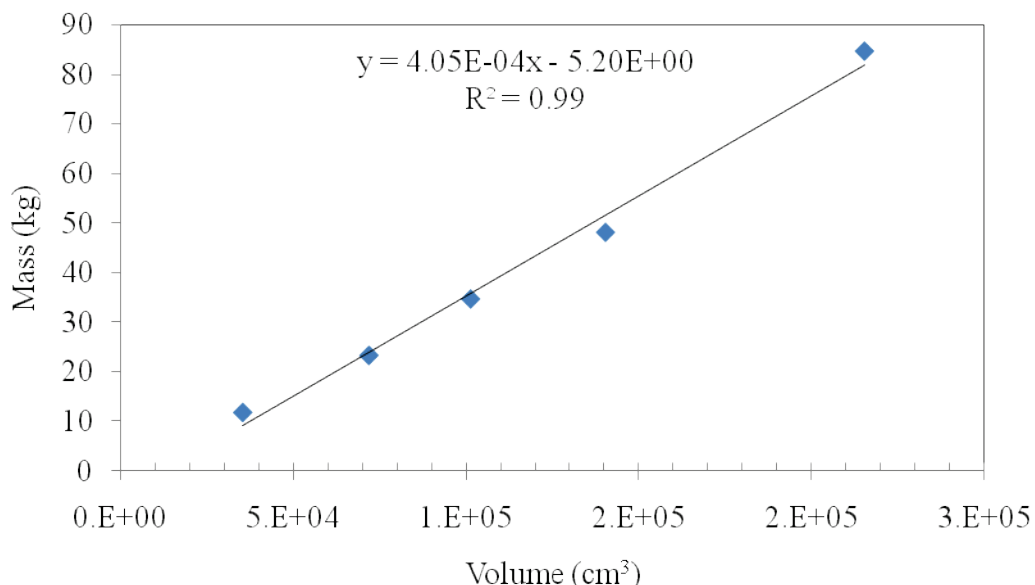


Figure 4-32. Calibration plot of mass vs. Calculated volume of fruits calculated after correcting the data with gridding method and removing the flap error

Validation. The same data were used for validation test and when the calibration equation was applied, there was a significant error in the volume. Table 4-16 shows that the percentage error and the SEP is more if the method of gridding and flap correction was not used. In addition, this error may increase if the conveyor is running for hours. In an ideal field conditions, the mechanical harvester does not stop that frequently unless there are problems or the workers are taking break. Thus, the flap error should be removed continuously during yield prediction.

Table 4-16. Standard and the percentage error in the actual and predicted mass 1.1 m/s

Actual Mass (kg)	Calculated Volume $\times 10^3$ (cm 3)	Calculated Mass (kg)	%Error
11.78	35.33	10.24	13.08
23.27	71.91	25.18	8.24
34.65	101.34	37.21	7.38
48.08	140.45	53.19	10.63
84.58	215.50	83.86	0.85
RMSE (kg)			2.8

Results and Discussions. The volumetric yield monitoring system needs to validate for different set of data and also the flap error needed to decrease or removed from the data which will improve the performance of the system and reduce the amount error in yield prediction. The reason for the high error in volume might be the frequency which was 36 Hz.

Experiment B

In this experiment, the algorithm was modified to minimize the error produced by the flaps; also a new set of validation test was performed to see the performance of the volumetric yield measurement system. Also to increase the data acquisition frequency from 36 Hz to 75 Hz, the angular resolution was changed to 1^0 from 0.5^0 .

Calibration. For the system calibration, the fruits were weighed from 4 to 41 kg and put into the bins then for each speed the fruit bins were dropped onto the conveyor and the data were collected. The system performance was tested for three different speeds. For each mass, the experiments were performed three times, to see the repeatability in volume calculation. Then the validation tests were performed with five different mass. When the data were processed, the volume for the amount of fruits on the conveyor system was calculated. Table 4-17, 4-18 and 4-19 shows the data collected with 0.587, 0.785, and 1.1 m/s speeds. When the actual mass versus

the volume calculated were plot it showed linear trend with the coefficient of correlation $R^2 = 0.98$ as shown in Figure 4-33, 4-34, 4-35. The calibration equations with different speeds were applied on the validation set to check the performance of the volume measurement system.

Validation. System calibration shows a linear trend with coefficient of correlation 0.99 between the actual mass and the calculated volume as shown in Figure 4-33, 4-34 and 4-35. These calibration equations were used to validate the system. A data set with different speeds was collected and the calibration equations were applied to calculate mass of fruits in kg on the conveyor system. Table 4-20, 4-21, 4-22 shows calculated mass from the amount of volume on the conveyor system with speeds 0.586, 0.785 and 1.1 m/s respectively.

Results and Discussions

The result showed that for different speeds the error reduces as the amount of fruit on the conveyor increases. As shown in the Figure 4-36, for each speed the percentage error has reduced and it is less than 5% for the mass more than 20 kg. This trend shows that in the actual field, percentage error will be less than 5% as the amount of load on the conveyor is more than 35 kg. The algorithm removes most of the flap error but it cannot completely remove it as the flap error is not consistent all the time. This flap error gets added if the conveyor runs without fruits for long time. In actual field conditions this situation may occur at the start or at the end of the citrus tree harvesting or when the mechanical harvester is moving from one tree to another. Also this condition may occur when the mechanical harvester starts harvesting and initially the conveyor is empty. This technique shows the potential use volumetric yield calculation using LMS SICK sensor in yield monitoring of citrus in mechanical harvester.

Table 4-17. Calibration data with speed 0.586 m/s

Actual Mass (kg)	Calculated Volume $\times 10^3$ (cm 3)
4.54	10.75
4.54	10.13
4.54	11.82
9.08	15.61
9.08	16.55
9.08	18.15
13.62	25.44
13.62	24.60
13.62	27.61
18.16	34.89
18.16	37.68
18.16	26.10
22.7	35.63
22.7	39.54
22.7	39.23
27.24	44.12
27.24	44.78
27.24	51.77
31.78	50.70
31.78	52.21
31.78	51.60
36.32	59.32
36.32	60.59
36.32	54.82
40.86	71.45
40.86	66.23
40.86	73.32

Table 4-18. Calibration data with speed 0.785 m/s

Actual Mass (kg)	Calculated Volume x 10 ³ (cm ³)
4.54	10.89
4.54	9.36
4.54	7.27
9.08	16.90
9.08	15.87
9.08	16.34
13.62	22.17
13.62	24.37
13.62	21.73
18.16	30.20
18.16	31.25
18.16	27.21
22.7	38.12
22.7	36.51
22.7	109.27
27.24	43.54
27.24	44.76
27.24	42.44
31.78	48.36
31.78	50.10
31.78	45.21
36.32	49.35
36.32	48.21
36.32	53.15
40.86	59.84
40.86	59.54
40.86	60.09

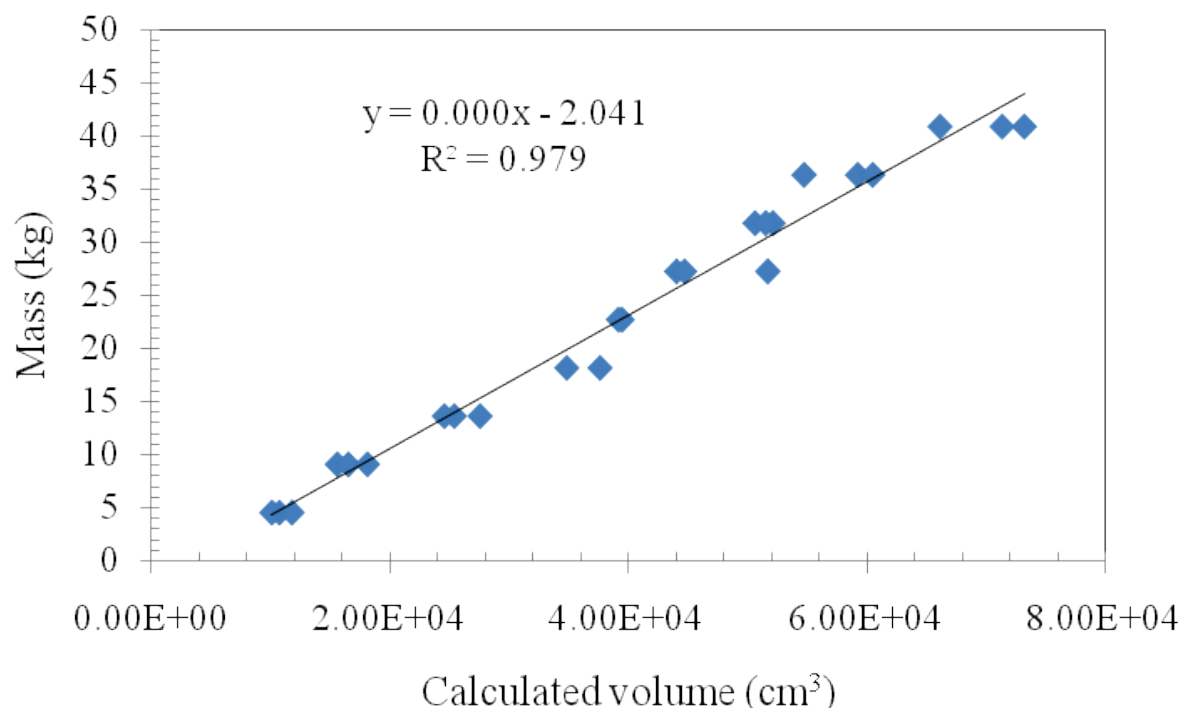


Figure 4-33. Calibration curve with speed 0.586 m/s

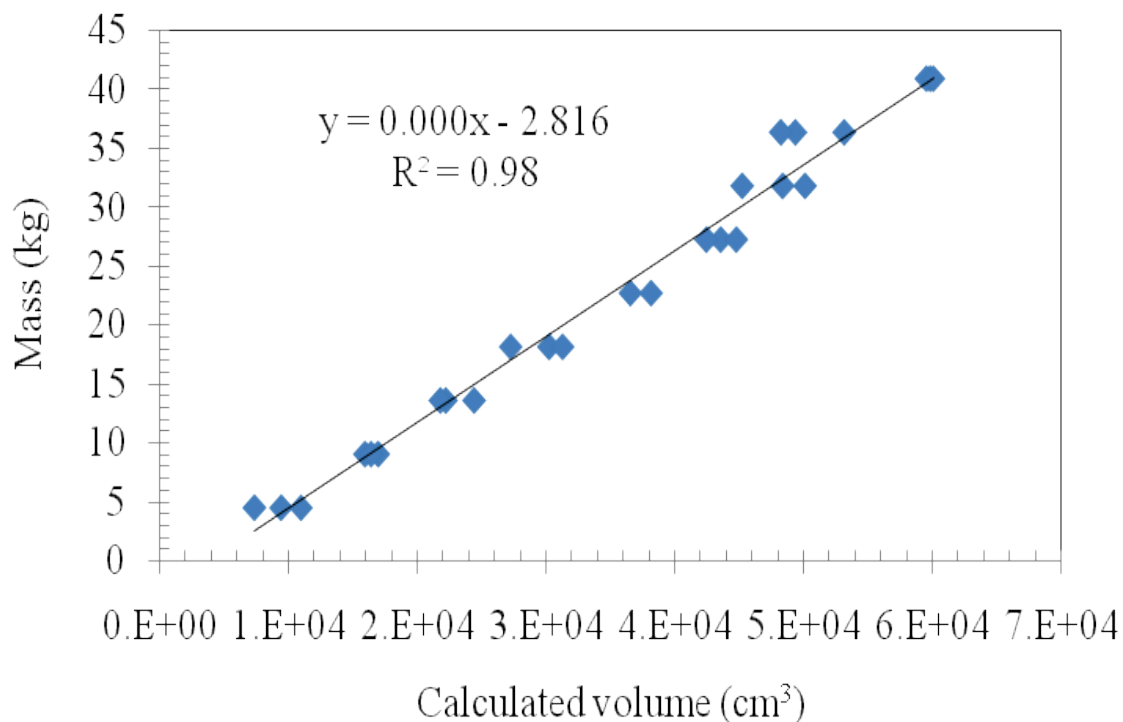


Figure 4-34. Calibration curve with speed 0.785 m/s

Table 4-19. Calibration data with speed 1.1 m/s

Actual Mass (kg)	Calculated Volume x10 ³ (cm ³)
4.54	13.51
4.54	15.08
4.54	9.67
9.08	17.25
9.08	16.39
9.08	17.03
13.62	26.21
13.62	23.05
13.62	28.45
18.16	34.04
18.16	68.25
18.16	45.13
22.7	38.68
22.7	37.51
22.7	38.11
27.24	44.07
27.24	40.55
27.24	42.56
31.78	52.07
31.78	47.88
31.78	56.84
36.32	57.92
36.32	61.22
36.32	59.26
40.86	66.64
40.86	63.64
40.86	64.22

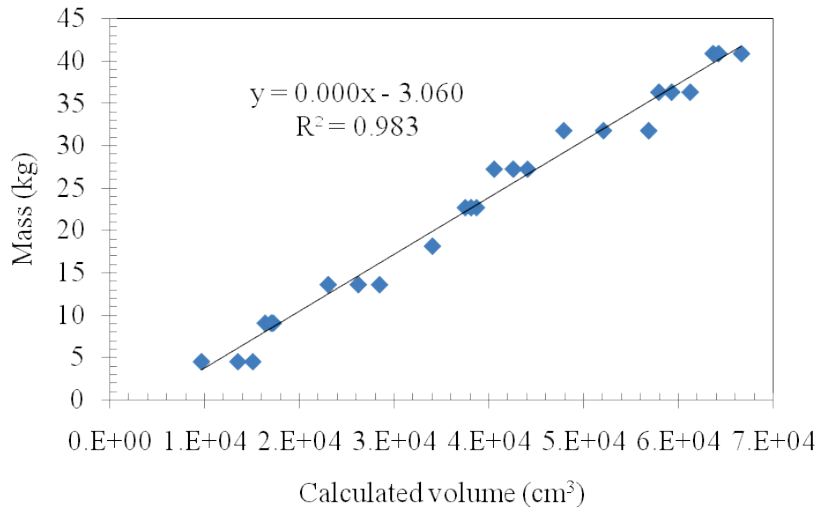


Figure 4-35. Calibration curve with speed 1.1 m/s

Table 4-20. Validation data and error with speed 0.586 m/s

Actual Mass (kg)	Calculated Volume	Calculated Mass (kg)	% Error	$(Y-Y')^2$
6.67	12.48	5.77	13.47	0.81
11.58	20.49	10.80	7.62	0.61
19.84	32.51	18.33	6.75	2.29
26.92	47.68	27.83	-3.36	0.82
38.25	64.16	38.15	0.24	0.01
RMSE (kg)				0.95

Table 4-21. Validation data and error with speed 0.785 m/s

Actual Mass (kg) Y	Calculated Volume $\times 10^3 (\text{cm}^3)$	Calculated Mass (kg) Y'	% Error	$(Y-Y')^2$
6.67	11.57	5.62	15.84	1.12
11.58	15.18	8.24	5.45	11.15
19.84	29.66	18.76	32.89	1.17
26.92	36.24	23.54	12.57	11.46
38.25	55.45	37.49	1.99	0.58
RMSE (kg)				2.25

Table 4-22. Validation data and error with speed 1.1 m/s

Actual Mass (kg) Y	Calculated vol wt grid and flap correction x 10 ³ (cm ³)	Calculated Mass (kg) Y'	% Error	(Y-Y') ²
38.25	63.23	39.43	-3.07	1.39
26.92	41.24	24.65	8.43	5.16
19.84	32.71	18.92	22.74	0.85
11.58	17.89	8.96	4.64	6.86
6.67	13.87	6.26	6.23	0.17
RMSE (kg)				1.69

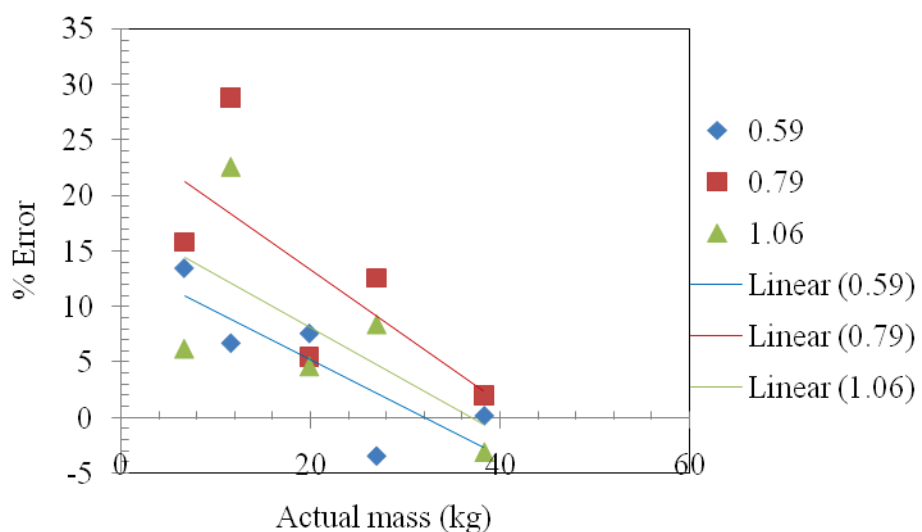


Figure 4-36. Error spread with different speeds

CHAPTER 5 YIELD MONITORING INTERFACE

As discussed in Chapter 1, one of the components of yield monitor is the user interface and a console unit located in the combine's cab as shown in Figure 5-1. This unit was integrated with the other yield monitor components such as the speed sensor, mass or volume of the grain/fruits flow sensor, grain moisture sensor, GPS / DGPS receiver unit. The console was also used to enter the operator specified information such as the fieldname, block number, grain/fruit type, calibration numbers, and correlation factors.

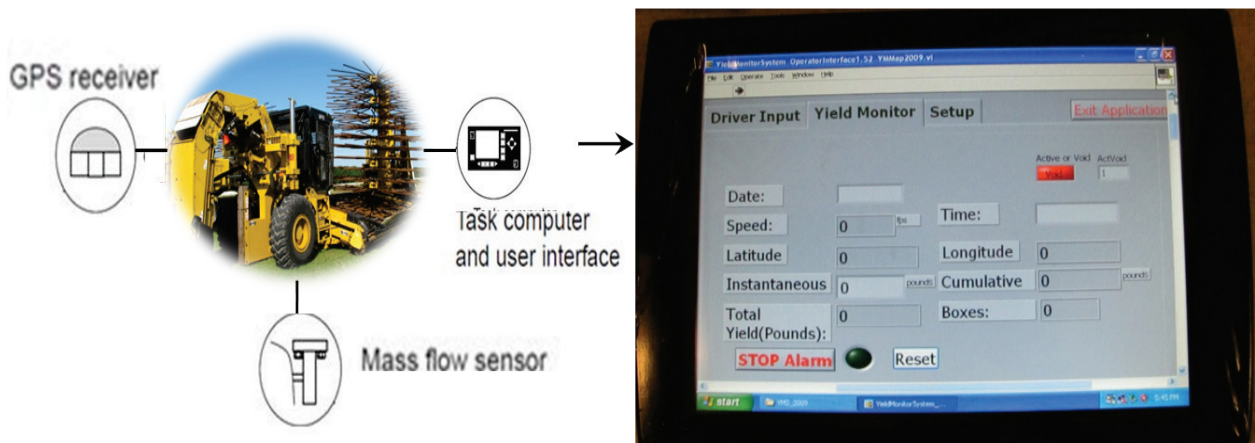


Figure 5-1. Yield monitor components (left), Yield monitor 8" touch Screen Panel (right)

The yield monitor interface unit provides the medium to store all this information which will then be used for the post processing. This information was also used by the user interface on-the-go to calculate the yield of the harvested grain/fruits. The console connected with the DGPS receiver stores the harvester position related information. These spatially indexed data were combined with the yield information and later used to produce the yield maps. Most yield monitors can display the instantaneous yield and the total amount of yield harvested at a given time and provides statistics for loads or batches of grain / fruits within an area of a field.

Importance of Yield Monitoring Interface

A load cell based yield monitoring system was developed by Maja et al., (2009) that used load cell to measure the impact force and correlate it to the mass of citrus fruits getting harvested. The load cell sensors were attached to a plate made up of a carbon fiber and was placed at the end of the conveyor belt of an Oxbo machine.

Due to the large sets of data, all of the computation for yield was done off line. The real time data were actually stored in a flash disk and then was transferred to the PC once a month for processing. The yield data were then made available to the growers on a monthly basis. A real time data logging and display or interface would prove very beneficial for the growers and at the same time for the operator of the machine. Most of the times the yield monitoring systems are calibrated and once it is calibrated then the calibration information is used to calculate the amount of fruits harvested in kg. The calibration information, such as the slope and the intercept is recorded in the yield monitor interface before the mechanical harvesters start to harvest the fruits in the grove. The yield monitor interface is explained in detail in the next paragraph.

Design and Development

The yield monitor interface was developed for the load cell based yield monitoring system (Maja et al., 2009). The system can be used for any other yield monitoring system with minor changes in existing software. The load cell based system produced the analog voltage for the continuous impact produced by the harvested fruits on the plate and this analog output from the entire load cells were combined using the summing board. Also, the position of the harvester was recorded using the GPS unit mounted on the mechanical harvester. The GPS information and the summed analog voltage was combined together and sent wirelessly to the yield monitor interface for further processing. Figure 5-2 shows the snapshot of the data sent wirelessly to the interface console.

```

data0.txt - Notepad
File Edit Format View Help
$GPRMC,120501,A,2721.6156,N,08108.4030,w,000.0,099.4,060509,005.3,w*7D,93
$GPRMC,120502,A,2721.6154,N,08108.4031,w,000.0,099.4,060509,005.3,w*7D,100
$GPRMC,120503,A,2721.6152,N,08108.4032,w,000.0,099.4,060509,005.3,w*79,110
$GPRMC,120504,A,2721.6150,N,08108.4033,w,000.0,099.4,060509,005.3,w*7D,96
$GPRMC,120505,A,2721.6149,N,08108.4033,w,000.0,099.4,060509,005.3,w*74,93
$GPRMC,120506,A,2721.6148,N,08108.4033,w,000.0,099.4,060509,005.3,w*76,93
$GPRMC,120507,A,2721.6147,N,08108.4034,w,000.0,099.4,060509,005.3,w*7F,94
$GPRMC,120508,A,2721.6146,N,08108.4034,w,000.0,099.4,060509,005.3,w*73,92
$GPRMC,120509,A,2721.6145,N,08108.4034,w,000.0,099.4,060509,005.3,w*73,98
$GPRMC,120510,A,2721.6144,N,08108.4034,w,000.0,099.4,060509,005.3,w*7A,100
$GPRMC,120511,A,2721.6144,N,08108.4034,w,000.0,099.4,060509,005.3,w*7B,89
$GPRMC,120512,A,2721.6143,N,08108.4034,w,000.0,099.4,060509,005.3,w*7F,101
$GPRMC,120513,A,2721.6143,N,08108.4034,w,000.0,099.4,060509,005.3,w*7E,94
$GPRMC,120514,A,2721.6142,N,08108.4035,w,000.0,099.4,060509,005.3,w*79,104
$GPRMC,120515,A,2721.6142,N,08108.4035,w,000.0,099.4,060509,005.3,w*78,92
$GPRMC,120516,A,2721.6142,N,08108.4035,w,000.0,099.4,060509,005.3,w*7B,97
$GPRMC,120517,A,2721.6142,N,08108.4035,w,000.0,099.4,060509,005.3,w*7A,104
$GPRMC,120518,A,2721.6141,N,08108.4035,w,000.0,099.4,060509,005.3,w*76,88
$GPRMC,120519,A,2721.6141,N,08108.4035,w,000.0,099.4,060509,005.3,w*77,93
$GPRMC,120520,A,2721.6141,N,08108.4035,w,000.0,099.4,060509,005.3,w*7D,93
$GPRMC,120521,A,2721.6141,N,08108.4034,w,000.0,099.4,060509,005.3,w*7D,82
$GPRMC,120522,A,2721.6141,N,08108.4034,w,000.0,099.4,060509,005.3,w*7E,91
$GPRMC,120523,A,2721.6140,N,08108.4034,w,000.0,099.4,060509,005.3,w*7E,92
$GPRMC,120524,A,2721.6140,N,08108.4034,w,000.0,099.4,060509,005.3,w*79,92
$GPRMC,120525,A,2721.6140,N,08108.4034,w,000.0,099.4,060509,005.3,w*78,87
$GPRMC,120526,A,2721.6140,N,08108.4034,w,000.0,099.4,060509,005.3,w*7B,90

```

Figure 5-2. Snap shot of the data from GPS and load cell

During the harvest season, two mechanical harvesters move side by side in a row, harvesting the citrus trees, collecting the fruit and transferring the harvested fruit to the haul truck (sometimes referred to as the “goat truck”) as shown in Figure 5-3. The fruit collection frame of one of these two mechanical harvesters in a row is on top of the fruit collection frame of other mechanical harvester (bottom) in the second row. In mechanical harvesting operation the top row refers to the row where a mechanical harvester frame is on top of the another. The fruit gets harvested by these two harvesters, so the yield monitor interface can be installed on either one of the harvester. The yield related data and the GPS position information from the individual harvesters is transferred wirelessly to the interface.



Figure 5-3. Mechanical harvesting machines on top and bottom rows in the grove



Figure 5-4 Yield monitoring interface mounted in the Oxbo machine

The yield monitor interface was developed using Labview® software from National Instruments. This software was then installed on an 8" touch screen panel (Comfile technology model CUPC-P80). As shown in Figure 5-5, the interface shows six tabs on the interface such as the Driver's input, Yield monitor top, Yield monitor bottom, Combined, Setup 1, and Setup 2. The machine operator is responsible to input the information about the grove such as field, block, crop type, the goat truck capacity, the calibration data (the slope and the intercept) and other information shown in Figure 5-5.

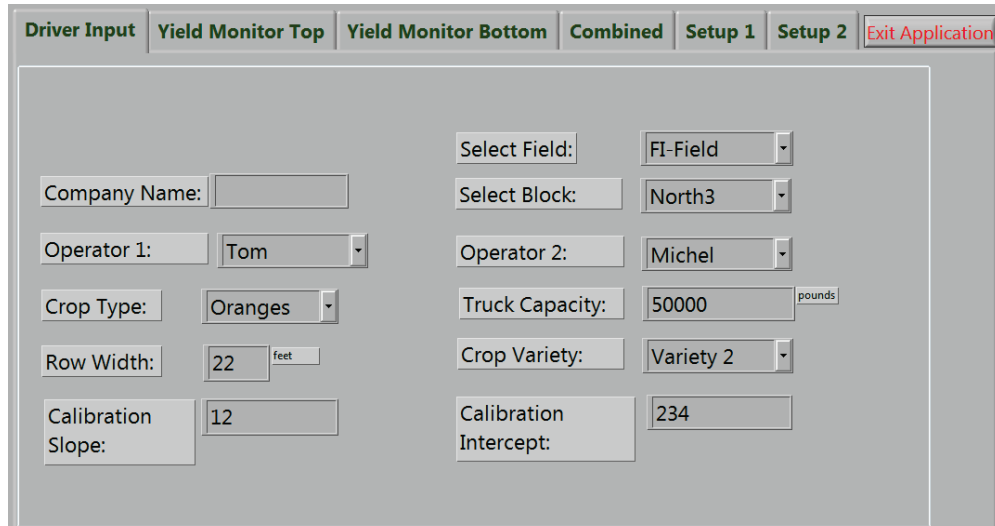


Figure 5-5. Yield monitor interface with driver's input tab

The calibration information is used to calculate the amount of fruit harvested in mass, kg as the mechanical harvester moves along the row and harvest the fruits. The Yield monitor top tab as shown in Figure 5-6, shows the information about the mechanical harvester on the top row. It shows the amount of fruits harvested by calculating the instantaneous yield using the calibration slope and the intercept constant specified by the operator in the driver's input tab. It calculates the total fruits harvested in terms of the cumulative yield and the number of boxes. The calibration information such as the slope and intercept can be computed by running a simple test on the Oxbo machine with a defined weigh of oranges and correlate it with the impact data from the control box. It can be done once before the harvesting starts and the calibrated slope and intercept can be used for the whole harvest season. One of the nice features of the interface build was the alarming system. The operator can set the trailer capacity in one of the interface input and when the citrus trailer reach its capacity, the system alarms the operator that the trailer is full and a new trailer should be used by the goat truck. This feature can save the trailers from overloading its capacity and eventually avoid the possibility of paying the fines for littering the fruits on the road.



Figure 5-6. Yield monitor interface with top row mechanical harvester information tab

The mechanical harvester bottom row as shown in Figure 5-7, is the same as for the top row. This interface collects the yield related information from the other mechanical harvester on the bottom side.



Figure 5-7. Yield monitor interface with bottom row mechanical harvester information tab

The next tab (Figure 5-8) with combine yield shows the amount of fruits harvested by both of these top and bottom side mechanical harvesters. This tab gives the information about the yield and total number of boxes harvested combined by the two harvesters.



Figure 5-8. Yield monitor interface with bottom row mechanical harvester information tab

The setup1 and setup 2 tabs as shown in Figure 5-9 and 5-10 are used to set the RS-232 terminals for the wireless input from the GPS and the impact plate output ports from the two harvesters. Setup shows the additional alarm playing setting after the fruit trailer reaches to its specified capacity.

The yield monitoring software processes the data from the two mechanical harvesters and creates two files. The first file is the raw data file and the other one is for the processed data. When the yield monitoring interface starts collecting the data, it creates a folder named YieldMonitor_Interfacedata on ‘C:\’ drive of the panel and creates two subfolder in the main folder called RawData and ProcessedData. Once these folders get created it creates another two files for the raw data received from the two mechanical harvesters and three processed data files

after processing the individual data from the respective harvesters such as top and bottom side mechanical harvesters and a third file which was the combination of the processed data.

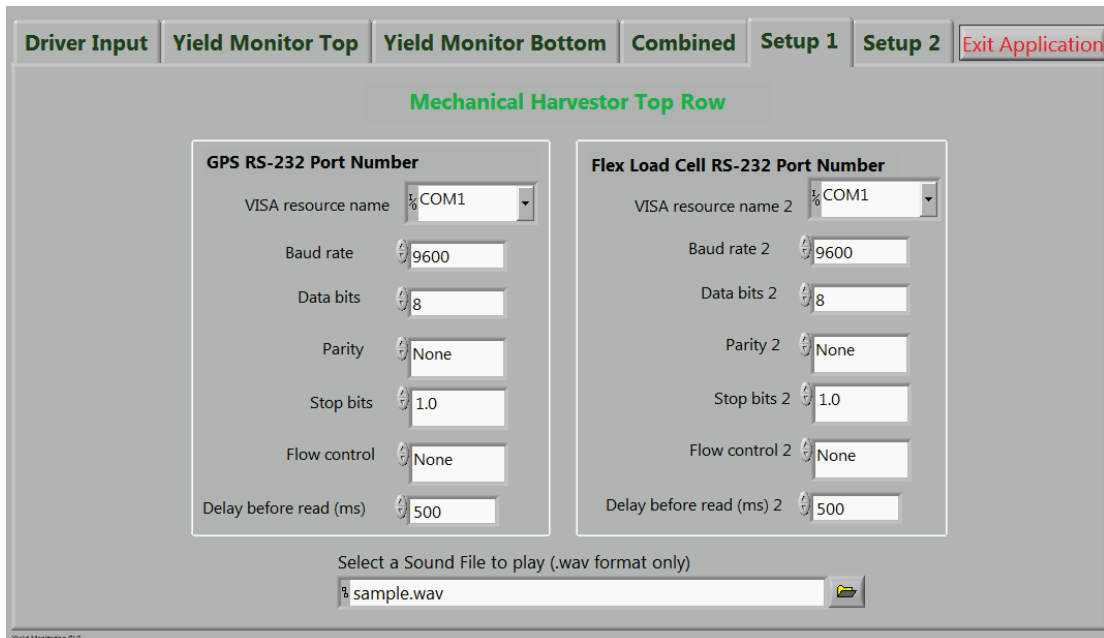


Figure 5-9. Yield monitor interface top row mechanical harvester data communication port setting tab

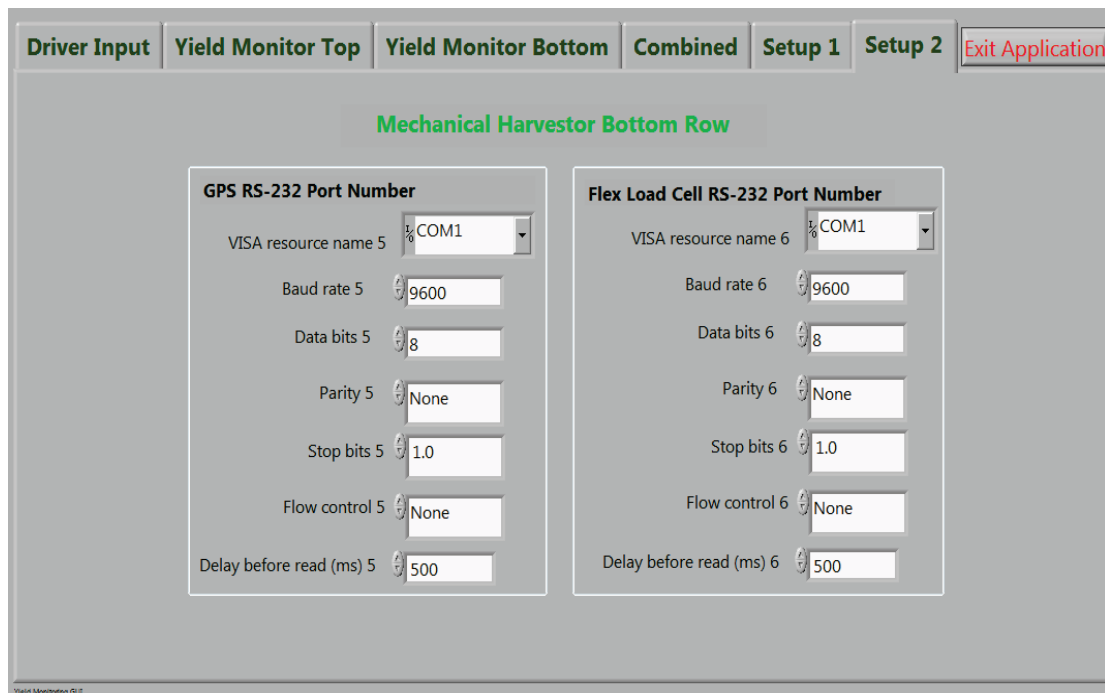


Figure 5-10. Yield monitor interface bottom row mechanical harvester data communication port setting tab

The sample files generated are shown in Figure 5-11. The Figure 5-11(a) and (b) shows the sample file raw data received from the top and bottom side mechanical harvester respectively. Figure 5-11 (c) shows the sample file generated after processing the raw data received from the mechanical harvesters. These files are stored in the panel memory and used later to generate yield maps.

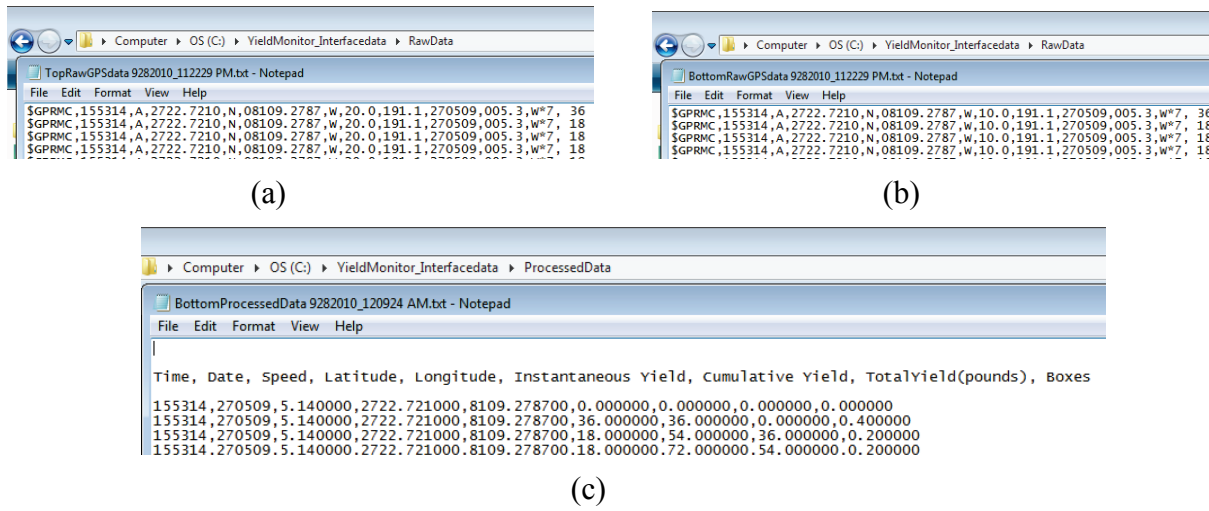


Figure 5-11. (a), (b) Snap shot of raw data for the top and bottom row harvesters, (c) The processed data after combining raw data from top and bottom row harvesters.

Conclusion and Discussion

The yield monitor interface developed for the impact based system can be modified and used for the volumetric yield monitoring system. As presented earlier, it shows that there was information that needs to be placed in the program for this to work properly. One of the most important parts of it was the calibration, e.g., slope and intercept which can be made available by doing a simple test of known weights. The yield monitoring interface also has very important feature that tell the operator of the harvester that the trailer which is located outside the harvested block is already full based on its current harvest and thus another trailer should be used. This saves both time and money for the grove owners as they will know that the trailer that transports their fruits from their grove to the processing plant is not overloaded.

CHAPTER 6

CONCLUSION AND FUTURE WORK

The overall objective of this study was to explore the use of non-contact method specifically LIDAR technology to measure volumetric flow on a conveyor system to predict the yield of citrus fruits. A methodology was developed to use the cross-sectional information captured over specified amount of time to calculate the amount of mass and thus fruits harvested and collected on the citrus mechanical harvester and the trash removal machine.

This objective was achieved by testing two types of laser sensors to measure the cross sectional information. The first sensor system consisted of a linear array of IR sensors from which data were available in Cartesian co-ordinate system while the second sensor was a single LMS SICK sensor which measures the data in polar co-ordinate system. An algorithm was developed to process the data collected by these sensors and generate the amount of volume passing on the conveyor system by doing time integration of the information. A linear calibration curve was developed to calculate the actual mass (kg) of the fruits and thus yield in terms of measured fruit volume on the conveyor system.

Five different laboratory experiments were conducted to achieve this objective. The first experiment was performed by mounting a linear array of (Sharp GP2Y0A02) sixteen IR laser sensors on the conveyor system. The repeatability of the sensor was questionable with measured volumes showing errors anywhere from 10% to 100%. Sensors were found to interfere with each other when the distance between them was less than 4 cm. Sensors were also found to be sensitive to the ambient lighting conditions. Additional possible source of error could be sensor synchronization or rather lack of it. The highest possible sensor frequency of 23Hz is found to be insufficient for the conveyor speeds of more than 1 m/s, the number of data points per fruit were less than three which adds error in fruit volume calculation.

Two experiments were conducted by mounting the LMS SICK laser sensor on the horizontal conveyor system of trash removal machine. The results were encouraging with error less than 5% for citrus fruits weighing more than 40 kg with conveyor speed of 1.34 m/s. The mass measurement error was found to be less than 8% with a conveyor speed of 1.71 m/s, the maximum possible setting of current trash removal machine.

Additional two experiments were performed using the same sensor on an inclined conveyor system present in the mechanical harvester. This conveyor has flaps of height 8 cm to hold the fruits and to carry them towards the fruit collecting bins or containers. These flaps introduce error in the volume measurement, which was corrected by using a 30 second dry run of conveyor as a reference. The volumetric yield calculation system was calibrated for the speeds of 0.58, 0.875 and 1.1 m/s and the linear calibration curve information was used to predict the citrus fruit mass in kg. The results showed that for the maximum speed of 1.1 m/s, the coefficient of determination, R^2 between the actual yield and the predicted yield was 0.989 and the RMSE was 1.69 kg for a measurement range of 4 to 41 kg. The error is expected to reduce with increase in mass, which increases the conveyor occupancy. The error in predicted mass was found to be less than 5% for the fruit mass of more than 20 kg. It will be safe to conclude that in the actual field, percentage error will be less than 5% as the amount of load on the conveyor is normally more than 35 kg. Thus the non-contact measurement method using the LIDAR technology was successfully implemented and its usefulness in measuring volumetric flow of fruit and the yield was successfully demonstrated for citrus mechanical harvester as well as the trash removal machine.

As future work, field trials can be conducted to ascertain the performance observed in the laboratory setting. Using more than one LMS SICK sensors can be explored to further reduce the

error in predicted yield. The current volume calculation algorithm can be further developed for real-time yield measurement.

APPENDIX

LMS SICK DATA COLLECTION ALGORITHM

This appendix gives an algorithm implemented in Matlab software to process the data collected when the LMS SICK scanner was mounted on the conveyor system. Two algorithms were implemented to process the SICK sensor data, one for the horizontal conveyor system in trash removal machine and the inclined conveyor system in the citrus mechanical harvester machine.

Algorithm for Horizontal Conveyor System in Trash Removal Machine

```
clear all  
close all  
% x-axis is along conveyor  
% y-axis is across conveyor  
% z-axis is along depth, starting at conveyor face  
%% Load data from a txt file  
vdata = load ('Test1_Speed5_30s_Error.dat', '-ascii'); % Voltage data  
% time in seconds between when the sensor data collection starts and the conveyor starts moving  
% corresponding data should be removed from the 'vdata'  
conveyorwaittime = 0;  
%% Required inputs  
drate = 75; % Sensor frequency in Hz  
convspeed = 1.032955665*1000; % mm/sec conveyor speed  
dsenseconv = 25*10; % mm distance between sensor and conveyor surface  
wallheight = 4*10; % conveyor side wall height (mm) to be considered in calculation  
senstortwall = 32*10; % mm distance between sensor mid and conveyor right side wall
```

```

conveyorwidth = 63*10; % conveyor width in mm

totalangle = 180; % total angle in y-z plane for which data is collected by the sensor

angspace = 1; % anglespacing is the interval between 2 data points in y-z plane

flappitch = 40*10; % average distance between two flaps on conveyor

% total_vol = 6.3566e+006 volume for 94 flaps when conveyorwaittime = 0;

flapvolcorfact = 0; %7.9122e+007/99; % calculated volume per flap when conveyor was run

empty (it will give volume due to flaps alone)

% total_vol1 = 1.0883e+008 volume for 94 flaps when used grid data

flapvolcorfact_griddata = 0; % calculated volume per flap when conveyor was run empty when

the data is corrected using grid technique(it will give volume due to flaps alone)

%%

% delete initial data, when conveyor is not moving

vdata(1:ceil(drate*conveyorwaittime),:)=[];

%Size of vdata in c rows and d columns

[l,m] = size(vdata); % gives size of data, 'c' rows and 'd' columns

sensortorightwall = senstortwall*dsenseconv/(dsenseconv-wallheight); % mm distance between

sensor mid and conveyor right side wall

sensortoleftwall = (conveyorwidth*dsenseconv/(dsenseconv-wallheight))-sensortorightwall; %

mm distance between sensor mid and conveyor left side surface

convsensheight = dsenseconv;

rangle = 180/pi()*atan(sensortorightwall/convsensheight); % Angle setting for matlab analysis, it

is scanning included angle

```

```

langle = 180/pi()*atan(sensortoleftwall/convsensheight); % Angle setting for matlab analysis, it
is scanning included angle

anglesetting = langle + rangle;

%% Erase side wall data

% left side

rightsidestart = 1;

rightsideend = floor((totalangle/2-rangle)/angspace)-1;

leftsideend = totalangle/angspace - rightsideend+1;

leftsidestart = floor(leftsideend - ((totalangle/2-langle)/angspace));

vdata(:,rightsidestart:rightsideend) = [];

vdata(:,leftsidestart:leftsideend) = [];

% vdata(:,end)=[];

%% Internal calculations

% Size of vdata in c rows and d columns

[c,d] = size(vdata); % gives size of data, 'c' rows and 'd' columns

sensorspoints = d; % number of points across conveyor

dt = 1/drate; % data frequency in seconds

% x-axis data

t = [0:dt:(c-1)*dt]; % time scale

for i=1:length(t)

x(i,:)=t(i)*convspeed*[ones(1,d)]; % distance between 2 area scans

end

```

```

% z axis and y axis data

at=angspace*pi()/180; % reading at the rate of 'at' radians

startang=(90-rangle)*pi()/180;

for i=1:c

    angle = startang; % for every scan in y-z plane, starting angle is 0 deg

    for j=1:d

        theta(i,j) = angle; % current angle

        z(i,j) = vdata(i,j)*sin(theta(i,j)); % z = r*sin(theta)

        y(i,j) = vdata(i,j)*cos(theta(i,j)); % y = r*cos(theta)

        angle=angle+at; % increment angle by 0.5 deg for next data point

    end

end

z = dsenseconv*ones(size(z))-z; % gives distance from conveyor surface to fruit top surface

%% Plotting

figure

% surface data points plot

% subplot(1,2,1),

surface(x,y,z)

xlabel('Along conveyor (mm)')

ylabel('Across conveyor (mm)')

zlabel('Depth (mm)')

title('Surface plot : data points')

axis equal

```

```

axis tight
shading interp
view([-40 20])
colorbar
for i=1:c
    for j=1:d
        if z(i,j)<45
            z(i,j)=0;
        end
        if z(i,j)>85
            z(i,j)=80;
        end
    end
end
y = y - min(min(y)); % this makes wall = 0, gives distance from conveyor side wall to fruit top
surface
%% Elemental volume (4 adjacent points), linear interpolation
[a, b] = size(x);
for i=1:a-1 %
    dx(i) = x(i+1)-x(i); % elemental length along x-axis
    for j=1:b-1
        dy(i,j) = (y(i,j)-y(i,j+1)+y(i+1,j)-y(i+1,j+1))/2; % avg elemental length along y-axis
        zavg(i,j) = (z(i,j)+z(i,j+1)+z(i+1,j)+z(i+1,j+1))/4;
    end
end

```

```

vol(i,j) = zavg(i,j)*dx(i)*dy(i,j);

dxpoint(i,j) = x(i)+dx(i)/2;

dypoint(i,j) = y(i,j)+dy(i,j)/2;

end

xslice_vol(i) = sum(vol(i,:)); % volume of all elements between 2 xslices

end

total_vol = sum(sum(vol(:, :))), % total volume

% removing volume corresponding to flaps

xrange = max(max(x)); % finds out what is the length of the conveyor we have considered in
data analysis

flapvolume = floor(xrange/flappitch)*flapvolcorfact;

total_vol_flapcor = total_vol - flapvolume, % total volume with flap correction

%% Plotting

figure

% surface data points plot

% subplot(1,2,1),

surface(x,y,z)

xlabel('Along conveyor (mm)')

ylabel('Across conveyor (mm)')

zlabel('Depth (mm)')

title('Surface plot : data points')

axis equal

axis tight

```

```

shading interp
view([-40 20])
colorbar

%% Working on data achieved through grid data

% data reshaping - uniform x and y co-ordinates, interpolate z co-ordinate

% Presently we have kept the data size same. increasing data size might improve results

X1 = x; % keeping the original x data

Y1 = ones(c,1)*[floor(max(y(:,1))):-floor(max(y(:,1)))/(d-1):0]; % changing y data to get
uniformly spaced y data

% floor(y(:,1)) gives rounded down value of maximum element in the 1st column of y data

Z1 = griddata(x,y,z,X1,Y1,'cubic'); % 'linear' interpolation of z data, we can use 'cubic' as well

% elemental volume (4 adjacent points), linear interpolation

[a, b] = size(X1);

% check due to interpolation if we get any element of Z1 as NaN, if we do,
% then replace that element with original z value, we can do this because
% we have kept the size of x,y,z same when it becomes X1, Y1 and Z1

Z1check=isnan(Z1); % checks if any of the element of Z1 is 'NaN' and returns '1' else '0' at that
element

for i=1:a
    for j=1:b
        if Z1check(i,j)== 1
            Z1(i,j)=z(i,j);
        end
    end
end

```

```

end

end

for i=1:a

    for j=1:b

        if Z1(i,j)<45

            Z1(i,j)=0;

        end

        if Z1(i,j)>85

            Z1(i,j)=80;

        end

    end

end

for i=1:a-1 %

    dx1(i) = X1(i+1)-X1(i); % elemental length along x-axis

    for j=1:b-1

        dy1(i,j) = (Y1(i,j)-Y1(i,j+1)+Y1(i+1,j)-Y1(i+1,j+1))/2; % avg elemental length along y-axis

        zavg1(i,j) = (Z1(i,j)+Z1(i,j+1)+Z1(i+1,j)+Z1(i+1,j+1))/4;

        vol1(i,j) = zavg1(i,j)*dx1(i)*dy1(i,j);

    end

    dxpoint1(i,j) = X1(i)+dx1(i)/2;

    dypoint1(i,j) = Y1(i,j)+dy1(i,j)/2;

end

```

```

xslice_vol1(i) = sum(vol1(i,:)); % volume of all elements between 2 xslices
end

total_vol1 = sum(sum(vol1(:, :))), % total volume

%removing volume corresponding to flaps

X1range = max(max(X1)); % finds out what is the length of the conveyor we have considered in
data analysis

flapvolume1 = floor(X1range/flappitch)*flapvolcorfact_griddata;

total_vol1_flapcor = total_vol1 - flapvolume1, % total volume with flap correction

% plotting

figure

% % surface data points plot

% subplot(1,2,1),
surface(X1,Y1,Z1)

% mesh(X1,Y1,Z1)

xlabel('Along conveyor (mm)')
ylabel('Across conveyor (mm)')
zlabel('Depth (mm)')
title('Surface plot : data points')

axis equal

shading interp

view([-40 20])

colorbar

```

Algorithm for Horizontal Conveyor System in Citrus Mechanical Harvester Machine

```
clear all

close allangspace

%% About the File

% This file shows the walls properly than other versions in this folder

% x-axis is along conveyor

% y-axis is across conveyor

% z-axis is along depth, starting at conveyor face

%% Load data from a txt file

vdata = load ('test.dat', '-ascii'); % Voltage data

conveyorwaittime = 0;

conveyorwaittimeend = 0;

%% Required inputs

drate = 75; % Sensor frequency in Hz

convspeed = 1.057669527*1000; % mm/sec conveyor speed

dsenseconv = 35.6*10; % mm distance between sensor and conveyor surface

wallheight = 5*10; % conveyor side wall height (mm) to be considered in calculation

senstortwall = 36.5*10; % mm distance between sensor mid and conveyor left side wall

conveyorwidth = 76*10; % conveyor width in mm

dbar = 55; %in mm error data other than fruit data

% time in seconds between when the sensor data collection starts and the conveyor starts moving

% corresponding data should be removed from the 'vdata'

totalangle = 180; % total angle in y-z plane for which data is collected by the sensor
```

```

angspace = 1; % anglespacing is the interval between 2 data points in y-z plane

flappitch = 40*10; % average distance between two flaps on conveyor

% total_vol = 3.4908e+007 volume for 80 flaps when conveyorwaittime = 0;

% calculated volume per flap when conveyor was run empty (it will give volume due to flaps
alone)

flapvolcorfact = 3.72E+07/80;

% total_voll = 3.4006e+007 volume for 96 flaps when used grid data

% calculated volume per flap when conveyor was run empty when the data is corrected using
grid technique(it will give volume due to flaps alone)

flapvolcorfact_griddata = 3.26E+07/80;

%%

% delete initial data, when conveyor is not moving

vdata(1:ceil(drate*conveyorwaittime),:)=[];

[aa,bb]=size(vdata);

vdata((aa-ceil(drate*conveyorwaittimeend)):end,:)=[];

%Size of vdata in c rows and d columns

[l,m] = size(vdata); % gives size of data, 'c' rows and 'd' columns

sensortorightwall = senstortwall*dsenseconv/(dsenseconv-wallheight); % mm distance between
sensor mid and conveyor right side wall

sensortoleftwall = (conveyorwidth*dsenseconv/(dsenseconv-wallheight))-sensortorightwall; %

mm distance between sensor mid and conveyor left side surface

convssensheight = dsenseconv;

```

```

rangle = 180/pi()*atan(sensortorightwall/convsensheight); % Angle setting for matlab analysis, it
is scanning included angle

langle = 180/pi()*atan(sensortoleftwall/convsensheight); % Angle setting for matlab analysis, it
is scanning included angle

anglesetting = langle + rangle;

%% Erase side wall data

% left side

rightsidestart = 1;

rightsideend = floor((totalangle/2-rangle)/angspace)-1;

leftsideend = totalangle/angspace - rightsideend+1;

leftsidestart = floor(leftsideend - ((totalangle/2-langle)/angspace));

vdata(:,rightsidestart:rightsideend) = [];

vdata(:,leftsidestart:leftsideend) = [];

% vdata(:,end)=[];

%% Internal calculations

% Size of vdata in c rows and d columns

[c,d] = size(vdata); % gives size of data, 'c' rows and 'd' columns

sensorspoints = d; % number of points across conveyor

dt = 1/drate; % data frequency in seconds

% x-axis data

t = [0:dt:(c-1)*dt]; % time scale

for i=1:length(t)

```

```

x(i,:)=t(i)*convspeed*[ones(1,d)]; % distance between 2 area scans

end

% z axis and y axis data

at=angspace*pi()/180; % reading at the rate of 'at' radians

startang=(90-rangle)*pi()/180;

for i=1:c

    angle = startang; % for every scan in y-z plane, starting angle is 0 deg

    for j=1:d

        theta(i,j) = angle; % current angle

        z(i,j) = vdata(i,j)*sin(theta(i,j)); % z = r*sin(theta)

        y(i,j) = vdata(i,j)*cos(theta(i,j)); % y = r*cos(theta)

        angle=angle+at; % increment angle by at deg for next data point

    end

end

```

$z = dsenseconv * \text{ones}(\text{size}(z)) - z;$ % gives distance from conveyor surface to fruit top surface

%% Plotting

```

figure

% surface data points plot

% subplot(1,2,1),

surface(x,y,z)

xlabel('Along conveyor (mm)')

```

```

ylabel('Across conveyor (mm)')
zlabel('Depth (mm)')
title('Surface plot : data points')
axis equal
axis tight
shading interp
view([-40 20])
colorbar
for i=1:c
    for j=1:d
        if z(i,j)<dbar
            z(i,j)=0;
        end
        if z(i,j)>85
            z(i,j)=85;
        end
    end
end

y = y - min(min(y)); % this makes wall = 0, gives distance from conveyor side wall to fruit top
surface
%% Elemental volume (4 adjacent points), linear interpolation
[a, b] = size(x);

```

```

for i=1:a-1 %
dx(i) = x(i+1)-x(i); % elemental length along x-axis

for j=1:b-1

dy(i,j) = (y(i,j)-y(i,j+1)+y(i+1,j)-y(i+1,j+1))/2; % avg elemental length along y-axis
zavg(i,j) = (z(i,j)+z(i,j+1)+z(i+1,j)+z(i+1,j+1))/4;
vol(i,j) = zavg(i,j)*dx(i)*dy(i,j);
dxpoint(i,j) = x(i)+dx(i)/2;
dypoint(i,j) = y(i,j)+dy(i,j)/2;

end

xslice_vol(i) = sum(vol(i,:)); % volume of all elements between 2 xslices

end

total_vol = sum(sum(vol(:, :))), % total volume

% removing volume corresponding to flaps

xrange = max(max(x)); % finds out what is the length of the conveyor we have considered in
data analysis

flapvolume = floor(xrange/flappitch)*flapvolcorfact;
total_vol_flapcor = total_vol - flapvolume, % total volume with flap correction

%% Plotting

figure

% surface data points plot

% subplot(1,2,1),
surface(x,y,z)

xlabel('Along conveyor (mm)')

```

```

ylabel('Across conveyor (mm)')

zlabel('Depth (mm)')

title('Surface plot : data points')

axis equal

axis tight

shading interp

view([-40 20])

colorbar

%% Working on data achieved through grid data

% data reshaping - uniform x and y co-ordinates, interpolate z co-ordinate

% Presently we have kept the data size same. increasing data size might improve results

X1 = x; % keeping the original x data

Y1 = ones(c,1)*[floor(max(y(:,1))):-floor(max(y(:,1)))/(d-1):0]; % changing y data to get

uniformly spaced y data

% floor(y(:,1)) gives rounded down value of maximum element in the 1st column of y data

Z1 = griddata(x,y,z,X1,Y1,'cubic'); % 'linear' interpolation of z data, we can use 'cubic' as well

% elemental volume (4 adjacent points), linear interpolation

[a, b] = size(X1);

% check due to interpolation if we get any element of Z1 as NaN, if we do,

% then replace that element with original z value, we can do this because

% we have kept the size of x,y,z same when it becomes X1, Y1 and Z1

Z1check=isnan(Z1); % checks if any of the element of Z1 is 'NaN' and returns '1' else '0' at that

element

```

```

for i=1:a
    for j=1:b
        if Z1check(i,j)== 1
            Z1(i,j)=z(i,j);
        end
    end
end

for i=1:a
    for j=1:b
        if Z1(i,j)<dbar
            Z1(i,j)=0;
        end
        if Z1(i,j)>85
            Z1(i,j)=80;
        end
    end
end

for i=1:a-1 %
    dx1(i) = X1(i+1)-X1(i); % elemental length along x-axis
    for j=1:b-1
        dy1(i,j) = (Y1(i,j)-Y1(i,j+1)+Y1(i+1,j)-Y1(i+1,j+1))/2; % avg elemental length along y-axis
        zavg1(i,j) = (Z1(i,j)+Z1(i,j+1)+Z1(i+1,j)+Z1(i+1,j+1))/4;
        vol1(i,j) = zavg1(i,j)*dx1(i)*dy1(i,j);
    end
end

```

```

dxpoint1(i,j) = X1(i)+dx1(i)/2;
dypoint1(i,j) = Y1(i,j)+dy1(i,j)/2;
end

xslice_vol1(i) = sum(vol1(i,:)); % volume of all elements between 2 xslices
end

total_vol1 = sum(sum(vol1(:,:))), % total volume

%% removing volume corresponding to flaps

X1range = max(max(X1)); % finds out what is the length of the conveyor we have considered in
data analysis

flapvolume1 = floor(X1range/flappitch)*flapvolcorfact_griddata;

total_vol1_flapcor = total_vol1 - flapvolume1, % total volume with flap

% correction

%% weight calculation

% weight = 1.38E-06*total_vol1_flapcor - 4.50E+00, % 0.5864 m/s

% weight = 1.60E-06*total_vol1_flapcor - 6.14E+00, % 0.785 m/s

weight = 1.48E-06*total_vol1_flapcor - 6.74E+00, % 1.1 m/s

%% plotting

figure

% % surface data points plot

% subplot(1,2,1),
surface(X1,Y1,Z1)

% mesh(X1,Y1,Z1)

```

```
xlabel('Along conveyor (mm)')
```

```
ylabel('Across conveyor (mm)')
```

```
zlabel('Depth (mm)')
```

```
title('Surface plot : data points')
```

```
axis equal
```

```
shading interp
```

```
view([-40 20])
```

```
colorbar
```

LIST OF REFERENCES

- Abidine, A., S. K. Upadhyaya and J. Leal. 2003. Development of an electronic weigh bucket. In *ASAE Paper No. 031043*, St. Joseph, MI, USA: ASAE.
- Annamalai, P. 2004. Color vision system for estimating citrus yield in real-time. MS Thesis. UFL: University of Florida, Agricultural and Biological Engineering Department.
- Behme, J. A., J. L. Schinstock, L. L. Bashford and L. I. Leviticus. 1997. Site-specific yield for forages. In *ASAE Paper No. 971054*. St. Joseph, MI, USA: ASAE.
- Benjamin, C. E. 2002. Sugar cane yield monitoring system. MS diss. Baton Rouge, Louisiana: Louisiana State University, Department of Biological and Agricultural Engineering.
- Bora, G. C., R. Ehsani, K. Lee and W. Lee. 2006. Development of a test rig for evaluating a yield monitoring system for citrus mechanical harvesters. In *ASAE Paper No. 701P0606*, St. Joseph, MI, USA: ASAE.
- Campbell, R. H., S. L. Rawlins and S. F. Han. 1994. Monitoring methods for potato yield mapping. In *ASAE Paper No. 94-1584*, St. Joseph, MI, USA: ASAE.
- Cerri, D. G., S. K. Upadhyaya and J. Leal. 2004. Development of an electronic weigh bucket. In *ASABE, Paper No: 041097*, St. Joseph, MI, USA: ASABE.
- Chinchuluun, R., W. S. Lee and R. Ehsani. 2007. Citrus yield mapping system on a canopy shake and catch harvester. In *ASAE Paper No: 073050*, St. Joseph, MI, USA: ASAE.
- Churchill, D. B., H. R. Sumner and S. L. Hedden. 1976. Developments in citrus pickup equipment. *Agricultural Research Service, ARS-S-84. New Orleans, LA*.
- Coppock, G. E. 1976. Catching frame development for a citrus harvest system. *Transaction of the ASAE* 19(4): 75-1045.
- Coppock, G. E. 1967. Harvesting early and midseason citrus fruit with tree shaker harvest systems. *Proc. Fla. State Hort. Soc.* 80:98-104.
- Coppock, G. E. and S. L. Hedden. 1968. Design and development of a tree shaker harvest system for citrus fruit. *Transactions of the ASAE* 11(3): 339-342.
- Cundiff, J. S. and Y. Sharobeem. 2003. Development of yield monitor (Part one). In *ASAE Paper No: 031036*, St. Joseph, MI, USA: 2003.
- Ehlert, D. 2000. Measuring mass flow by bounce plate for yield mapping of potatoes. *Precision agriculture* 2(2): 119-130.
- Ehsani, M. R., T. E. Grift, J. M. Maja and D. Zhong. 2009. Two fruit counting techniques for citrus mechanical harvesting machinery. *Computers and Electronics in Agriculture* 65(2): 186-191.

- Ehsani, R. and D. Karimi. 2010. Yield monitors for specialty crops. *Advanced engineering systems for specialty crops: A review of precision agriculture for water, chemical, and nutrient application, and yield monitoring*. Spec. Issue of Landbauforschung vTI Agriculture and Forestry Research 340: 31-43
- FDOC. 2010. Marketing, research and regulation of the Florida citrus industry: Bartow, FL.: Available at: <http://dev08.floridajuice.com>. Accessed 15 May 2010
- Gogineni, S., J. G. White, J. A. Thomasson, P. G. Thompson, J. R. Wooten and M. Shankle. 2002. Image-Based Sweetpotato Yield and Grade Monitor. In *ASAE Paper No: 021169*, St. Joseph, MI, USA: ASAE.
- Grift, T., R. Ehsani, K. Nishiwaki, C. Crespi and M. Min. 2006. Development of a yield monitor for citrus fruits. In *ASABE Paper No: 061192*, Portland, Oregon, USA: ASABE.
- Hall, A. and J. Louis. 2009. Chapter 3: Vineclipper: A Proximal Search Algorithm to tie GPS field locations to high resolution grapevine imagery. In *Innovations in Remote Sensing and Photogrammetry*, 361-372. ed. W. CartwrightGartner, G.Meng, L. and Peterson, M., Springer Berlin Heidelberg.
- Hedden, S. L. and G. E. Coppock. 1971. Comparative harvest trials of foliage and limb shakers in 'Valencia'oranges. In *Proc. Fla. State Hort. Soc.* 88-92.
- Heidman, B. C., U. A. Rosa, P. H. Brown and S. K. Upadhyaya. 2003. Development of a pistachio yield monitoring system. In *ASAE Paper No. 031040*, St. Joseph, MI, USA: ASAE.
- Hofstee, J. W. and G. J. Molema. 2003. Volume estimation of potatoes partly covered with dirt tare. In *ASAE Paper No:031001*, Paper No: 031001. St. Joseph, MI, USA: ASAE.
- Hume, H. H. 1926. *The cultivation of citrus fruits*. New York, NY.: The Macmillan Company.
- Konstantinovic, M., S. Woeckel, P. S. Lammers, J. Sachs and M. Minneapolis. 2007. Evaluation of a UWB radar system for yield mapping of sugar beet. In *ASABE Paper No. 071051*, Minneapolis, Minnesota: ASABE.
- Kuhar, J.E. 1997. *The precision-farming guide for agriculturists*. Moline, IL.: John Deere Publ
- Lee, W. S., T. F. Burks and J. K. Schueller. 2002. Silage yield monitoring system. In *ASAE Paper No: 021165*, St. Joseph, MI, USA: ASAE.
- Labview®. 2008. *Labview for Windows*. ver. 8.6.: National Instruments Corporation, Austin, TX, USA
- Magalhães, P. S. G. and D. G. P. Cerri. 2007. Yield Monitoring of Sugar Cane. *Biosystems Engineering* 96(1): 1-6.

- Maja, J. M. and R. Ehsani. 2009a. Development of a yield monitoring system for citrus mechanical harvesting machines. *Precision Agriculture* 1-13.
- Maja, J. M. and R. Ehsani. 2009b. Development of a yield monitoring system for citrus mechanical harvesting machines. *Precision Agriculture* 1-13.
- Miller, W. M. and J. D. Whitney. 1999. Evaluation of weighing systems for citrus yield monitoring. *Applied Engineering in Agriculture* 15(6): 609-614.
- MATLAB®. 2009. *Matlab for Windows*. ver. 2009a: The Mathworks Inc., Natick, MA, USA
- Molin, J. P. and L. A. A. Menegatti. 2004. Field-testing of a sugar cane yield monitor in Brazil. In *ASAE Paper No. 041099*, St. Joseph, MI, USA: ASABE.
- Pelletier, G. and S. K. Upadhyaya. 1999. Development of a tomato load/yield monitor. *Computers and Electronics in Agriculture* 23(2): 103-117.
- Persson, D. A., L. Eklundh and P. A. Algerbo. 2004. Evaluation of an optical sensor for tuber yield monitoring. *Transactions of the ASAE* 47(5): 1851-1856.
- Peterson, D. L. 1998. Mechanical harvester for process oranges. *Applied Engineering in Agriculture* 14(5): 455-458.
- Price, R. R., J. Larsen and A. Peters. 2007. Development of an optical yield monitor for sugar cane harvesting. In *ASABE Paper No. 071049*, Minneapolis, Minnesota, USA: ASABE.
- Qarallah, B., K. Shoji and T. Kawamura. 2008. Development of a yield sensor for measuring individual weights of onion bulbs. *Biosystems engineering* 100(4): 511-515.
- Rains, G. C., D. L. Thomas and C. D. Perry. 2002. Pecan mechanical harvesting parameters for yield monitoring. *Transactions of the ASAE* 45(2): 281-285.
- Rains, G. C., C. D. Perry and G. Vellidis. 2005. Adaptation and Testing of the Agleader Cotton Yield Sensor on a Peanut Combine. *Applied Engineering in Agriculture* 21(6): 979-983.
- Roades, J. P., A. D. Beck and S. W. Searcy. 2000. Cotton yield mapping: Texas experiences in 1999. In *Proceedings of the Beltwide Cotton Conference*, 404-408. 404-407 San Antonia, TX. Jan 4-8, 2000. Memphis, TN: National Cotton Council of America.
- Salehi, F., J. D. Whitney, W. M. Miller, T. A. Wheaton and G. Drouillard. 2000. An automatic triggering system for a citrus yield monitor. In *ASAE Paper No. 001130*, St. Joseph, MI, USA: ASAE.
- Schueller, J. K., J. D. Whitney, T. A. Wheaton, W. M. Miller and A. E. Turner. 1999. Low-cost automatic yield mapping in hand-harvested citrus. *Computers and Electronics in Agriculture* 23(2): 145-153.

- Schueller, J. K. and Y. H. Bae. 1987. Spatially attributed automatic combine data acquisition. *Computers and Electronics in Agriculture* 2(2): 119-127.
- Searcy, S. W., J. K. Schueller, Y. H. Bae, S. C. Borgelt and B. A. Stout. 1989. Mapping of spatially variable yield during grain combining. *Transactions of the ASAE* 32(3): 826-829.
- Spiegel-Roy, P. and E. E. Goldschmidt. 1996. *Biology of citrus*. Cambridge, UK: Cambridge University Press.
- Sumner, H. R. and D. B. Churchill. 1977. Collecting and handling mechanically removed citrus fruit. *Proc. Int. Soc. Citriculture* 2413-418.
- Thomasson, J. A. and R. Sui. 2004. Optical peanut yield monitor: development and testing. In *ASABE Paper No. 041095*, St. Joseph, Michigan, USA: ASABE.
- Tumbo, S. D., J. D. Whitney, W. M. Miller and T. A. Wheaton. 2002. Development and testing of a citrus yield monitor. *Applied Engineering in Agriculture* 18(4): 399-403.
- Upadhyaya, S. K., U. A. Rosa, M. Ehsani, M. Koller, M. Josiah and T. Shikanai. 1999. Precision farming in a tomato production system. In *ASAE Paper No. 99-1147*, St. Joseph, MI: ASAE
- USDA. 2009. The USDA Economics, Statistics and Market Information System: 2008-2009. National Agricultural Statistics Service. Washington, D.C.: USDA National Agricultural Statistics Service. Available at: www.nass.usda.gov. Accessed 15 May 2010.
- Vellidis, G., C. D. Perry, J. S. Durrence, D. L. Thomas, R. W. Hill, C. K. Kvien, T. K. Hamrita and G. Rains. 2001. The peanut yield monitoring system. *Transactions of the ASAE* 44(4): 775-785.
- Whitney, J. D., Q. Ling, W. M. Miller and T. A. Wheaton. 2001. A DGPS yield monitoring system for Florida citrus. *Applied Engineering in Agriculture* 17(2): 115-119.
- Whitney, J. D. 1995. A review of citrus harvesting in Florida. *Applied Engineering in Agriculture* 4133-39.
- Whitney, J. D. 1968. Citrus fruit removal with an air harvester concept. *Proc. Fla. State Hort. Soc* 8143-48.
- Whitney, J. D. and J. M. Patterson. 1972. Development of a citrus removal device using oscillating forced air. *Transactions of the ASAE* 15(5): 849-855.
- Whitney, J. D., W. M. Miller, T. A. Wheaton, M. Salyani and J. K. Schueller. 1999. Precision farming applications in Florida citrus. *Applied Engineering in Agriculture* 15(5): 399-403.
- Whitney, J., Q. Ling, W. Miller and T. Wheaton. 2001. A DGPS yield monitoring system for Florida citrus. In 115-119.

- Whitney, J. D., T. A. Wheaton, W. M. Miller, M. Salyani and J. K. Schueller. 1998. Site-specific yield mapping for Florida citrus. *Proc. Fla. State Hortic. Soc.* 111: 148-150.
- Wild, K. and H. Auernhammer. 1999. A weighing system for local yield monitoring of forage crops in round balers. *Computers and Electronics in Agriculture* 23(2): 119-132.
- Wilkerson, J. B., F. H. Moody, W. E. Hart and P. A. Funk. 2001. Design and evaluation of a cotton flow rate sensor. *Transactions of the ASAE* 44(6): .
- Ye, X., K. Sakai, A. Sasao and S. Asada. 2008. Potential of airborne hyperspectral imagery to estimate fruit yield in citrus. *Chemometrics and Intelligent Laboratory Systems* 90(2): 132-144.
- Zaman, Q. U., A. W. Schumann and H. K. Hostler. 2006. Estimation of citrus fruit yield using ultrasonically-sensed tree size. *Applied Engineering in Agriculture* 22(1): 39-44.
- Zaman, Q. U., A. W. Schumann, D. C. Percival and R. J. Gordon. 2008. Estimation of wild blueberry fruit yield using digital color photography. *Transactions of the ASAE* 51(5): 1539-1544.

BIOGRAPHICAL SKETCH

Ujwala Jadhav was born in year 1982, to Mangal Jadhav and Subhash Jadhav, in Satara, Maharashtra, India. She attended University of Pune, India from year 1999-2004 where she earned her Bachelor of Computer Science degree in 2002 and Master of Computer Science degree in year 2004. Later she worked as a software engineer in three reputed Indian companies and gained quality experience in software project development. She joined University of Florida to pursue her higher education in year 2008 and worked in Precision Agriculture Lab on Citrus yield monitoring project for mechanical harvesters. She will receive her concurrent degrees in computer science as well as agricultural and biological engineering in December 2010.